Multifunction PAPR

(NIOSH Contract 200-2202-00531)
National Personal Protection Technology Laboratory

Final Report

Arthur T. Johnson
Professor
Fischell Department of Bioengineering
University of Maryland
College Park, MD 20742

William H. Scott, Jr.
Faculty Research Assistant

Frank C. Koh
Faculty Research Assistant

Timothy E. Rehak
General Engineer
National Personal Protection Technologies Laboratory
National Institute for Occupational Safety and Health
Pittsburgh, PA

Ken Y. H. Chiou
Graduate Student

Stephanie J. Phelps
Graduate Student

Erica B. Frances
Graduate Student

Erika R. Lopresti
Graduate Student

04 September 2007

Table of Contents

I. Contributor Information

We would like to thank John Kovac for his help with the preparation of this report.

II. Executive summary

A. Contract Objective

The objective of this contract is to formulate new comprehensive test recommendations for certifying multifunction Powered Air Purifying Respirators (PAPR). The specific PAPR involved is the Centurion Max Multifunction PAPR manufactured by Martindale Protection, Norfolk, UK but testing standards are to be applicable to all similar protective devices. There is a focus on the Centurion because manufacturers wanted to use this type of respirator in the mining industry but there were no NIOSH standards for these multifunction PAPRs.

B. Summary

Although this contract specifically targeted certification of multifunction PAPRs such as the Centurion MAX, some more general questions were posed that related to all PAPRs, both loose-fitting and tight-fitting. The opportunity to extend the state of knowledge was seized, and experiments were conducted. Each of these research questions resulted in a prepared manuscript that either has been, or will be, submitted for publication in a peer-reviewed journal. Current drafts of these manuscripts are appended to this report.

It needed to be determined if the current NIOSH standards were sufficient to test the multifunction PAPR or if there needed to be more. Applicable standards and testing recommendations are reviewed in Appendix 1.

The first question posed addressed the possibility of overbreathing a PAPR. Peak flows during strenuous work are likely to exceed blower capacity. Also, PAPR worn for long periods of time are likely to have discharged batteries, and these would have less power to blow air to their full capability. In either case, overbreathing the air capacity of a PAPR blower is likely. The first study Exercise Performance While Wearing a Tight-Fitting Powered Air Purifying Respirator with Limited Flow (Appendix 2), was designed to see what the impact overbreathing would have on wearer performance. It was found that a decrease in flow rate did lead to a decrease in the time subjects were able to perform while wearing the mask.

Next it needed to be determined, in the event of overbreathing, how much air is overbreathed. The study *Overbreathing a Loose-Fitting PAPR* (Appendix 3) was conducted to answer this question. All subjects inhaled more air than was supplied by the PAPR blower, but only one of them exceeded the 1.4 L dead volume of the PAPR facepiece. This indicated that the dead volume of the PAPR was protective.

The next study, *Inhalation Flow Rates During Strenuous Exercise* (Appendix 4) was conducted to characterize peak inhalation flow rates during heavy exercise. Knowing this information is essential in determining if the respirator blower can satisfy the demands of the wearer. Because the blower, batteries, and filter of PAPRs are often located on top of the wearer's helmet, powerful blowers require more mass to be carried on the head. The study titled *Effects PAPR Helmet Weight on Voluntary Performance Time at 80-85% of Maximal Aerobic Capacity* (Appendix 5) was performed to determine the effect on wearer performance when the power of the blower was increased. It was found that performance time decreased linearly with an increase in helmet weight.

The next four studies were performed to examine flow patterns within multifunction PAPRs. In the study *Flow Visualization in a Loose-Fitting PAPR* (Appendix 6), a novel approach was developed to visualize air as it is drawn into the PAPR through the filter and travels to the wearer's mouth. Using this method with a breathing machine, it was determined that there was leakage in a loose-fitting PAPR. However, in a situation where contaminants entered the facepiece, up to 1.4 L could be inhaled before the contaminant reached the mouth. Using similar flow visualization techniques in the study *Inward Leakage in Tight-Fitting PAPRs* (Appendix 7), it was determined that tight-fitting PAPRs would provide adequate protection for the wearer because contaminated air would not reach the mouth. Flow visualization was next used to test leakage in a loose-fitting PAPR when human subjects were used in the study *Human Subject Testing of Leakage in a Loose-Fitting PAPR* (Appendix 8). This study confirmed that the dead volume of a respirator is protective. The subjects could inhale up to 1.1 L of air before any contaminants that entered the facepiece would reach the mouth.

Protection Factors and Net Contaminant Volumes Inhaled While Wearing Respirators (Appendix 9), the final study of this report, was conducted to determine how much contaminant could be expected to be inhaled when overbreathing of a respirator did occur. In this study, we investigated measurement of respirator protection factors using a different method of a challenge gas and collection of exhaled breath. Other methods to measure protection have shortcomings. Visual detection of fog is not a direct indication of contaminant protection offered by the respirator. Respirator protection factors, which are defined as contaminant concentration outside the facepiece divided by contaminant concentration inside the facepiece, cannot be used accurately for rapidly changing

particle counts. This concentration ratio can also be influenced by moisture particles from and deposition of particles in the respiratory system. Therefore, a different technique was needed to assess protection provided by a respirator when more air is inhaled than is supplied by the PAPR blower.

III. Background

The multifunction PAPR is a personal protective device incorporating respiratory protection, head protection, hearing protection, and eye protection. Respiratory protection is provided by a battery-powered blower and filter supplying air to the face piece; head protection incorporates a helmet and head harness able to absorb impact loads; hearing protection is supported by ear muffs perhaps supplemented with ear plugs; eye protection is given by a visor or eye lenses. The Centurion Max is a loose-fitting device with face shield, hearing protection, helmet, and blower with particulate filter. A blouse around the edges of the face shield provides a partial barrier to air flow from outside of the shield. The Centurion Max PAPR is worn voluntarily by miners in contaminant conditions that do not require respiratory protection. Other multifunction PAPRs may or may not be worn by miners, construction workers, medical personnel, or others. None is presently NIOSH certified.

NIOSH standards (Appendix 10) for the multifunction PAPR offer cranial, eye, hearing, and respiratory system protection. Current NIOSH standards show that the multifunction PAPR can be tested with all of these except for the respiratory protection standards.

IV. Scope

The scope of this report is to first review existing standards and suggest standards applicable to testing multifunction PAPRs. New test standards will be recommended as a result of the findings of additional experiments conducted. Authority to decide whether these standards will be used rests with NIOSH and not with the authors.

V. Approach

After reviewing existing standards, it was concluded that there needed to be additional respiratory protection standards in order to adequately test the multifunction PAPR. Eight studies were performed to help make new testing recommendations for the multifunction PAPR. This report aims to answer a series of questions that developed as each study was completed. Might there be a problem with wearers overbreathing the PAPR? If there is a problem with overbreathing, to what degree? What peak inhalation flow rates could be expected with PAPR wear? How would increasing blower power to meet these flow rates affect wearer performance? After these questions were answered (Appendices 2-5), techniques were developed to visualize the air flow pathway from the environment to the subject's mouth. These flow visualization techniques were used to test both loose and tight-fitting PAPRs on breathing machines (Appendices 6 and 7). Human subjects were then used to test leakage with loose-fitting PAPRs (Appendix 8). Finally, the last study (Appendix 9) was performed to address the problem of current methods of measuring respiratory protection being inadequate.

VI. Test Methodology

A. Test equipment used

The first four studies used human subjects exercising on a standard treadmill. Prior to the start of each experiment, a maximal oxygen consumption test ($\dot{V}O_2$max test) was performed on each subject using a Quinton (Bothell, WA) motorized treadmill and a modified Bruce incremental treadmill exercise protocol. Subjects were asked to warm-up and stretch for approximately 5-10 minutes prior to the start of the test, and were then equipped with a Hans Rudolph (Kansas City, MO) one-way breathing valve configured with a rubber adaptable mouthpiece. This apparatus was interfaced with a standard Fleisch (Phillips and Bird, Richmond, VA) pneumotach and Perkin Elmer (Pomona, CA) model 1100 mass spectrometer to monitor continuous expired airflow.

In the first study, *Exercise Performance While Wearing a Tight-Fitting Powered Air Purifying Respirator with Limited Flow* (Appendix 2), all subjects wore the PAPR blower and filter (FR-57, 3M, St. Paul, MN) on their waists without the battery pack. Subjects exercised on a standard treadmill and electrodes were used to monitor heart rate continuously during the test. The PAPR was powered by a dc power supply to give flow rates of 0%, 30%, 66%, 94%, and 100% of rated maximum blower capacity of 110 L/min.

The second study, *Overbreathing a Loose-Fitting PAPR* (Appendix 3), had subjects exercising on a treadmill while wearing the Centurion MAX loose-fitting PAPR inside a Portable Breathing Chamber.

In the study, *Inhalation Flow Rates During Strenuous Exercise* (Appendix 4), instantaneous inhalation flow rates for subjects exercising on a treadmill have been

measured for the following conditions: 1) at 80-85% $\dot{V}O_2$ max without a respirator, 2) at 100% $\dot{V}O_2$ max without a respirator, and 3) at 80-85% $\dot{V}O_2$ max while wearing a breath-responsive PAPR.

In the fourth study, *Effects PAPR Helmet Weight on Voluntary Performance Time at 80-85% of Maximal Aerobic Capacity* (Appendix 5), subjects were tested with four lead-weighted construction helmets of 0.54, 1.03, 1.85, and 3.36 kg.

Tests in the study *Flow Visualization in a Loose-Fitting PAPR* (Appendix 6) were conducted with the Centurion MAX and the Racal AirMate 3 respirators mounted on a head form. This setup was placed inside a portable breathing chamber. Visible glycerol fog was introduced into the chamber and the flow pathways of the air in the facepiece were recorded with a digital video recorder.

In the next study, *Inward Leakage in Tight-Fitting PAPRs* (Appendix 7), a combination of fog flow visualization and local flow measurement techniques was used to determine the inward leakage for two tight-fitting Powered Air-Purifying Respirators (PAPRs), the 3M Breathe-Easy PAPR and the SE 400 breathing demand PAPR. They were mounted on a breathing machine head form and flows were measured from the blower and into the breathing machine. A bronchoscope was located at the mouth of the headform to detect inhaled fog and capture digital video images.

For the study *Human Subject Testing of Leakage in a Loose-Fitting PAPR* (Appendix 8), ten human volunteers were asked to wear the Centurion MAX inside a fog-filled chamber. Their inhalation flow rates were measured with small pitot-tube flowmeters held inside their mouths. They were video imaged while they breathed deeply, and the points at which the fog reached their mouths were determined.

In the final study, *Protection Factors and Net Contaminant Volumes Inhaled While Wearing Respirators* (Appendix 9), CO_2 was used as a tracer gas in the ambient air, and several loose-and tight-fitting respirators were tested on a breathing machine. CO_2 concentration in the exhaled breath was monitored as well as CO_2 concentration in the ambient air. Respirators tested were the Racal AirMate 3 (Racal; Frederick, MD) loose-fitting PAPR; Breathe Easy (3M; St. Paul, MN) tight-fitting PAPR, Butyl Head Cover with Cape, #522-02-23 (3M) loose-fitting hood, Centurion MAX (Martindale Protection; Thetford, Norfolk, UK) multi-purpose loose-fitting PAPR, SE 400 (SEA; Meadowlands, PA) breath-responsive PAPR, and FRM 40 (3M) air-purifying respirator. Pneumotach were adapted to blower inlets for the Racal, Centurion, and SEA devices. Pneumotachs were placed in the connecting hose between blower and facepiece for the two 3M powered devices. An inlet hose was connected to the filter of the FRM40.

B. Test subjects

Human test subjects were used in 5 of the studies (Appendices 2, 3, 4, 5, and 8). Subjects were healthy volunteers between the ages of 18 and 42. Most were college students.

VII. Results

It was found in the study, *Exercise Performance While Wearing a Tight-Fitting Powered Air Purifying Respirator with Limited Flow* (Appendix 2), that as flow rate was reduced, so was performance time. There was a 20% reduction in performance time as blower flow changed from 100% to 0% of maximum. Significant differences in Breathing Apparatus Comfort and Facial Thermal Comfort were found as flow rate varied.

In the study, *Overbreathing a Loose-Fitting PAPR* (Appendix 3), all subjects inhaled more air than was supplied by the PAPR blower, and all of them exceeded the 1.4 L dead volume of the PAPR face piece. The PAPR blower provided only 110 L/min instead of the 205 L/min specified by the manufacturer.

Results from the third study, *Inhalation Flow Rates During Strenuous Exercise* (Appendix 4), showed that there is a linear relationship between peak flow rate and average minute volume. A peak inhalation flow rate of up to 379 L/min (BTPS) was measured for subjects exercising at 80-85% $\dot{V}O_2$ max without a respirator. Peak flow rates of up to 440 L/min (BTPS) have been measured for subjects exercising at 80-85% $\dot{V}O_2$ max while wearing a breath-responsive PAPR

It was discovered in the fourth study, *Effects PAPR Helmet Weight on Voluntary Performance Time at 80-85% of Maximal Aerobic Capacity* (Appendix 5), that performance time in minutes was linearly related to helmet mass. A linear least square regression line to describe the data was: time = 20.25 – 2.552 * kg.

In the study *Flow Visualization in a Loose-Fitting PAPR* (Appendix 6), it was found that the loose-fitting PAPR without a scarf offered no protection against the fog, whereas the PAPR with a scarf allowed up to 1.4 L of inhaled breath before the fog reached the mouth. Tilting the head affected the amount of protection given by the PAPR.

Results from the study *Inward Leakage in Tight-Fitting PAPRs* (Appendix 7) show a small amount of leakage through the exhalation valves of both tight-fitting PAPRs. However there was no evidence of contaminant reaching the mouth of the breathing machine.

In the study, *Human Subject Testing of Leakage in a Loose-Fitting PAPR* (Appendix 8), results showed that an average of 1.1 L could be inhaled before contaminated air reached the mouth. As long as the blower purges contamination from inside the face piece during exhalation, the 1.1 L acts as a buffer against contaminants leaked due to overbreathing of blower flow rate.

Results from the final study, *Protection Factors and Net Contaminant Volumes Inhaled While Wearing Respirators* (Appendix 9), show that protection factors were found to range from 1.1 for the Racal AirMate loose-fitting PAPR to infinity for the 3M Hood, 3M Breath-Easy PAPR and SE 400 breath-responsive PAPR. Inhaled contaminant volumes depend on tidal volume, but ranged from 2.02 L to 0 L for the same respirators, respectively. Blower effectiveness was about 1.0 for tight-fitting APRs, 0.18 for the Racal, and greater than 1.0 for two of the loose-fitting PAPRs. With blower effectiveness greater than 1.0, some blower flow during the exhalation phase contributes to the subsequent inhalation.

VIII. Findings

The first study, *Exercise Performance While Wearing a Tight-Fitting Powered Air Purifying Respirator with Limited Flow* (Appendix 2), showed that when flow rates are not adequate, there is a performance decrement. Reducing blower air flow rates also causes a decrease PAPR comfort and facial cooling.

Two major findings came out of the study *Overbreathing a Loose-Fitting PAPR* (Appendix 3). First, the Centurion MAX PAPRs should only be used in atmospheres containing minimal, if any, contamination. The level of contamination must be below the Permissible Exposure Limit. Second, one reasonable recommendation would be that a

more powerful blower be used with this PAPR to supply higher air flow rates.

In the study *Inhalation Flow Rates During Strenuous Exercise* (Appendix 4), it was discovered that instantaneous inhalation flow rates were found to vary greatly among subjects and at different times for each subject. Measured flow rates for the pressure-demand PAPR are higher than breathing flow rates. Estimated peak flow rates can be calculated for various strenuous work conditions.

It was found in the study, *Effects PAPR Helmet Weight on Voluntary Performance Time at 80-85% of Maximal Aerobic Capacity* (Appendix 5), that an increase in blower capacity leading to an increase in helmet weight would lead to a decrease in respirator wearer performance. Each additional kilogram mass on the head could be expected to result in 2.5 min performance penalty at this rate of work.

Results of the study, *Flow Visualization in a Loose-Fitting PAPR* (Appendix 6), indicated that the dead volume (1.4 L) of the PAPR was protective. In other words, 1.4 L of contaminated air could be inhaled before any contamination reached the wearer's mouth. The presence of the Centurion MAX scarf makes the Centurion much more protective than the Racal.

It was concluded from the results in the study *Inward Leakage in Tight-Fitting PAPRs* (Appendix 7), that the tight fitting PAPRs tested would provide adequate protection for the wearer because contaminated air would not reach the mouth.

In the study, *Human Subject Testing of Leakage in a Loose-Fitting PAPR* (Appendix 8), the average volume inhaled before contaminants (fog) reached subjects' mouths was 1.11 L. For tidal volume less than this value, airborne contaminants leaking

in from around the periphery of this respirator would not be inhaled by an average wearer.

In the last study, *Protection Factors and Net Contaminant Volumes Inhaled While Wearing Respirators* (Appendix 9), a new way to measure respirator efficacy was developed. It was found that wearer protection factors do not match well with OSHA assigned protection factors. PAPR blower flow rates are not constant flow for the tight-fitting PAPRs. Finally, as confirmed by earlier studies dead space can be effective against inhaling contamination.

IX. Summary and Conclusions

There was found to be potential for an overbreathing problem for the loose-fitting PAPR (Appendix 3). Peak inhalation flow rates were explored and it was discovered that increased blower power may be necessary (Appendix 4). However, increasing blower power has the disadvantage of decreasing wearer performance (Appendix 5).

The four flow visualization studies (Appendixes 6-9) provided valuable information about the protection provided by loose- and tight-fitting PAPRs. It was found that there was significant leakage in a loose-fitting PAPR but not the tight-fitting PAPR. It was found in the last study (Appendix 9) that measurements of contaminant concentration inside the face piece can be incorrect, given that there are regions of high and low contaminant concentrations in close proximity. Wearer protection factors do not agree well with expected respirator protection factors.

Each study confirmed that dead volume in the PAPR proved to be important in adding protection against inhaling contamination. This is a different way to look at dead volume. Dead volume in air-purifying respirators is considered to be a problem,

accumulating CO_2 and limiting physical work performance. Dead volume in powered air-purifying respirators (PAPRs) in contrast, can actually be a significant help to provide wearer protection. PAPR dead volume might be purposely designed to be large in order to achieve protection goals. A recommendation to be made is that PAPR blowers do not need to supply peak flow rate, but should function by cleaning dead volume of contamination during exhalation phase. Also, the method of taking the ratio of CO_2 in exhaled air to the concentration in ambient air may be a better way to measure respiratory protection than methods currently used.

APPENDIX 1

Standards and Recommended Test Procedures

A. Testing Recommendations

The Centurion Max Multifunction PAPR can be tested using existing standards for most of its functions. Research has shown that, used in an environment with low contaminant levels, this respirator can be safely used. Improved protection can be obtained by increasing the air supply capacity of the battery-blower combination to meet or exceed the peak instantaneous inhalation flow rate expected from active wearers. Some performance penalty may be paid because of the extra weight that would result, but the difference would be minor. Other configuration and indicator recommendations are given for blower power and filter life.

1. Configuration

The configuration is the fit and arrangement of the mask components around the wearer's facial features. It is essential in ensuring successful mask performance and comfort to the wearer. Assumed in these recommendations is that appropriate configuration adjustments are able to be made. That is, the face visor does not contact any part of the face, hair, beard, or eye glasses and that it can be lowered to its operating position. The helmet must be able to fit comfortably upon the head and not slide around. The helmet harness should be able to be adjusted to give adequate protection. Hearing protector ear muffs must be able to be fitted over the ears and any hearing-assist devices being used. Cushion pressure at the ear shall not exceed 4500 Pa (DIN EN 352-3:1996), and as much

accommodation as possible made with eye glass temples. All these adjustments are described in standards applicable to separate components. These recommendations are an essential component to ensuring the mask's ability to protect the wearer as designed.

2. Head Protection

Multifunction PAPRs offer protection to the wearer's head from electric shock, impact and penetration of objects through the helmet. ANSI Z89.1 – 1987 is required by 29 CFR 1910.135B. Protective helmets purchased after 5 July 1994 must comply with ANSI Z89.1 – 1986, and, by extension, ANSI Z89.1 – 1997. Thus head protection offered by the helmet of the multifunction PAPR is adequately covered by the existing standard.

3. Hearing Protection

PAPR wearers often need protection against loud noise in the work environment that may lead to hearing damage. Protection against environmental sound levels is difficult to apply to the multifunction PAPR. Noise levels at the ear are specified by existing standards at a level not to exceed a weighted average of 80 dBA irrespective of environmental sound levels and time-varying changes. Thus, the individual hearing protection device included in the multifunction PAPR cannot be tested without additional standards and test procedures being developed.

There are several approaches that could be used. The first is to pick some ceiling noise value, say 125 dB at 5000 Hz for instance, and test

the multifunction PAPR hearing protection for a constant external sound level at the ear to 80 dB.

Another approach would be to use a number of different noise protection devices, each with its own Noise Reduction Ratio (NRR), to give the required upper limit of 80 dBA when challenged by sound levels in the workplace. This would require different devices to be made available and a multifunction PAPR that would allow protective devices to be interchanged.

Even these two approaches would not adequately meet requirements of present standards because the requirement relates to the average and not the peak sound level at the ear.

A combination of the two approaches above is recommended. First, testing should use a constant external sound level, and the protective device should reduce this external sound level to 80 dBA at the ear, and, second, the multifunction PAPR should allow a choice of protective devices to be used depending on the environmental noise level challenge.

When testing hearing protection with ear muffs and while wearing eye glasses, a 5 dB correction is routinely applied to the noise level at the ear (E.H. Berger, Aero Co., Indianapolis). Because the hearing protection with the multifunction PAPR uses ear muffs, and glasses are so common, this correction should be applied whenever hearing protection is tested.

4. Communications

Communications in the work environment can be very important for normal activities and for transmitting emergency information. The multifunction PAPR has intrinsic hearing protection plus a blower that generates a low level of noise. Both of these contribute to difficulty hearing speech generated in a noisy environment.

There are existing standards for testing communications effectiveness. However, unless a powered speech communications system is to be installed in a multifunction PAPR, it is recommended that the multifunction PAPR not be expected to allow communications through voice. Rather, it is important that adequate vision be present for hand signaling and written communication. Therefore, it was determined that a speech conveyance or speech intelligibility test is not necessary for this application.

5. Vision

Vision standards are essential to protect the wearer's eyes from damage. Adequate standards exist for eye protection, and these need to be applied. Vision, however, goes beyond eye protection because, as explained in the section above, communications with a multifunction PAPR must necessarily rely on visual signals (touch, of course, can also be important, but information content of touch is not too detailed).

29 CFR 1910.133 specifies minimum shade numbers for exposures to harmful light levels. Very dark shades cannot be used with the

multifunction PAPR if they prevent adequate visual communications to occur, thus potentially allowing an unsafe condition to develop. Thus, it is important that eye protection given by the multifunction PAPR also maintain adequate optical clarity, field of view, and color discrimination for visual communication.

Spectacles prescribed to be worn by the worker must be accommodated by the multifunction PAPR. The spectacles themselves cannot interfere with the hearing protection device, and the hearing protection device cannot cause spectacles to develop pressure concentrations on the bridge of the nose, temples, or cheeks. Spectacles must be able to be worn as prescribed and not altered in lens-to-eye distance or angle presented to the face. Spectacles should not interfere with the visor or other eye protection of the multifunction PAPR. Development of additional test standards as described above, relating spectacles to the other elements of the multifunction PAPR is recommended.

6. Respiration I (blower and battery)

Standards for respiratory protection fall into one of three areas: blower and battery, air flow routes, and filter protection. These sections are discussed individually here because they are tested separately. The PAPR blower must provide adequate flow to prevent the wearer from inhaling contaminants. Flow rate requirements for a tight-fitting PAPR are 115 L/min and for a loose-fitting PAPR it is 170 L/min. Laboratory

testing has identified a number of deficiencies in the multifunction PAPR model supplied. Correction of these deficiencies requires new standard test procedures to be developed. The first of these is concerned with inadequate blower flow rate. The blower was specified to supply 205 L/min of air to the face shield with no back pressure, as specified in European standard EN 146/EN 1294. It is not likely that the flow path from blower to outlet will be completely unobstructed, so the blower should be able to supply the peak inspiratory flow rate of the wearer with some small pressure drop in the flow channel. Peak inspiratory flow rates are approximately 440 L/min (Appendix 4), as measured in our laboratory during maximal exercise. This value depends on the individual and on the work rate. Depending on the particular configuration, contaminated air may be drawn into the face piece by the blower. Although additional testing (Appendix 8) has shown that this contamination does not necessarily reach the mouth and threaten the wearer, it has been found that as long as the blower clears air from the facepiece during the exhalation phase the threat to the wearer is minimal. Thus, a test procedure should be developed to test blower capacity while in place and with some partial obstruction (represented, for example, by a dirty particulate filter) of the flow channel.

Blower capacity is directly affected by battery capacity. Useful battery life, defined as supplying enough power to maintain blower capacity at or above peak inspiratory flow rate, should probably be at least

the amount of time that a wearer would continuously depend on the PAPR for protection. This probably would be four hours or more.

A battery condition indicator should be present. The multifunction PAPR model supplied to the University of Maryland had no such indicator, and it was nearly impossible for wearers to detect when battery capability and blower performance had degraded seriously. Indicators for both battery and blower would be suggested.

The visor on the PAPR controlled a switch that operated the blower. The blower was not turned on until the visor was in the correct operating position. There were times during the exercise testing when the visor changed position, the blower turned off, and the wearer was not aware that the air supply had stopped. The visor position switch is unnecessary and gives trouble; therefore it should be replaced with a manual switch that is difficult to change inadvertently. A blower indicator should be added.

7. Respiration II (air flow routes)

Blower flow pathways should be tested to be sure that uncontaminated air is delivered uniformly to the face. Flow that is directed mainly to the mouth, for instance, can protect the respiratory system but perhaps not the eyes or facial skin. A test procedure is recommended to determine minimum acceptable flow delivery.

If exhaled air is allowed to accumulate at some point inside the face shield, then a CO_2 test is recommended. NIOSH has developed a test

plan for CO_2 based upon 42 CFR Part 84, Section 84.97. This should be adapted to locate regions of higher CO_2 concentration. Although CO_2 that is not re-inhaled has no stimulation effect on respiration, CO_2 concentrations still indicate regions where contaminated air could accumulate.

Likewise, oxygen concentrations need to be measured inside the face shield to be sure they are adequate (42CRF Part 84). High CO_2 and low O_2 are expected to exist together.

The flow path for contaminated air entering the face area from around the face shield should be established to determine if wearers are protected by the dead volume inside the face shield. Although this test will likely give a qualitative rather than a quantitative result, extreme preferential flow pathways must be avoided.

Flow pathway observation should also be used to assure that exhaled air is not directed toward the blower inlet. Such gas concentration feedback could result in high CO_2 and low O_2 air being delivered to the wearer.

The dead volume inside the face shield could be measured. As described in Appendix 3, the dead volume of this PAPR can be measured on a headform with all respirator cavities and the gaps between visor and headform taped shut. A known volume of dried lentils of known density is used to fill the visor dead volume. The weight of the lentils in the container after filling the dead volume is subtracted from the original

weight of lentils in the container. The difference, when multiplied by lentil density, gives the facepiece volume of the PAPR. Such information could be useful to determine how sensitive device protection is to external wind and high respiratory flow rates. An extremely high amount of dead volume would cause the loose-fitting PAPR to be less sensitive to variations in blower delivery.

8. Respiration III (filter protection)

The final area of respiratory protection to be tested concerns the filter on the PAPR. Filter life and resistance should be adequate to provide protection for some specified period of time. The applicable standard is 29 CFR 1910.134.

Filters should be able to be changed easily. The environment should be first characterized before selecting a filter; therefore, a change out schedule should be established. An end-of-service life indicator should be present because the filter often cannot be easily observed. This indicator needs to be placed downstream of the filter because particulates pile up on it. One atmospheric sensor and one sensor between the filter and the blower would serve to measure a pressure drop across the filter. Using a low flow indicator would not be able to isolate the problem to the filter, but a pressure drop indicator across the filter would.

9. Intrinsically Safe

As specified in MSHA 30 CFR 18.68, all devices to be used in mines must be unable to cause fire or explosion electrically detonated.

Multifunction PAPR's used in workplaces with fire dust (grain milling) or solvent vapors (paint shops) should also be intrinsically safe electrically.

B. A Review of Applicable Standards for Multifunction Air Purifying Respirators

1. Overview

Powered air purifying respirators (PAPRs) are respiratory protection devices that utilize a motorized fan to draw ambient air through the filtering element and deliver the cleaned air to the wearer in the face piece. Multifunction PAPRs are combination devices in which the filters, motor, and blower are located within a protective helmet shell that is equipped with hearing protection and a facial shield. Such a device is particularly useful for individuals who work within confined spaces, such as mines, because they have less space in which to maneuver. While individual standards are currently available for respiratory protective devices (42 CFR Part 84), vision, hearing, and head impact, no single standard exists for a device that incorporates all of these components and the interoperability with one another. Domestic standards that may be applicable to multifunction PAPRs are discussed below, and international standards are also listed. Although the multifunction PAPR must meet the requirements of 42 CFR 84 for OSHA compliance, international standards may be applicable if a unique feature needs to be tested that is not in 42 CFR 84.

2. Respiratory Protection Standards

42 CFR 84

Title 42 Code of Federal Regulations Part 84, Respiratory Protective Devices, June 8, 1995 gives specifications for respiratory protective devices, including requirements for respiratory, eye, ear, and face protection. This is a federally mandated standard for respirators to be in compliance with OSHA 29 CFR parts 1910 and 1926 that respirators must be approved under 42CFR part 84 to be in compliance with OSHA

regulations. Guidelines for proper respirator configuration are provided, and the procedures for obtaining NIOSH certification for respirators meeting general construction, performance, and respiratory protection requirements are specified for multiple classes of respirators in NIOSH SOP and STPs. Inspection, examination, and testing methods are also specified.

An overview of requirements by section is provided below. In some cases, requirements are provided for specific types of respirators, such as self contained breathing apparatuses (SCBA), and not for PAPRs. In those instances where requirements exist for one type of respirator that could also be applicable to PAPRs, those sections have been included.

84.72 Specifications for breathing tubes for SCBA require that they be designed to prevent the restriction of free head movement, disturbance of the fit of the face and mouthpiece, interference of wearer activities, and shutoff of airflow due to kinking or applied external pressure.

84.73 Harness installation and construction specifications for SCBA require that a suitable harness must be employed that is capable of holding the apparatus in proper position against the wearers body. The harness must be easy to remove.

84.76 Face and eyepiece requirements for SCBA stipulate that the wearer's vision must not be blocked or distorted by the device. Further, all face and eyepieces must be impact and penetration resistant.

84.89 Weight specifications for self SCBA require that the entire assembly weigh no more than 16 kg (35 lbs); however, if the assembly includes equipment designed to

increase wearer comfort (such as a cooling system), then the assembly may weigh no more than 18 kg (40 lbs).

84.139 Supplied-air respirator designs are required to protect the wearer's head and neck from the impact of abrasive materials.

84.140 The noise levels generated by the blower must be measured within the hood or helmet while the blower is operating at the maximum airflow rate. The noise level must not exceed 80 dBA.

84.254 Specific testing parameters with vinyl chloride are given for PAPRs, as well as maximum allowable penetration levels.

84.255 An end of service life indicator is required for each canister or cartridge approved under 84.254. The indicator must provide an obvious warning before the threshold value of 1 ppm vinyl chloride penetration is reached.

84.1141 Dust, fume, and mist respirators are required to meet certain performance and protection criteria specified in the tests described in sections 84.1141 and 84.1152 and tables 12 and 13.

29 CFR 1910.134

Under OSHA, Title 29 Code of Federal Regulations Part 1910, section 134, Fit Testing Procedures (Mandatory), provides practical guidelines for the proper selection, fit testing, and seal check for respirators. ANSI standards are also available that cover the testing procedures in greater detail.

Qualitative Fit Test Protocols

Isoamyl Acetate Protocol - Not appropriate for particulate respirators

Saccharin Solution Aerosol Protocol

First a taste threshold screening is performed to make sure the subject can taste saccharine. Subject will don an enclosure comparable to the 3M hood assembly with parts #FT 14 and #FT 15 combined. Respirator equipped with a particulate filter should be properly adjusted. A fit test solution containing 83 grams of sodium saccharine and 100 mL of warm water is sprayed into the enclosure with a nebulizer. The following fit test exercises are performed: (1) normal breathing, (2) deep breathing, (3) Turing head side to side as far as the subject is able to, inhaling at each side, (4) Moving the head up and down, inhaling at the "up" position, (5) Talking slowly and loudly enough to be heard by the test conductor. Saccharine mixture is sprayed into the enclosure every 30 seconds during this time. The subject alerts the test conductor if they detect any taste of saccharine and the test is failed. No detection of saccharine means fit is satisfactory.

Bitrex™ (Denatonium Benzoate) Solution Aerosol Qualitative Fit Test Protocol

This test is performed similar to the Saccharin Solution Aerosol Protocol except the fit test solution consists of 337.5 mg of Bitrex to 200 mL of a 5% salt (NaCl) solution in warm water.

Irritant Smoke (Stannic Chloride) Protocol

For this test, the respirator used should be equipped with a high efficiency particulate air (HEPA) or P100 series filter. No enclosure or hood is used. Subject dons respirator and is instructed to keep eyes closed. A stream of smoke is distributed (via a low flow air pump set to deliver 200 milliliters per minute or an aspirator squeeze bulb) 12 inches from the facepiece around the whole perimeter of the mask. If no irritant smoke is detected, the test proceeds. The fit test exercises described above are then performed. If irritant smoke is detected at any time, the fit test fails.

ANSI Z88.2 "Respiratory protection"

This standard provides guidance on the proper selection, use, and care of respirators, and contains requirements for establishing and regulating respirator programs. It is primarily directed toward persons who are directly responsible for ensuring proper respiratory protection programs, and is therefore not intended to be used in certifying a particular respiratory device. The standard is still applicable to PAPRs, however, in that a certified PAPR must still comply with the guidelines set forth within the document.

ANSI Z88.4 "Safety guide for respiratory protection against coal mine dust"

This standard provides recommended procedures for respiratory protection from coal mine dust inhalation. Coal dust concentration is identified as the basis for selection of respiratory protective devices, and the standard makes reference to the Federal Register, Subpart O, Part 70 "Mandatory Health Standards- Underground Coal Mines," in which coal dust concentration standards are established. These standards may be particularly applicable to multifunction PAPRs because of their utility and convenience in mining operations. Specific requirements stated in 30 CFR 70.100.

30 CFR 70.100

Title 42 Code of Federal Regulations Part 70, section 100, Respirable dust standards gives an average exposure of 2.0 milligrams of respirable dust per cubic meter of air inside the active workings of each mine

ANSI Z88.7 "Color coding of air purifying respirator canisters, cartridges, and filters"

This standard seeks to facilitate rapid identification of filtering devices by employing a color coding scheme that is consistent among respirator manufacturers.

Table 1 is given in the document as a guideline for color assignments according to atmospheric contaminants. The standard requires that the color of the label must be clearly visible from a distance of 1 m, must cover at least 75% of the filtering device or container, and must be resistant to peeling, fading, bleaching, and blistering.

ANSI Z88.10 "Respirator fit testing methods"

Specific testing procedures are covered in this standard, and are intended to assist wearers in selecting the appropriate respirator. The standard outlines several tests that may be used to check the seal and fit of respirators using taste, touch, and smell. Each test is performed by allowing the wearer to don the respirator and then exposing the wearer to a test chemical. If the wearer is able to sense the chemical inside the face piece of the respirator, then the fit is insufficient to protect the wearer from airborne contaminants. The following is a summary of the four main tests that are employed in assessing the fit of respirators:

Fit test method	test	chemical agent
Smell	Odor test	Isoamyl acetate
Taste	Sweetener aerosol	Sodium saccharine
	Bitter aerosol	Denatonium benzoate
Feeling	Irritating aerosol	Stannic chloride

International standards

BS EN 136 "Respiratory protective devices – Full face asks – Requirements, testing, marking"

BS EN 143 "Particle filters used in respiratory protective equipment"

BS EN 12941 "Respiratory protective devices – Powered filtering devices incorporating a helmet or hood – Requirements, testing, marking"

JIS T 8157 "Powered air purifying respirators (PAPR)"

3. Eye and Face Protection Standards

29 CFR 1910.133

Under OSHA, Title 29 code of Federal Regulations Part 1910, section 133(b)(1), Eye and face protection, provides guidelines for the selection of eye and face personal protective equipment, and requires that such equipment purchased after July 5, 1994 must comply with ANSI Z87.1 "Eye and Face Protection.

The employer is required to ensure that workers use appropriate face and eye protection when hazards such as flying particles, molten metal, liquid chemicals, acids or caustic liquids, chemical gases or vapors, or potentially injurious light radiation are present. (133(a)(1)) Workers are further required to wear eye protection that provides side protection when flying objects are present. (133(a)(2)).

Workers are expected to wear their prescription lenses along with their eye and face equipment. This may be accomplished either by wearing eye protection that incorporates the prescription into the lens, or by wearing the equipment over the worker's prescription lenses. If the latter option is selected, the protective equipment must not interfere with the proper fit of the prescription lenses.

Workers must use filter lenses that have a shade number appropriate for the type of light radiation present. A table is provided that gives minimum protective shade numbers for various activities that entail exposure to harmful light radiation.

ANSI Z87.1 "Practice for occupational and educational eye and face protection"

This standard provides minimum requirements for eye and face protective devices and guidance for the selection, use, and maintenance of these devices. In order for a device to claim compliance with the standard, the device must meet all requirements set forth in the standard.

The testing procedures outlined in the standard utilize the Alderson 50th percentile male headform under normal laboratory ambient conditions unless otherwise specified. Compliance with the standard requires that the device be put through a battery of tests for physical and optical performance. Criteria and interpretation of test results are given for different types of devices, such as goggles, lenses, and face shields. An overview of tests follows:

- High velocity impact test. The test is designed to assess the level of protection provided from high velocity, low mass projectiles. Steel balls (6.35 mm, 1.06 g) are used to impact the lens of the device at several locations, with a total of 20 impacts for the entire device. If more than one of the trials results in failure, then the device fails.
- High mass impact test. The test is intended to assess the level of protection provided from high mass, low velocity projectiles. A missile with a heat-treated steel tip (30^{o} conical tip, 500 g, mm diameter) is used in the test, and is dropped from a predetermined height. Four trials are completed, and failure of any one of them indicates failure of the device.

- Flammability resistance. The test is intended to measure the resistance of the device to sustaining flame after it has been ignited. Ignition time (the time a fire source must be in contact with the protector that is required to sustain burning) is measured using a Bunsen burner with a 50 mm blue flame and 25 mm inner cone.
- Optical test methods. These tests include a test for prismatic power, refractive power, astigmatism, definition, prism imbalance, haze, and transmittance.
- There is a NIOSH Haze, Luminous Transmittance and Abrasion Resistance in statement of standard for CBRN Full Facepiece Air Purifying Respirators, Rev 2 April 4, 2003 section 3.7.
- Corrosion-resistance test for metal parts. The test is performed by submerging the device in boiling 10% sodium chloride solution, followed by immersion in room temperature 10% sodium chloride solution. The device is allowed to dry for one day, and is then rinsed and examined for corrosion.

International standards

AS/NZS 1337 "Industrial eye and face protection"

DIN/BS EN 166 "Personal eye protection- specifications"

DIN/BS EN 167 "Personal eye protection- optical test methods"

DIN/BS EN 168 "Personal eye protection- non-optical test methods"

This standard provides a method for testing resistance to fogging of oculars. Fogging may be an important test parameter for multifunction

PAPRs, as they are likely to be used in environments like mines that have cool ambient conditions and in which condensation would be likely to occur.

ISO 4849 "Personal eye protectors- specifications"

ISO 4854 "Personal eye protectors- non-optical test methods"

ISO 4856 "Personal eye protectors- synoptic tables of requirements for oculars and eye protectors"

4. Cranial Protection Standards

29 CFR 1910.135

Under OSHA, Title 29 Code of Federal Regulations Part 1910, section 135, Head Protection, requires that protective helmets be used in environments where there is a risk of head injury from falling objects, and requires that such equipment purchased after July 5, 1994 must comply with ANSI Z89.1. It further requires the use of helmets that reduce the risk of electric shock if the wearer is anticipated to work in such an environment.

ANSI Z89.1 "Industrial head protection"

The standard describes the types and classes, materials, physical and performance requirements, and tests for protective helmets. It establishes minimum performance requirements for protective helmets to reduce force of impact and penetration, and also gives requirements for protection from high voltage electric shock. Partial use of the standard is prohibited, and any device claiming compliance with the standard must meet all requirements. Helmets meeting the requirements of the standard are intended to provide protection against one blow.

The standard gives physical requirements for the construction of safety helmets. Specifications for headbands, sweatbands, crown straps, protective padding, accessories, chin straps, winter liners, and mounting brackets are detailed. Markings are required to be printed on the helmet giving the manufacturer's name, date of manufacture, the American National Standard Designation, type and class designations, and the approximate headband size range. Criteria and interpretation of test results are given for each certification test. An overview of tests follows:

- Flammability. A flame (as described in the flammability test for lenses) is applied to the helmet for five seconds, and inspected for continued burning after five seconds of removal (section 9.1). No flame shall be visible 5 seconds after removal of the test flame (section 7.1.1).
- Force transmission. In this test, the helmets being tested are preconditioned for hot and cold, and are placed one at a time on a headform that records force transmission. An impactor is then dropped on the helmet from a height that produces an impact velocity of 5.5 m/s. Averages are taken over each preconditioning group. (Section 9.2) Helmets shall not transmit a force to the test headform in excess of 4450 N (1000 lbf). Averaged values of the maximum transmitted force of individual test samples cannot exceed 3780 N (850 lbf).
- Apex penetration. In this test, the helmets are preconditioned as above and placed on a headform. The impactor (1.0 kg) must have a steel tip, and must impact the helmet at 7.0 m/s. The headform is designed such that if penetration of the helmet occurs, an electronic sensor on the headform is

activated. (Section 9.3) "The penetrator shall not make contact with the top of the test headform under any of the test conditions specified" (section 7.1.3).

- Off center penetration. The test above is repeated with impact occurring above the dynamic test line but not at the helmet apex. (Section 9.5) "For each condition specified, the penetrator shall not make contact with the test headform when struck anywhere above the DTL." (Section 7.2.2)
- Impact energy attenuation. In this test, the helmet is mounted on a headform with an electronic force sensor and dropped from a height resulting in a velocity of 3.5 m/s at impact. The maximum G value for each test is recorded. (Section 9.4) They cannot exceed 150 (section 7.2.1).
- Chin strap retention. Deflection of the helmet after impact is measured. (Section 9.6). "The chin strap needs to remain intact such that the loading device does not become detached during the test and the residual elongation of the chin strap does not exceed 25 mm (1.0 in.)." (Section 7.2.3).
- Electrical insulation. The helmet is filled with tap water up to the static test line, and then placed in a bath of tap water up to the level of the same line. A voltmeter and milliammeter are then used to measure the current leakage through the helmet when a voltage of 2200 V is applied. (Section 9.7). Class E helmets need to be able to withstand 20,000 volts, AC, 60

Hz, for 3 minutes with maximum leakage of 9 milliamperes. (Section 7.2.1).

International standards

AS/NZS 1801 "Occupational protective helmets"

BS EN 397 "Specifications for industrial safety helmets"

ISO 3873 "Industrial safety helmets"

5. Intrinsic Safety Standards

30 CFR 18.68

Under MSHA, Title 30 Code of Federal Regulations Part 18, section 68, provides requirements for electronic device components for use in environments where air composition may increase the likelihood of explosions, as in underground mines. Components affecting intrinsic safety must meet the following requirements:

- Current limiting components shall consist of two equivalent devices, and shall not be used at greater than 50% of their maximal rating.
- Reliable materials must be used for components, and they must be mounted as to mitigate shock and vibration during normal use.
- Semiconductors must be amply sized. Rectifiers, transistors, and Zener diodes are given limitations.
- Electrolytic capacitors may not be used at greater than 2/3 of their rated voltages.
- If failure of one component occurs, the circuit must remain intrinsically safe.

- The circuit will be considered intrinsically safe if during the course of testing no ignition occurs. Testing procedures for intrinsic safety are outlined in the CFR.

6. Hearing Protection Standards

29 CFR 1910.95

Under OSHA, Title 29 Code of Federal Regulations Part 1910, section 95, provides methods for measuring the adequacy of hearing protector attenuation. The standards for hearing protection differ somewhat from standards for other personal protective devices in that they base compliance on testing the devices as workers use them in their work environment. The devices are therefore not pre-certified by completing a series of tests successfully in a laboratory setting. Rather, compliance is determined by calculating a time-weighted average (TWA) for sound exposure based on the amount of exposure to noise in the workplace. The standard gives computational methods for determining a worker's time weighted average for noise exposure.

Appendix B of this CFR indicates that employees must wear hearing protection that is able to reduce their TWA to 85dBA. It further specifies that employers must select a method outlined in the document to estimate the adequacy of hearing protector attenuation, and suggests that the most convenient method is the Noise Reduction Rating (NRR) developed by the Environmental Protection Agency (EPA). Detailed methodology is provided.

ANSI S12.6 "Method for measuring the real-ear attenuation of hearing protectors"

This standard provides laboratory-testing procedures for measuring, analyzing, and reporting the noise reduction capabilities of hearing protection devices. Two

measurement methods are provided; the "experimenter supervised fit" and the "subject fit". The former method is intended to describe the upper limits of hearing protector performance and is intended for ideal laboratory conditions. The latter is conducted with subjects who are naïve with respect to the use of hearing protection and takes into consideration human factors and real world considerations. For the experimenter supervised fit, subjects are given precise instructions and are aided in fitting the device. For the subject fit, the experimenter does not give the subject any assistance.

Detailed testing procedures are provided in the standard that may be used to rate the capabilities of the hearing protection device; however, this standard is not intended to certify the device. Rather, devices must comply with 29 CFR 1910.95 in the context of the individual work environment.

ANSI S12.19 "Measurement of Occupational Noise Exposure"

This standard provides testing methods that may be used to measure the noise exposure received in the workplace. All types of noise may be assessed using the methodology, including continuous, fluctuating, intermittent, and impulse/impact. Measurements are given as sound levels and durations, TWA's, or noise doses. The standard gives examples for how to calculate noise exposure as a TWA.

ANSI S12.42 "Microphone in real ear and acoustic test fixture methods for the measurement of insertion loss of circumaural hearing protection devices."

This standard provides methods for measuring insertion loss in circumaural earmuffs, helmets, and communication headsets. Two methods are provided; the measurements may be made on human subjects or on a test fixture. Procedures are provided for locating ear-mounted microphones and hearing protection devices to

measure sound pressure levels in the ear, and methods are given to calculate insertion loss values.

7. Other Applicable Standards

Statement of Standard for CBRN Full Facepiece Air Purifying Respirator (APR), Section 4.6, 4 April 2003, Communications

This standard states that a performance rating of seventy percent or greater on a Modified Rhyme Test (MRT) is needed to meet the communications requirement. A steady background noise of 60 dBA of broadband "pink" noise is used for the MRT and a distance of 3 meters between listeners is required.

ANSI S3.2 "Method for measuring the intelligibility of speech over communication systems"

This standard gives methods for the assessment of speech intelligibility of monosyllabic words over communication systems using pre-prepared word lists. While this standard is specifically intended for communication systems, it may also be applicable for assessing verbal communication limitations imposed by respirators. In the case of a multifunction PAPR, this issue may be particularly important due to the sound attenuation properties of the hearing protection components and the additional noise exposure of the wearer by the blower fan located within the helmet. Limited verbal communication may place the wearer in a compromised situation in terms of safety (if instructions cannot be heard) or may limit productivity (if collaborative conversation is limited).

Application of this standard, or of a unique but similar standard designed specifically for respirator assessment, may mitigate the problems associated with limited

communication ability imposed by the respirator. A new standard may also wish to include visual communication tests (hand signals), or a combination of visual and auditory tests. Devices tested under such a standard should be donned in the manner specified by the manufacturer, particularly with regards to the placement of the earmuffs and face piece. The blower fan should be on, and the unit should be fully charged during testing.

APPENDIX 2

Exercise Performance While Wearing a Tight-Fitting Powered Air Purifying Respirator with Limited Flow

Arthur T. Johnson

Kathryn R. Mackey

William H. Scott

Frank C. Koh

Ken Y.H. Chiou

Stephanie J. Phelps

Biological Resources Engineering

University of Maryland

College Park, MD 20742

USA

Telephone: 301-405-1184

Fax: 301-314-9023

E-mail:aj16@umail.umd.edu

Abstract:

Sixteen subjects exercised at 80-85% $\dot{V}0_2$ max on a treadmill while wearing a tight-fitting FRM40-Turbo Powered Air Purifying Respirator (PAPR). The PAPR was powered by a dc power supply to give flow rates of 0%, 30%, 66%, 94%, and 100% of rated maximum blower capacity of 110 L/min. As flow rate was reduced, so was performance time. There was a 20% reduction in performance time as blower flow changed from 100% to 0% of maximum. Significant differences in Breathing Apparatus Comfort and Facial Thermal Comfort were found as flow rate varied.

Introduction

Powered air purifying respirators (PAPR) are the protection of choice for a broad range of wearers and tasks. They have the advantages of requiring less inspiratory effort to draw air across the filters, and of blowing cooling air across the face in warm environments. As long as pressure inside the facepiece remains positive, protection provided by a PAPR should exceed that of a non-powered air purifying respirator (APR); faceseal and expiratory valve leakage should be of little consequence.

As long as respiratory flow rates do not exceed blower flow rates, apparent inspiratory resistance of a PAPR should be slightly negative. That is, breathing in the PAPR should be easier than it would be if just inhaling without wearing a respirator. The positive pressure inside the facepiece assists the respiratory muscles to draw air into the lungs.

The same effect that assists inspiration works against expiration. So, PAPRs should make it somewhat harder to exhale than if no respirator were being worn. This effect would most likely be more noticeable at rest than during strenuous work because exhalation at rest is nearly passive (no active muscle contraction is involved for exhalation at rest) but exhalation during work is active (abdominal muscles contract to push air out). Exhaling against a positive pressure is easier and less noticeable if muscles can produce somewhat greater force to compensate for the increased pressure.

Based on anecdotal evidence, the increased exhalation pressure does not seem to cause a problem for wearers. This may be because of two factors: 1) PAPR may be worn mostly during strenuous work, when exhalation is active, and 2) the presence of the exhalation valve limits the positive pressure inside the facepiece to a low value (typically

2.6 cm H_20 at 85 Lpm). Of the two, the second is likely to be more important to PAPR wearers.

Peak flows during strenuous work are likely to exceed blower capacity. Also, PAPR worn for long periods of time are likely to have discharged batteries, and these would have less power to blow air to their full capability. In either case, overbreathing the air capacity of a PAPR blower is likely. What would happen in this case?

The answer is not easy to predict. Overbreathing the fan would cause the wearer to have to breathe through the resistance of the filter, fan, and tubing. How this resistance affects performance is not easy to determine.

Attempts to analyse this situation to predict the outcome of overbreathing a tight-fitting PAPR, demonstrate its complexity. In Figure 1 is shown an equivalent electrical schematic for the PAPR on a wearer. The blower is diagrammed as a pressure source, P_b, and the flow through the blower is given by $\dot{V}_b$. Resistance of the blower, filter, and tubing is indicated by the resistance labeled R_f. Blower flow can take one of two paths: it either is breathed ($\dot{V}_r$) or leaked through the exhalation valve ($\dot{V}_e$). The respiratory system of the wearer is represented by a pressure source (P_r) in series with respiratory resistance (R_r). The exhalation pathway is represented by a diode (allowing one-way flow only) and a resistance (R_e). Mask face piece pressure is given as the symbol P_m. For simplicity, the resistances R_f, R_r, and R_e, and the blower pressure P_b are assumed to be constant.

All flows flowing into the node marked P_m are defined as positive. In actuality, $\dot{V}_e$ will be negative and $\dot{V}_r$ will be bipolar. With these definitions and conventions, a series of equations can be written:

$$\dot{V}_b + \dot{V}_r + \dot{V}_e = 0 \qquad (1)$$

$$\dot{V}_r = \frac{P_r - P_m}{R_r} \qquad (2)$$

$$\dot{V}_b = \frac{P_b - P_m}{R_f} \qquad (3)$$

$$\dot{V}_e = \frac{-P_m}{R_e} \qquad \text{for } P_m > 0 \qquad (4a)$$

$$\dot{V}_e = 0 \qquad \text{for } P_m \leq 0 \qquad (4b)$$

There are two flow domains of interest: 1) no overbreathing ($P_m > 0$), and 2) overbreathing ($P_m \leq 0$). The condition of no overbreathing includes exhalation and some part of inhalation. Overbreathing only occurs during strong inhalation.

Algebraic manipulation yields the following for face piece pressure:

$$P_m = R_e\,(\dot{V}_b + \dot{V}_r) \qquad \text{no overbreathing} \qquad (5)$$

$$P_m = P_b + \dot{V}_r\,R_f \qquad \text{overbreathing} \qquad (6)$$

and respiratory pressure:

$$P_r = \dot{V}_r\,R_r + R_e(\dot{V}_b + \dot{V}_r) \qquad \text{no overbreathing} \qquad (7)$$

$$P_r = P_b + \dot{V}_r(R_r + R_f) \qquad \text{overbreathing} \qquad (8)$$

One effect of overbreathing is to shift the reference pressure for both P_r and P_m from atmospheric ($P = 0$) to blower pressure (P_b).

The results of this analysis are diagrammed in two graphs of Figure 2. The upper graph shows facepiece pressure plotted against the excess flow through the blower ($\dot{V}_b + \dot{V}_r$). Overbreathing occurs when excess flow becomes negative. Otherwise, no

overbreathing occurs when ($\dot{V}_b + \dot{V}_r$) is positive. The slope of the line is just R_e for the no overbreathing condition, but, for overbreathing, it changes gradually to R_f.

The lower graph plots respiratory pressure (P_r) against respiratory flow rate ($\dot{V}_r$). The slope of the line is $\frac{P_r}{\dot{V}_r} = \mathrm{R_r} + \mathrm{R_e}\left(1 + \frac{\dot{\mathrm{V}}_\mathrm{b}}{\mathrm{V_r}}\right)$ for no overbreathing, and gradually becomes

$(R_r + \mathrm{R_f})$ for overbreathing. Zero respiratory flow can only occur if respiratory pressure is maintained at a positive pressure of $P_r = P_m = -R_e \dot{V}_e$ (remember that $\dot{V}_e$ is negative with our sign convention). This graph shows that exhalation is performed against a positive pressure that changes with flow rate, and that at high enough overbreathing rates, filter resistance must be overcome by respiratory pressure.

The resistances detected by the respiratory system are given by the slopes of the lines drawn from the origin of the lower graph to the points on the curve where the respiratory flow rates appear. The exhalation resistance, drawn to $\dot{V}_{r1}$, is positive and decreasing somewhat as exhalation flow rate increases. The effective inhalation resistance is negative for flow rate $\dot{V}_{r2}$, zero at the point where $\dot{V}_r = \dot{V}_b$, and again positive for $\dot{V}_{r3}$. To make matters even more complicated, blower flow rate ($\dot{V}_b$) may exceed respiratory flow rate ($\dot{V}_r$) within part of each breath and $\dot{V}_b$ may be exceeded by $\dot{V}_r$ during other parts of the same breath.

Previous experimental results have shown that exercise performance times are affected by levels of inhalation [1] and exhalation [2] resistances. In both cases, as respirator resistance increased, performance time decreased linearly. So, the expectation

is that overbreathing a PAPR might effectively increase resistance, but by how much, and to what effect, is anybody's guess. For this reason, overbreathing of a tight-fitting PAPR was put to an experimental test.

Methods

Sixteen volunteer subjects participated in this study, which was approved by the University of Maryland Institutional Review Board. Table I gives demographics for the subjects.

An investigator met with the prospective participant to explain test procedures and methods. The participant was then provided with an informed consent document, a brief medical history form, and a Physical Activity Questionnaire. The participant was asked to complete a Physical Activity Readiness Questionnaire (PAR-Q), which determined whether vigorous activity was appropriate.

A maximal oxygen ($\dot{V}O_2$ max) consumption test was performed before experimental treatments were begun on all prospective participants using a Quinton (Bothell, WA) motorized treadmill. Participants were asked to warm-up and stretch for approximately 5-10 minutes prior to the start of the test. After the warm-up the participants donned a Hans Rudolph (Kansas City, MO) one-way breathing valve configured with a rubber adaptable mouthpiece. This apparatus was attached to a standard Fleisch #4 (Phipps & Bird, Richmond, WA) pneumotach and mass spectrometer to monitor continuous expired airflow. Heart rate measurement was assessed using a standard ECG electrode configuration with the leads connected to a Hewlett Packard (Palo Alto, CA) Monitoring System. The initial work rate was established at a speed and grade designed to elicit 70% of the participant's age-predicted maximal heart rate

(approximately 60% $\dot{V}O_2$ max). The work rate (speed and grade) was adjusted every third minute until the participant experienced volitional fatigue, failed to display a rise in oxygen consumption (150 mlO_2) in accordance with the increase in work rate, or exhibited cardiovascular responses that contraindicated walking further. Most subjects completed $\dot{V}O_2$ max in about 9-15 minutes.

How rate to the respirator was controlled with a variable voltage power supply in place of the battery. In Table II and Figure 3 are shown the steady flows resulting from manipulating power supply voltage. All flow rates were measured with a Fleisch #4 pneumotach inserted in the hose between the blower and unworn face piece. Flow rate conditions were assigned to each subject in balanced random (Latin square) order.

Each participant was asked to warm-up and stretch for approximately 5-10 minutes prior to the start of each experimental test session. Respirator face pieces were put on the subjects immediately after the warm-up. Face seals were checked for leaks by blocking the inhalation port without the blower hose. Straps were adjusted for comfort and to eliminate leaks. All subjects wore the PAPR blower and filter (FR-57, 3M, St. Paul, MN) on their waists without the battery pack. The treadmill speed and grade were set at a work rate eliciting approximately 70% of the individual's age-predicated maximal heart rate. Electrodes were used to monitor heart rate continuously during the test. Work rate was slowly increased within 90 seconds to the speed and grade corresponding to 80-85% of the participant's maximal aerobic capacity as predetermined during the $\dot{V}O_2$ max test. Upon reaching the predetermined speed and grade, the timing was started. The participant was asked to exercise at this intensity until volitional fatigue. These

procedures were used in all conditions. Rating of perceived Exertion (RPE), Breathing Apparatus Comfort (BACS), Facial Thermal Comfort (FTC) and Overall Thermal Comfort (OTC) were used to objectively gage fatigue and comfort of the subject during each condition. These scales were assessed every two minutes. Each session took approximately 1 hour from start to the end of a five-minute cool down period of walking on the treadmill. All tests were conducted in an environmentally-controlled laboratory.

Results

Average performance time data appear in Figure 4. Performance times varied from 701 sec to 848 sec. There was a 21% difference from no blower flow to maximum blower flow. Paired-t tests showed statistically significant differences ($p=0.05$) between the 0% flow condition and either of the two highest flows.

In Table III is found a summary of other measurements. Breathing Apparatus Comfort (BACS), Rating of Perceived Exertion (RPE), Overall Thermal Comfort (OTC), Facial Thermal Comfort (FTC) and heartrate (HR) are given for termination and at the fourth minute into the test. We have found that termination values do not always discriminate among treatments, but sometimes values compared at some time before termination, when all subjects are still participating, do show differences. We have chosen to compare this measure taken at the fourth minute (240 sec).

As an example, consider the BACS, a scale that ranges from 0 (very, very uncomfortable) to 10 (very, very comfortable). Termination values of BACS discriminate between flow rate extremes, but are not overall statistically significant. The four-minute BACS is statistically significant at $p=0.05$ as determined by Analysis of

Variance (ANOVA). Paired t-tests indicate quite a few paired comparisons are statistically significant at p=0.5. The BACS value of 3.25 indicates "fairly uncomfortable", whereas the BACS value of 5.38 indicates 'fairly comfortable.'

The other statistically-significant effect is the FTC at four minutes. Facial thermal comfort ranges from 5.75 (warm) at 0% flow to 4.56 (neutral) at 100% flow. OTC at four minutes appears to have been affected somewhat by FTC at four minutes, although the face covers only 5% of body surface area. RPE and HR at termination differed little among flow rates. This indicates that subjects expended about the same amounts of effort for each flow rate, and demonstrates that performance times can be given credence.

The PAPR was tested on a Krug Life Sciences (San Antonio, TX) breathing simulator while the fan was powered by a 5 vdc power supply. The results are shown in Figure 5. There is a large similarity in shape between the pressure-flow characteristic measured on the Krug head form and the theoretical diagram shown in Figure 2. This demonstration supported the analysis given in the Introduction Section of this paper.

Discussion

The discussion in the introduction section summarizes what was known before testing began. Since there was no prediction of the experimental outcome, the results of this experiment cannot be said to conform to expectations. Nonetheless, it was anticipated that lower blower flow rates would cause the wearer to breathe through the filter resistance in increasing amounts. Based on previous studies, this would mean lower performance times. This informal anticipation was confirmed by the results.

As flow rate decreased, the beneficial effect for exhalation appears to be less than the detrimental effect for inhalation, so the overall effect is a performance penalty. Whether this penalty is significant in the workplace depends on many things. A 20% reduction in performance time for a 100% reduction in blower flow rate may not be important if the battery is maintained in a relatively high state of charge. However, during emergencies, when times of physical activity may be lengthened significantly, respiratory flow rates are higher than normal, and the luxury of battery recharge cannot be availed, then a 20% reduction in performance capability could be critical. It all depends on the situation.

Peak respiratory flow rates may be 400·L/min or more, depending on the person and the work rate. It is clear that this PAPR does not supply sufficient air to meet this demand. Hence, even if the battery is fully charged and the blower is working at full capacity, the wearer must expend some effort to breathe against the filter resistance. Judging from results from this study, some performance penalty could be expected.

The reason for PAPR wear preference is illuminated by the BACS and FTC scores. PAPR are significantly cooler and more comfortable, giving the wearer more capacity to work. If the wearer feels better, she or he will probably have a better attitude toward the work being done. If ambient air is not at a comfortable temperature, as it was in our laboratory (18-20°C), the cooling effect of the blower air might be more or less dependent on ambient temperature. However, evaporation of facial sweat could still be very important. The Speilberger State-Trait Anxiety Inventory (STAI) was given to the subjects before and after each session (Table IV). State anxiety increased for all flow

rates, but no differences achieved statistical significance. The smallest pre-post differences were for the highest flow rates.

Although the conditions of this study were not those expected in an actual workplace environment, the results can be useful nevertheless. A battery that dies completely and shuts off the blower is not likely to happen in a well-regulated environment, but all devices are inclined to fail at some time. As anyone who has needed a flashlight knows, the light often seems to go out when it is needed the most. The same is true of batteries in cars.

When conducting a scientific experiment, the protocol needs to be most sensitive to the anticipated effects of the treatments. We usually test at 80-85% $\dot{V}O_2$ max when we want to see whether treatments primarily affect the respiratory system. Likewise, we impose extreme conditions to reduce the relative importance of natural variation in responses. Overall trends are much easier are much easier to see if noise is relatively small. One can reduce relative noise by either using a very homogeneous group of subjects and testing procedures (not easily done), or by imposing a wide range of treatment levels. The latter is a common approach.

Conclusions

1. When flow rates are not adequate, there is a performance decrement.
2. Reducing blower air flow rates decrease PAPR comfort and facial cooling.

Funding source

This work was funded in part by the National Institute for Occupational Safety and Health (NIOSH Contract 200-2002-00531). The results published herein are solely the responsibility of the authors.

References

1. Johnson, A.., W.H. Scott, C.G. Lansted, M.B. Benjamin, J.M. Coyne, M.S. Sahota, and M.M. Johnson; Effect of Respirator Inspiratory Resistance Level on Constant Load Treadmill Work Performance, Amer. Ind. Hyg. Assoc. J. 60: 474-479 (1999).

2. Caretti, D.M., W.H. Scott, A. T. Johnson, K.M. Coyne, and F. Koh; Work Performance When Breathing Through Different Respirator Exhalation Resistances, Amer. Ind. Hyg. Assoc. J. 62:411-415 (2001).

Table 1. Subject Demographics

Gender	8 males, 8 females	
Age (y)	24.73±	5.66
Mass (kg)	67.61±	14.52
Height (cm)	168.40±	8.74
Maximal Oxygen Consumption (L/min)	2.66±	0.79
Maximal Heart Rate (bpm)	192.62±	9.13
Trait Anxiety	34.5±	9.69

Table II. Voltages and the corresponding flow rates produced by the tight fitting PAPR and the corresponding Percentages

Volts	Flow Rate (L/min)	Percent Max Flow Rate
4.8	109.82	100%
4.5	103.46	94%
3.28	72.11	66%
1.86	33.24	30%
0	0	0%

Table III. Summary of Test Data

Flow Rate (L/min)	0	33	72	103	110
Performance Time (sec)	701[a] ±477	683[b] ±367	790 ±492	772 ±365	848[a,b] ±122
BACS (Term)	1.75[a] ±0.48	1.50[b] ±034	2.00[c] ±0.45	2.25 ±0.51	3.00[a,b,c] ±0.55
BACS* (4 min)	3.25[a,b,c] ±0.48	3.60[d,e,f] ±0.45	4.25[a,d,g] ±0.36	4.62[b,e,h] ±0.40	5.38[c,f,g,h] ±0.54
RPE (Term)	17.7 ±0.53	18.1 ±0.28	18.3 ±0.30	18.1 ±0.29	18.2 ±0.25
RPE (4 min)	14.8[a] ±0.63	14.5 ±0.49	14.2 ±0.53	14.2 ±0.41	14.1[a] ±0.59
OTC (Term)	6.12 ±0.22	6.12 ±0.20	6.31 ±0.18	6.31 ±0.22	6.12 ±0.22
OTC (4 min)	5.25[a] ±0.23	5.27[b,c] ±0.23	5.12 ±0.22	4.88[b] ±0.26	4.69[a,c] ±0.28
FTC (Term)	6.44 ±0.18	6.62 ±0.12	6.44 ±0.18	6.38 ±0.29	6.31 ±0.28
FTC* (4 min)	5.75[a,b,c] ±0.21	5.47[d,e,f,h] ±0.24	5.06[a,d,g] ±0.25	4.75[b,e,g] ±0.27	4.56[c,f,h] ±0.27
HR (Term)	184[a] ±2.6	183 ±3.0	185 ±2.9	186 ±2.6	189[a] ±3.4
HR (4 min)	178[a] ±2.3	173[b] ±3.8	175 ±2.8	177[b,c] ±2.3	179[a,c] ±3.1

*Denotes overall statistically significant effect at p=0.05 from ANOVA.
Superscript letters indicate statistically significant pairs at p=0.05 from paired t-test.

Table IV. Average State Anxiety Scores Before and After Each Test Session

PAPR Flow Rates (L/min)	STAI		Significance Level
	Pre	Post	
0	34.47 ± 6.85	37.40 ± 9.02	0.16
33.24	34.00 ± 7.09	37.75 ± 10.29	0.12
72.11	32.38 ± 7.80	36.94 ± 8.43	0.06
103.46	33.81 ± 8.44	36.50 ± 9.56	0.20
109.82	33.40 ± 9.96	33.80 ± 8.74	0.45

Figures

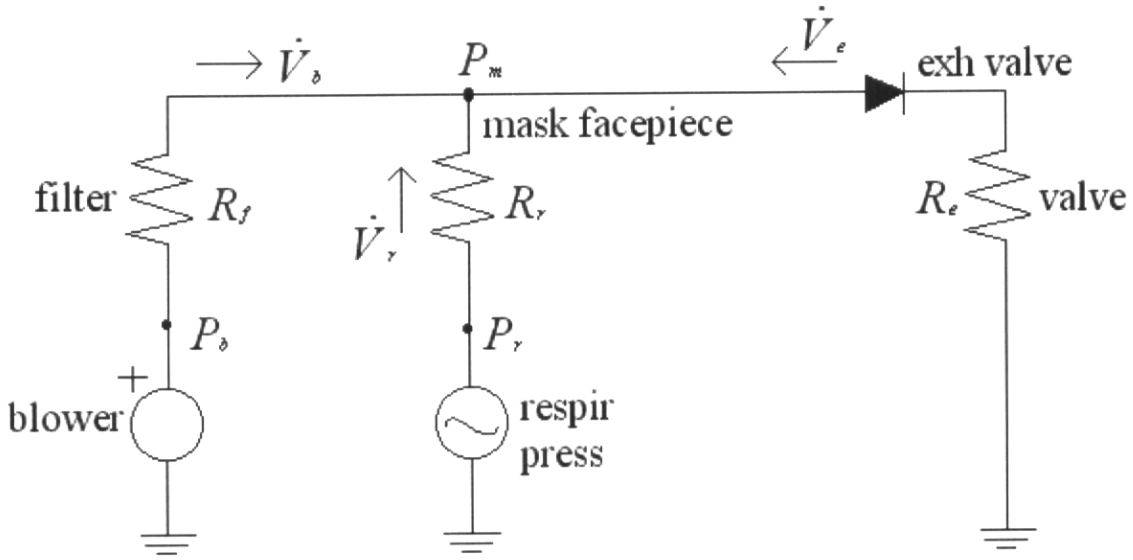
$\dot{V}_b$
P_m
$\dot{V}_e$
exh valve
mask facepiece
filter
R_f
$\dot{V}_r$
R_r
R_e
valve
P_b
P_r
+
blower
respir
press

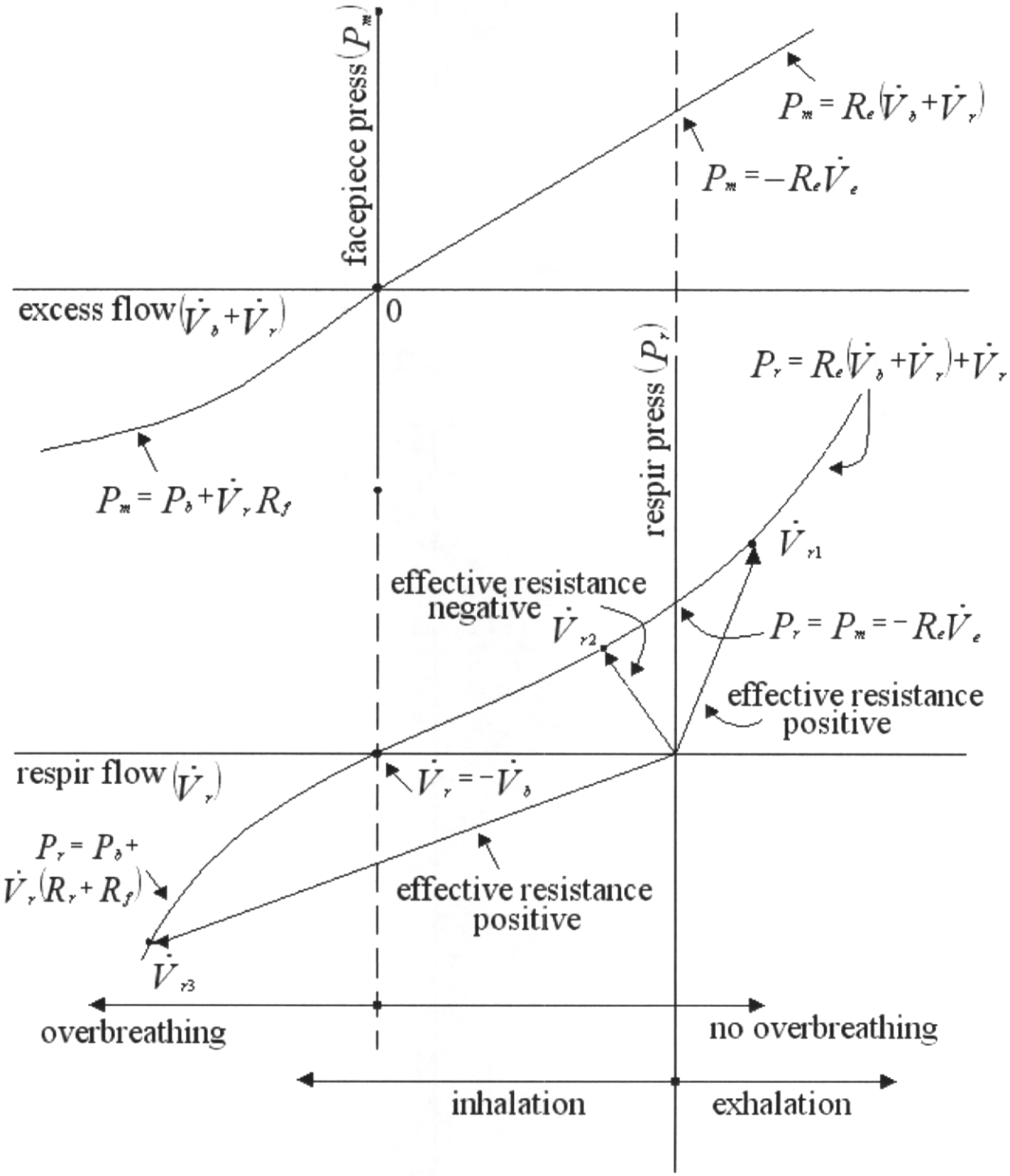
facepiece press (P_m)
$P_m = R_e(\dot{V}_b + \dot{V}_r)$
$P_m = -R_e\dot{V}_e$
excess flow $(\dot{V}_b + \dot{V}_r)$
0
respir press (P_r)
$P_r = R_e(\dot{V}_b + \dot{V}_r) + \dot{V}_r$
$P_m = P_b + \dot{V}_r R_f$
$\dot{V}_{r1}$
effective resistance negative
$\dot{V}_{r2}$
$P_r = P_m = -R_e\dot{V}_e$
effective resistance positive
respir flow $(\dot{V}_r)$
$\dot{V}_r = -\dot{V}_b$
$P_r = P_b + \dot{V}_r(R_r + R_f)$
effective resistance positive
$\dot{V}_{r3}$
overbreathing
no overbreathing
inhalation
exhalation

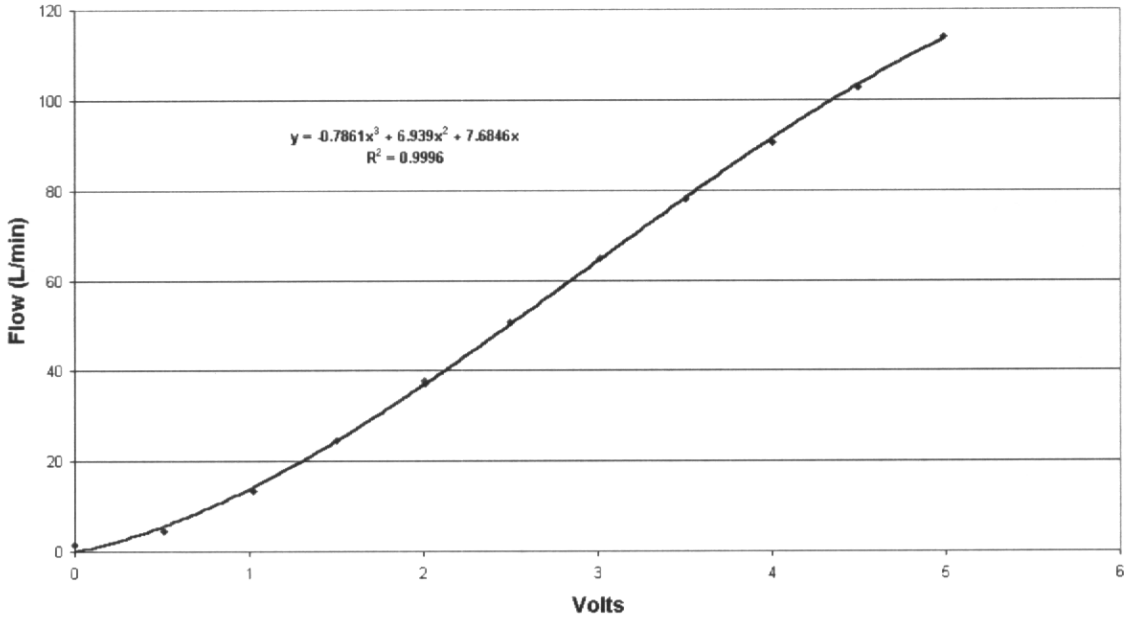
y = -0.7861x³ + 6.939x² + 7.6846x
R² = 0.9996
Flow (L/min)
Volts
0
20
40
60
80
100
120
0
1
2
3
4
5
6

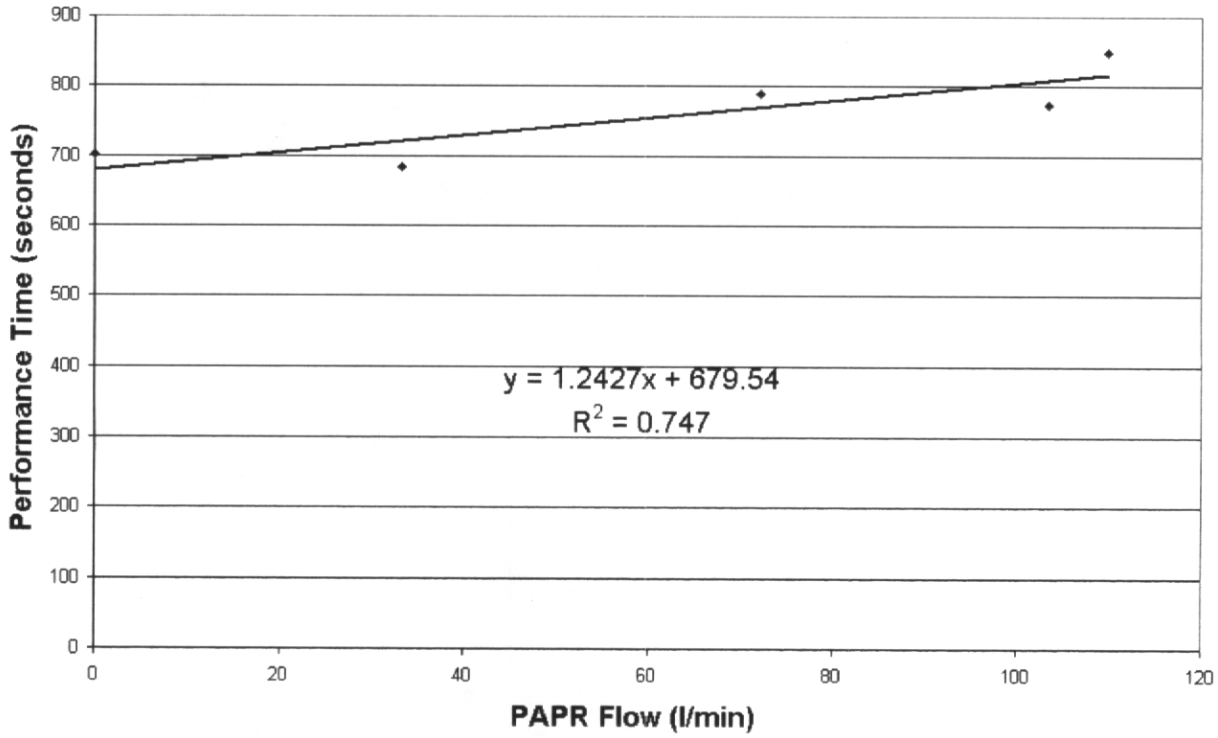
Performance Time (seconds)
900
800
700
600
500
400
300
200
100
0
0
20
40
60
80
100
120
PAPR Flow (l/min)
y = 1.2427x + 679.54
R2 = 0.747

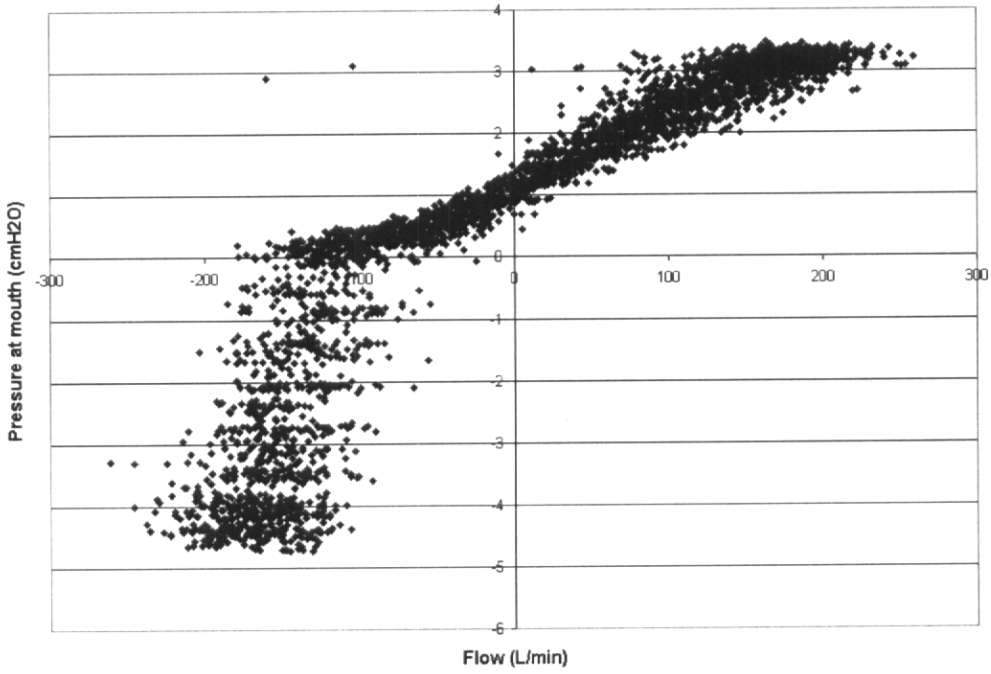
Pressure at mouth (cmH2O)
4
3
2
1
0
-1
-2
-3
-4
-5
-6
-300
-200
-100
0
100
200
300
Flow (L/min)

APPENDIX 3

Overbreathing a Loose-Fitting PAPR

Katherine R. M. Mackey
Arthur T. Johnson*
William H. Scott
Frank C. Koh

Biological Resources Engineering
University of Maryland

Timothy R. Rehak
National Institute for Occupational Safety and Health

*corresponding author:
Arthur T. Johnson
Biological Resources Engineering
University of Maryland
College Park, MD 20742
tel: 1-301-405-1184
email: ajohnso2@umd.edu

Abstract:

Loose fitting powered air purifying respirators (PAPRs) utilize a motorized fan to draw air through the respirator's air purifying elements, delivering clean air to the wearer through a facepiece that does not form an airtight seal with the wearer's face. Potential for wearer exposure to contaminants may exist if the breathing rate of the wearer exceeds the airflow rate supplied by the PAPR fan. In such an instance, ambient air could bypass the filters and enter the mask, potentially exposing the wearer to contamination. Cumulative dose depends on total volume overbreathed. This investigation assesses the extent to which overbreathing occurs in the Centurian MAX loose fitting PAPR. Fourteen subjects exercised at 80-85% $\dot{V}O_2$ max on a treadmill while wearing the PAPR inside a Portable Breathing Chamber (PBC). All subjects inhaled more air than was supplied by the PAPR blower, but only one of them exceeded the 1.4 L dead volume of the PAPR facepiece. Analysis of the one subject's data showed that potential contaminant exposure due to overbreathing would not likely have led to development of Coal Workers' Pneumoconiosis.

Introduction

Powered air purifying respirators (PAPRs) are respirators equipped with a blower and battery pack assembly that draw ambient air through the respirator filters and deliver it to the wearer via the facepiece. The PAPR design is intended to supply clean, breathable air to the wearer without relying on the inhalation of the wearer, thereby decreasing respiratory fatigue and increasing wearer comfort. Various types of facepieces are compatible with PAPRs, including half and full tight-fitting facepieces, as well as loose fitting hoods and helmets.

A significant benefit offered by both tight and loose fitting PAPRs is the reduction in inhalation resistance that the wearer experiences during tasks requiring work at 80-85% of their maximal oxygen consumption. During tasks occurring in this range, the wearer is most sensitive to respiratory stress[1]. Performance time at this work rate has been found to decrease linearly with increasing filter resistance[2]. A PAPR could therefore improve performance time by decreasing the amount of inhalation resistance experienced by the wearer.

Loose fitting PAPRs offer certain additional benefits to the wearer, including compatibility with facial hair and various facial structures. They may induce less feelings of claustrophobia in wearers, and they can be overbreathed without additional effort. In the case of helmet-style PAPRs, cranial protection is an additional benefit to the wearer that may be useful for tasks that carry the risk of head injury, as in mining or construction.

Most PAPR blowers supply a relatively constant airflow rate regardless of the breathing rate of the wearer. At fairly light work rates the wearer's breathing rate is likely to be less than the airflow rate supplied by the PAPR blower. However, at higher work rates the breathing rate may meet or exceed this airflow rate. When the wearer's breathing rate exceeds the blower

airflow rate, "overbreathing" of the PAPR blower occurs. In a tight fitting PAPR the wearer overbreathes by drawing air through the filters using his/her own inhalation effort. In a loose fitting PAPR, ambient air may bypass the filters and enter the mask directly through spaces between the wearer's skin and the facepiece, increasing wearer exposure to contaminants.

Preliminary testing in our laboratory indicates that for exercise occurring at 80-85% of the wearers' maximal oxygen consumption, instantaneous breathing flow rates in excess of 400 L/min may be observed, even if average air flow rates remain low (unpublished data). As many PAPR design specifications only incorporate fan airflow rates in the range of 120 L/min, overbreathing may be a significant concern at these work rates.

Understanding the physiological compatibility of a wearer with loose fitting PAPR components (like blower speeds) becomes particularly important for wearers working at unpredictable rates. Workers in mining, construction, emergency rescue, and agriculture, among others, may be required to perform tasks at high work rates that elicit overbreathing. Exposure to contaminants may therefore become a risk for these individuals[3].

The Occupational Safety and Health Administration (OSHA) has established regulatory guidelines for exposure to certain contaminants in the workplace. These permissible exposure limits (PELS) are based on input from physiological data, laboratory testing, and industry concerns, among other factors, and are given either as time weighted averages (TWAs) for an eight-hour workday or as ceiling values. Tables for individual contaminants are given in the Code of Federal Regulations[3] under 29 CFR 1910.1000s subpart Z, tables z1, z2, and z3. Similarly, the American Conference of Governmental Industrial Hygienists (ACGIH) has established recommendations for threshold limit values (TLVs) to be used as guidelines in industry for exposure to hazards[4]. However, these values are not legal standards. The

permissible respirable dose of a contaminant may be identified from either a PEL or a TLV by assuming a breathing flow rate if the ambient concentration of a contaminant is also known.

Overbreathing of a loose fitting PAPR would result in some measurable volume of ambient air entering the breathing vicinity of the wearer. The wearer's dose of contaminant depends, therefore, on his/her breathing rate in excess of the airflow supplied by the PAPR fan, the contaminant concentration, and the duration of exposure. The purpose of this study, then, was to measure overbreathing in one type of loose fitting PAPR, and determine if the resulting potential exposure would yield a contaminant dose in excess of those determined to be safe in PEL and/or TLV recommendations.

Methods

Fourteen subjects were recruited to participate in this study from the University of Maryland, College Park student body. The study was approved by the University of Maryland Institutional Review Board, and all subjects gave their informed consent to participate. Subjects completed a medical history questionnaire prior to testing that was used to ascertain general health information, as well as to screen for individuals with cardiovascular or respiratory disease, as these conditions would preclude their safe participation in the study. All subjects were categorized as non-anxious by the Spielburger State-Trait Anxiety Inventory (STAI), which was administered prior to testing. Subject statistics are given in Table I.

$\dot{V}O_2$max *Pre-Test*

Prior to the start of the experiment, a maximal oxygen consumption test ($\dot{V}O_2$max test) was performed on each subject using a Quinton motorized treadmill and a modified Bruce incremental treadmill exercise protocol. Subjects were asked to warm-up and stretch for

approximately 5-10 minutes prior to the start of the test, and were then equipped with a Hans Rudolph one-way breathing valve configured with a rubber adaptable mouthpiece. This apparatus was interfaced with a standard Fleisch (Phillips and Bird, Richmond, VA) pneumotach and Perkin Elmer (Pomona, CA) model 1100 mass spectrometer to monitor continuous expired airflow.

The initial work rate was established at a speed and grade designed to elicit 70% of the participant's age-predicated maximal heart rate. The work rate was adjusted by increasing the treadmill grade and speed every third minute until the participant experienced volitional fatigue, failed to display a rise in oxygen consumption (150 mL O_2) in accordance with the increase in work rate, or exhibited cardiovascular responses that contraindicated further assessment.

Sub-maximal oxygen consumption values (80-85% of each subject's $\dot{V}O_2$max) and testing conditions (treadmill speed and grade) were obtained from this testing. Efforts were made for the subject to achieve the 80-85% $\dot{V}O_2$max values at a treadmill speed and grade that would allow them to walk rather than run on the treadmill. These precautionary measures were taken in order to minimize unnecessary jostling of the testing apparatus, connecting hoses, and measurement devices.

Experimental Testing

Experimental testing commenced several days after the $\dot{V}O_2$max test. Subjects wore the loose fitting Centurian MAX Powered Respiratory Helmet, E140ISEW USA (Martindale Protection, Norfolk, UK). A switch on the PAPR visor activated the blower when the visor was in the down position. The visor sometimes interfered with the Portable Breathing Chamber, PBC (described below), causing the blower to turn off during testing. To solve this problem, the power connection to the blower was modified to connect directly to a dc power supply

maintained at a voltage corresponding to the full-charge battery voltage of 4.5v. During testing of this PAPR, it was found that the battery discharged at a rate too fast to allow multiple tests without recharging, and that this had a large effect on blower flow rate (Figure 1). Use of the dc power supply eliminated battery discharge as a consideration for our measurements.

Over the PAPR, subjects wore a portable breathing chamber (PBC) that was designed and constructed specifically for this investigation. The PBC was constructed from a large (39cm high x 39cm dia) polyethylene cylindrical food container (Figure 2). The container was used in the upside-down position, so that the top of the container (lid) was located at the subject's neck and the bottom of the inverted container rested above the PAPR helmet. The lid had a 23cm diameter circular hole and a slit from the edge to the hole, so that it could fit around the neck of the subject (Figure 3). A rectangular (14cm x 62cm) hole cut in front of the PBC was sealed with a visor of clear polycarbonate to allow the subject to see while walking on the treadmill. A piece of foam rubber in the PBC top cushioned the PAPR helmet from the PBC. The weight of the PBC was 1.9kg and the weight of the PBC and PAPR combination used in this study was 3.6kg.

The PBC body had two inlet/outlet ports installed. One port located near the nape of the wearer's neck allowed ambient air to reach the blower through a tube fabricated from a flexible heavyweight plastic material attached to the PAPR helmet blower intake port. The second port was designed to measure air exchange with the atmosphere that did not go through the blower and filter. Of particular interest was any indication of inhalation air through this port, because this was air required by the subjects over and above that supplied by the blower. This air was measured with a Fleish pneumotach connected to the PBC by a 1 m long piece of flexible tubing. Pressure across the pneumotach was measured with a Validyne (Northridge, CA) DP15

differential pressure transducer. Most measurements were made with a Fleisch #4 pneumotach (resistance = 0.067 $cmH_2O.sec/L$); some were made with a Fleisch #3 pneumotach (resistance = 0.13 $cmH_2O.sec/L$).

The Fleish pneumotach and Validyne pressure transducer were interfaced with a personal computer. Data were logged and recorded at 25 Hz using custom-designed software developed in Labview (National Instruments, Austin, TX) and Microsoft Excel specifically for this study.

Each participant was asked to warm-up and stretch for approximately 5-10 minutes prior to the start of each test session. The subject then sat and was prepared for testing. Heart rate electrodes were applied, and the neck of the subject was encircled with a flexible plastic cylinder made from a thick, durable plastic bag with the bottom cut open. The circular opening in the PBC lid was adjusted around the subject's neck. The bag was taped to the neck with tightness similar to a necktie. While probably not a completely airtight seal, the seal around the neck did assure that all or almost all overbreathed air would be measured by the low-resistance pneumotach.

Both PBC and PAPR visors were treated with anti-fog spray. The PAPR was put on the subject and chin strap adjusted for comfort. The PAPR visor was pulled down to the operate position. The PBC was placed over the PAPR and both air connections made. The PBC bottom was sealed to the top, and an inspection was made for leaks. The dc power supply was connected and air began to flow.

Tests were conducted while subjects walked on a treadmill at 80-85% $\dot{V}O_2$ max. Treadmill speed and grade were set initially to elicit 70% of the subject's age-predicted maximal heart rate. Speed and grade were slowly increased to predetermined values for 80-85% of

$\dot{V}O_2$ max. Each participant was asked to exercise at this intensity for 6 minutes. Air flow data of interest occurred during the last three minutes, after steady-state had been reached.

Overbreathing this loose fitting PAPR would not be harmful to the wearer if contaminated air did not reach the mouth or lungs of the wearer (exactly where harm would come depends largely on the type of contaminant, if and where it is deposited or absorbed, and its potency). If air is assumed to reach the mouth from all directions inside the visor, then the full dead volume of the visor in front of the face can be considered to be a margin of safety against overbreathing. The dead volume of this PAPR was measured on a headform with all respirator cavities and the gaps between visor and headform taped shut. A known volume of dried lentils of known density was used to fill the visor dead volume. The weight of the lentils in the container after filling the dead volume was subtracted from the original weight of lentils in the container. The difference, when multiplied by lentil density, gave the facepiece volume of the PAPR on the headform as 1.4 L.

Results

Inhalation portions of breaths during the last three minutes of the tests were analyzed for the occurrences of various overbreathing flow rate values. These occurrences were classified into different ranges, and the percentages of flow rates that fell into each range were calculated for each subject. Results for different subjects differed considerably. All subjects exceeded PAPR fan capacity during their tests.

In Figure 4 are results averaged over all subjects. Graphed in the Figure are volumes inhaled per breath above the volume of air supplied by the blower (overbreathed volumes). Volumes were categorized into ranges, with the percentage of breaths with volumes in each

particular range given by the height of the bars. All subjects overbreathed the PAPR. Only one subject, however, overbreathed with some volumes exceeding the 1.4 L dead volume of the PAPR visor. Data for this subject appear in Figure 5. Overbreathing flow rate categories as an average for all subjects are given in Figure 6. All instantaneous flow rates were above 19 L/min, 30% were above the 60-79 L/min range, and a small proportion of flows were in the 260-279 L/min range.

Discussion

Results from this test demonstrate conclusively that wearers working at the high rate used in this test regularly overbreathe this loose fitting PAPR. One subject inhaled volumes greater than the measured dead volume of the PAPR, and so would be at risk for contaminant exposure.

The Centurion MAX PAPR tested in this study has been used in the mining industry because of its ability to filter particulates in the size range of coal dust, the added cranial protection afforded by the built-in helmet, and the cooling effect of the PAPR blower. Because mine workers are known to wear the type of respirator tested in this study, some exposure calculations have been explored.

The TLV[4] for coal dust is 2ppm, or 2mg/m^3. If the ambient concentration of respirable coal dust is 2 mg/m^3 or less, then the TLV requirement is satisfied regardless of whether respiratory protection is used or not. Hence, overbreathing of a loose-fitting PAPR in this ambient dust concentration will not result in a condition outside recommended limits. At least in this respect, our results indicate that the performance of this PAPR is automatically acceptable under conditions of low contamination.

It is likely, however, that mine dust samples do not represent the extremes that could be reached near the face of the seam or near coal-handling equipment. It is also possible that the allowable legal limit for coal dust in U.S. mines could be increased in the future. Thus, there is concern that the respirator provides sufficient protection of worker health even under these conditions.

To assess the lifetime consequences of overbreathing this PAPR, one must first determine the dose-response of breathing mine dust. The most serious consequence of prolonged mine dust inhalation is Coal Workers' Pneumoconiosis[5] (CWP). Although the cumulative dose leading to CWP may appear somewhere, we have yet to locate such information. Therefore, a dose estimate will be developed from contributing factors[6]. Pon et al.[7] included a table of the prevalence of CWP among 18,388 mine workers examined between 1996 and 2002. These data appear in Table II.

Cumulative dose of coal dust leading to CWP can be calculated from a conceptual model equation:

$$\text{dose} = \dot{V}_A \cdot c_c \cdot \text{rf} \cdot \text{PF}^{-1} \cdot \text{ret} \cdot \text{time} \qquad (1)$$

where dose = grams of coal dust retained in the lung

$\dot{V}_A$ = alveolar ventilation rate, L/min

c_c = ambient concentration of coal dust, g/L

rf = respirable fraction (5-10 microns or less)[8] of the coal dust, dimensionless

PF = protection factor of respiratory protection[8] dimensionless

ret = retention fraction of dust that reaches the alveolar level,

dimensionless

time = total exposure time, min

Alveolar ventilation rate ($\dot{V}_A$) is the rate of airflow to the farthest reaches of the lung. $\dot{V}_A$ can be calculated from[9].

$$\dot{V}_A = \dot{V}_E - V_D f_{br} \qquad (2)$$

where $\dot{V}_E$ = sustained minute ventilation rate, L/min

$\dot{V}_D$ = respiratory dead volume, L

f_{br} = breathing rate, breaths/min

From Johnson and Dooly[10], the minute ventilation rate that can be sustained for an 8-10 hour day is 22 L/min. Respiration rate for the same period of time is about 26/min. Respiratory dead volume is typically 0.180L. Thus, $\dot{V}_A$ = 17.32 L/min.

The coal mine dust standard is 2 mg/m^3. However, Attfield[11] presented evidence that 1.5 mg/m^3 might be a more realistic dust concentration. Thus, c_c is 1.5 x 10^{-6} g/L. All of this dust is respirable[12], thus rf is 1.0. Miners may or may not wear respiratory protection. It is likely that older workers, in particular did not wear respirators[13]. Thus, PF will be assumed to be 1.0, and ret will also be assumed to be 1.0 in order to reflect a maximal exposure estimate.

Exposure time estimation is based upon 10 hour days, 240 working days per year, and the number of years spent in the mine. Thus, time = 144 x 10^3 $\cdot$ yr , in minutes. The number of years was taken to be the longest working time in each category in Table II; the number of years for the last category was taken to be 30.

Calculated dosage estimates appear in Table II, and indicate that increased dosages incur higher risks for developing CWP, as expected.

Determining the risk of exposure to coal dust by overbreathing this PAPR can be accomplished in a similar manner, except the $\dot{V}_A$ term must be replaced by the volume of overbreathed air inhaled per breath, the number of breaths per minute, and the fraction of the time this high flow rate can be sustained during the day:

$$\text{dose} = (f_{br}\, f_w \sum f_v (V_I - V'_D)) \cdot c_c \cdot rf \cdot PF^{-1} \cdot ret \cdot time \qquad (3)$$

where all terms are identical to those in equations (1) and (2) except:

V_I = volume inhaled per inhalation, L

V'_D = dead volume of PAPR facepiece plus respiratory system, L

f_v = fraction of inhalation volumes in each volume category, dimensionless

f_w = fraction of time that work at 80-85% $\dot{V}O_2$ max can be sustained during the day, dimensionless.

For this analysis, the following assumptions will be made:

1. The miner achieves high inhalation volumes throughout his entire career.
2. Blower delivery rate remains constant.
3. No contamination reaches the wearer from the blower.
4. Contaminated air does not reach the wearer if inhalation overbreathing volume does not exceed facepiece dead volume.
5. Workers perform in cycles of 80-85% $\dot{V}O_2$ max for as long as possible, followed by minimum recovery times.
6. Overbreathing does not exceed dead volume during recovery.
7. The effect of the contaminant is cumulative.

For the subject whose data appears in Figure 5, 14% of overbreathed inhalation volumes were in the range of 1.40 – 1.59 L, and 2% of inhalation volumes were in the range of 1.60 – 1.79 L.

The midpoints of each of these ranges are 1.5 L and 1.7 L, respectively. Total dead volume is 1.6 L (1.4 L for facepiece and 0.18 L in the respiratory system). Hence, only the 2% of inhalation volumes in the rage of 1.60 – 1.79 L contribute to lifetime dose. Therefore, $f_v = 0.02$.

Calculation of f_w, the fraction of the day during which work can be accomplished at 80-85% $\dot{V}O_2$ max requires determining both performance time and recovery time according to the Kamon formulas[9]:

$$t_{perf} = 120\left(\frac{\dot{V}0_{max}}{\dot{V}0_2}\right) - 117 = 120\left(\frac{1}{0.85}\right) - 117 = 24 \text{ min} \qquad (4)$$

$$t_{rest} = 8.8 \ln\left[\left(\frac{\dot{V}0_2}{\dot{V}0_{2\,max}}\right) - 0.5\right] + 24.6 = 8.8 \ln[0.85 - 0.5] + 24.6$$

$$= 15 \text{ min} \qquad (5)$$

$$f_w = \frac{24}{24+15} = 0.61$$

A person could work at this high work rate for more than half of the day. Respiration rate for this work rate will be taken to be 45/min. Values for c_2, rf, PF, ret, and time will be the same as previously.

Hence this subject could receive a lifetime (30 year) dose of:

$$\text{dose} = [45 \cdot 0.61 \cdot 0.02\,(1.7 - 1.6)] \cdot 1.5 \times 10^{-6} \cdot 1.0 \cdot 1.0 \cdot 1.0 \cdot 144 \times 10^3 \cdot 30 = 0.36 \text{ g}$$

Comparing this dosage to the ones calculated in Table II indicates that even if someone were to breathe with high volumes for an entire career, the chances of developing CWP are minimal (perhaps 0.005%).

Much of this analysis depends on the assumptions made. Certainly, one would not expect a miner to work at this rate for a full day, much less an entire lifetime. In this respect, the calculated dose is a very conservative estimate. On the other hand, the assumption that

contaminated air enters the facepiece equally from all directions so that the entire 1.4 L dead volume protects the worker may not be correct. That still leaves the question about the efficiency of the simple particulate filter used in this PAPR. If respirable dust penetrates the filter, then the 1.4 L dead volume of the facepiece no longer serves to protect the wearer against contaminant inhalation. The ability of the respirator to provide clean air to the wearer is dependent on the quality and age of the filters, which is determined in part by wearer compliance with manufacturer specifications for filter maintenance, storage, and replacement.

Also, we found in our testing that the blower battery voltage degraded relatively rapidly (Figure 7). If we had not used a dc power supply, overbreathing inhalation volumes would likely have been higher. The blower in this particular PAPR does not seem to be very powerful, so the use of the Fleisch #4 pneumotach, with a low resistance of 0.067 cm $H_2O \cdot$ sec/L (a very low resistance, approximately 2.5% of the standard resistance of a U.S. Army M17 air purifying respirator filter), was necessary if flow rate delivery was not to be changed by the flow rate measurement. It would probably be good for the manufacturer to improve both the blower and the battery. According to the data in Figure 6, the blower flow rate could increase by about 300 L/min to eliminate all overbreathing.

The visor switch controlling blower operation was extremely sensitive. If the visor hit the chest or shoulder of the wearer, the blower was sometimes found to turn off . In a high noise environment it was not always possible to hear whether the blower was operating. No other blower operation indicator was provided, and it was so easy to breathe air circumventing the blower and filter that breathing contaminated air was often undetectable.

For the same reason, different hair styles may obstruct either the blower inlet or outlet, and this would be hard to detect. Thus, the analysis of cumulative dose that appears to demonstrate minimal risk of CWP may instead be in error by a very large amount.

Funding source

This work is funded in part by the National Institute for Occupational Safety and Health (NIOSH Contract 200-2002-00531). The authors would like to thank mine workers at Cumberland Mine in Pennsylvania for their valuable comments and insights related to this study. The results published herein are solely the responsibility of the authors.

Table I: Subject Demographics. Values given are means ± standard deviations

Age (y)	24.73 ± 5.66
Mass (kg)	67.61 ± 14.52
Height (cm)	168.40 ± 8.74
Maximal Oxygen Consumption (L/min)	2.66 ± 0.79
Maximal Heart Rate (bpm)	192.62 ± 9.13
Trait Anxiety Score	34.5 ± 9.69
Sex	8 males, 8 females

Table II. Prevalence of Coal Workers' Pneumoconiosis in Underground Coal Miners In the U.S.[7]

Years Working	CWP Prevalence (Percent)	Estimated Cumulative Dose (grams)
0 – 9	1.1	34
10 – 14	1. 6	52
15 – 19	2.8	71
20 – 24	3.4	90
≥25	5.4	112

Figures

References

1. Johnson, A. T., and E. G. Cummings: Mask Design Considerations; *Amer. Indus. Hyg. Assoc. J.* 36:220-228 (1975).

2. Johnson, A. T., W. H. Scott, C. G. Lausted, M. B. Benjamin, K. M. Coyne, M. S. Sahota, and M. M. Johnson: Effect of Respirator Inspiratory Resistance Level on Constant Load Treadmill Work Performance, *Amer. Indus. Hyg. Assoc. J.* 60:474-479 (1999).

3. OSHA, "Toxic and Hazardous Substances," *Code of Federal Regulations*, 2001 ed., Title 29, Pt. 1910.1000Z, www.osha.gov/pls/oshaweb/owadisp.show__document? P-table = STANDARD&p_id. . . (accessed March 2004).

4. ACGIH, "PELS and TLV's for Chemical Substances," www.gettsysburg.edu/ /administration/ehs/policies/GCCHP/Appendices/Appendix K/ap. (accessed March 2004).

5. Stellman, S.D.: "Issues of Causality in the History of Occupational Epidemiology, S0z.- *Prä ventivmed.* 48:151-160, 2003, www.epidemiology.ch/history/papers/SPM% 2048(3) 151-60 Stellman.pdf (accessed 16 May 2004).

6. Vincent, J.H., D. Mark, A.D. Jones, and K. Donaldson, A Rational for Assessing Exposure-Dose Response Relationships for Occupational Dust-Related Lung Disease, *Proc. VII Intern. Pneumoconioses Conf.*, pp. 151-157, 1998, www.cdc.gov/niosh/90-108. html (accessed 16 March 2004).

7. Pon, M.R.L., R.A. Roper, E.L. Petsonk, M.L. Wang, R.M. Castellan, M.D. Attfield, and G.R. Wagner: Pneumoconiosis Prevalence Among Working Coal Miners Examined in Federal Chest Radiograph Surveillance Programs—United States, 1996-2002-, *MMWR* 52(15):336-340, (2003), www.cdc.gov/mmwr/preview/mmwrhtml/mm 5215a 3.htm (accessed 16 March 2004).

8. Cotton, C.E., and L.M. Brosseau, ed.: *Respiratory Protection*, AIHA, Fairfax, VA. p. 159 (2001).

9. Johnson, A.T.: *Biomechanics and Exercise Physiology*, J. Wiley and Sons, New York (1991), now at www.bre.umd.edu/johnson.htm.

10. Johnson, A.T., and C.R. Dooly: Exercise Physiology, in *The Biomedical Engineering Handbook*, 2nd ed., J.D. Bronzino, ed. CRC Press, Boca Raton, FL, pp. 26-1 to 26.9 (2000).

11. Attfield, M.D.: The Fourth Round of the National Study of Coalworkers' Pneumoconiosis: A Preliminary Analysis, *Proc. VII Intern. Pneumoconiosis Conf.* p. 141-148, 1988, www.cdc.gov/niosh/90-108.html (accessed 16 March 2004).

12. Haney, R.: MSHA Dust Standard, personal communication, (20 March 2004).

13. Kravitz, J.: Mine Workers' Protection Against Dust, personal communication, (19 March 2004).

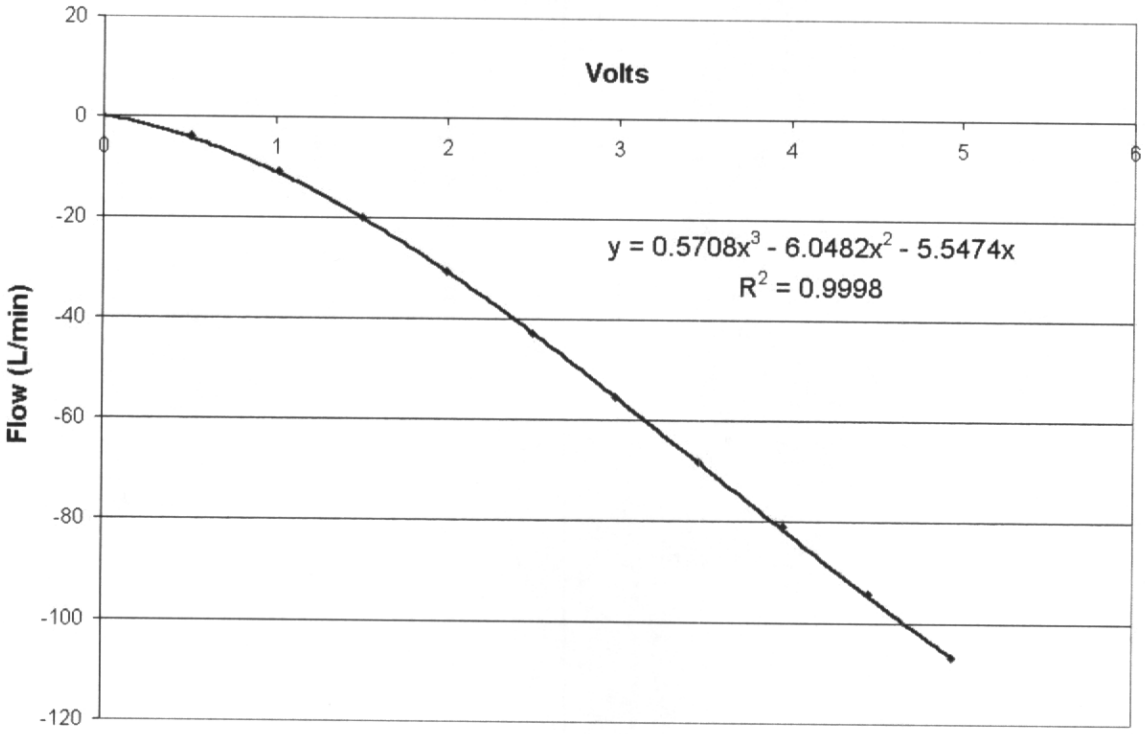

Figure 1. Battery voltage-flow rate characteristic of the Centurion MAX PAPR used in this study. Steady state flow rate was measured with a Fleisch #3 pneumotach in series with the blower and filter. At a battery voltage of 4.5v, steady state flow rate was 95.5 L/min.

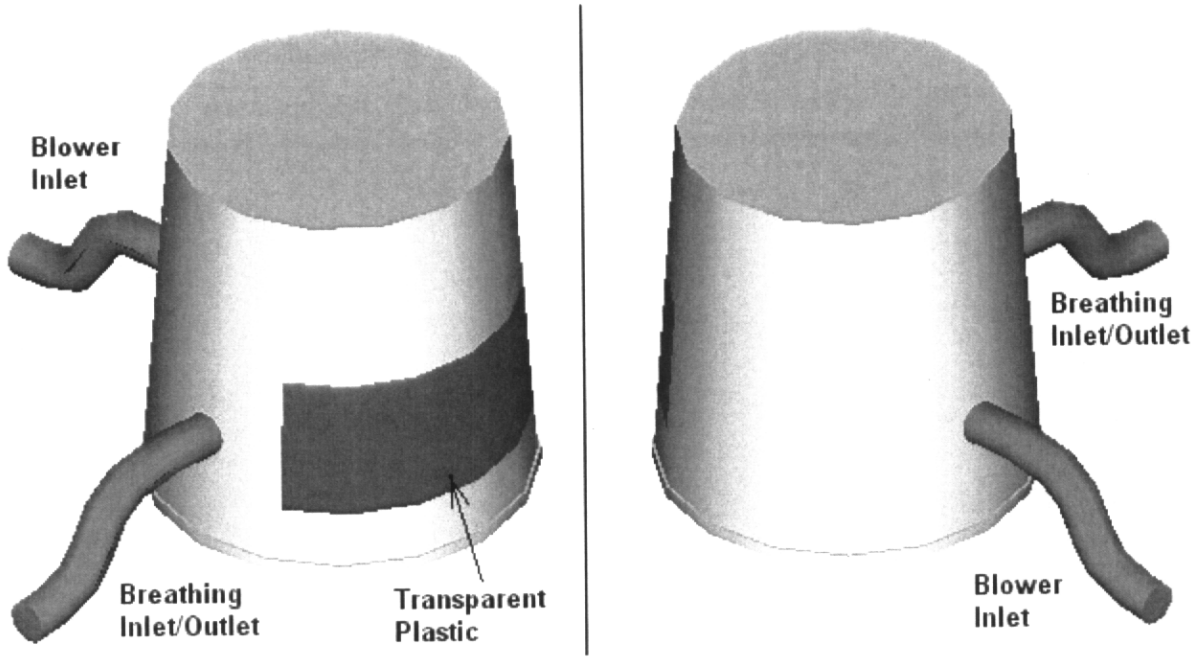

Figure 2. Diagram of the Portable Breathing Chamber (PBC).

Figure 3. Photo of the PBC as worn. The subject's face can be seen through the visor.

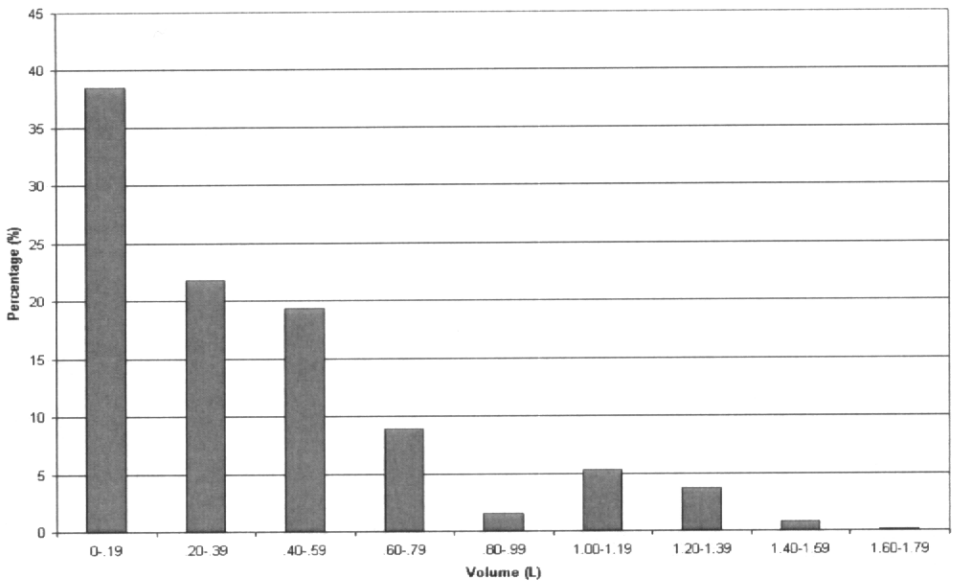

Figure 4. Overbreathing inhalation volumes averaged for all subjects. Percentages of breaths with volumes in each category are shown on the vertical axis.

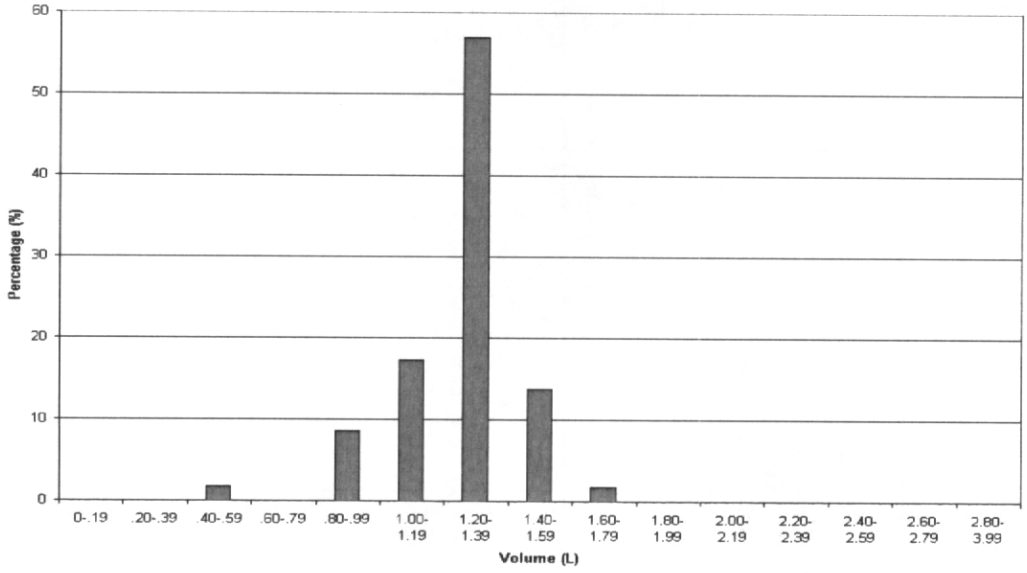

Figure 5. Overbreathing volumes for the one subject who exceeded the 1.4 L dead volume of the visor.

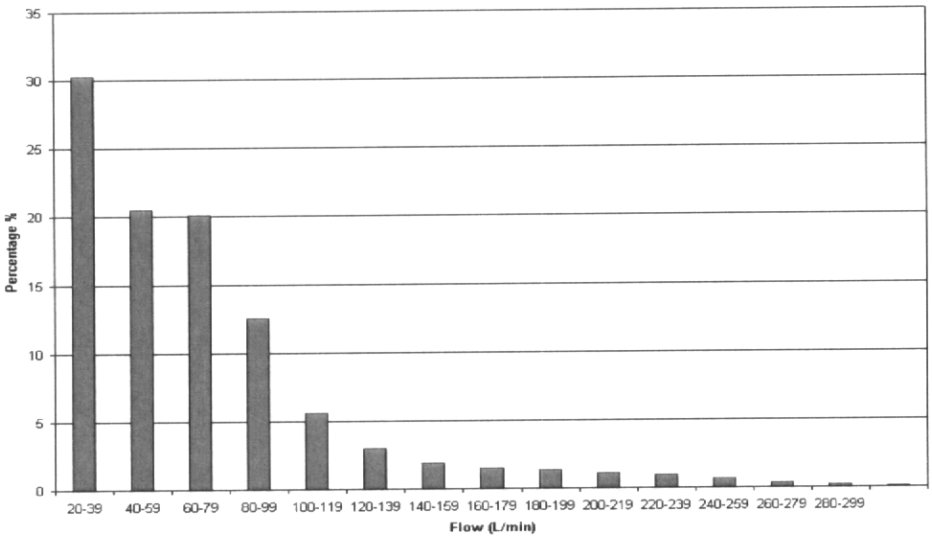

Figure 6. Flow rate ranges for the occurrence of overbreathing. Values given are the average for all subjects.

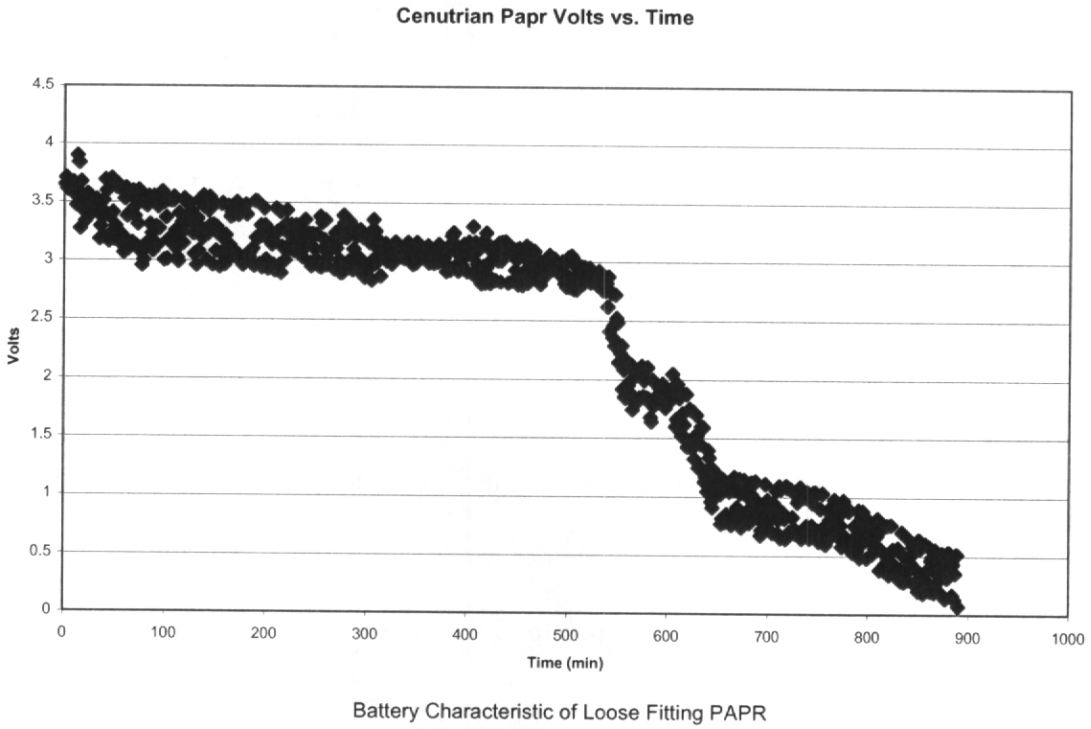

Figure 7. PAPR battery voltage with time during use. Battery voltage decreased very rapidly, especially after 500 min.

** It should be noted that there is a large difference in blower flow rates between our results reported here (95.5L/min at 4.5v) and test results supplied by the manufacturer (205 L/min at 4.8v). There are several possible explanations for this large discrepancy, including faulty batteries (not likely because most of our testing used a dc power supply in place of the battery), one of the two blower fans was inoperative (not likely, since operation of both fans was checked before each test), or the addition of extra pneumotach and hose resistance in the air flow circuit (this is possibly the reason). Devices were tested by the manufacturer using the European standard EN 146/EN 12941. Flow rate is determined by a zero pressure difference method: flow is introduced into a chamber by the device under test, and flow rate out is produced by a blower independently controlled to match the flow rate of the blower under test. When the pressure in the chamber equals the pressure outside the chamber, then flow rates from both blowers are matched. So, the additional pneumotach and tubing resistance likely contributed to the smaller flow rates we measured compared to the manufacturer's data.

Despite the difference in method and results, what are the likely consequences of added resistance in the blower circuit? The resistance of our flow-measuring instruments was very small. It is possible that a wearer's hair or a filter clogged with dust could provide at least as much resistance as our measuring devices, so it is likely that flow rates could be severely reduced.

At this point, the path of overbreathed air into the facepiece is not known, and must be determined by subsequent investigation. If there is preferential direction for outside air to enter the facepiece, then the entire 1.4L facepiece volume would not be protective. There seem to be differing opinions about whether the entire facepiece volume must be breathed before contamination reaches the mouth, but no scientific study reports have been found to illuminate

this issue. It is possible that the cloth barrier to be worn around the face when using the PAPR could be counter-productive by directing air through specific pathways rather than allowing the air to come in from all directions. Only further testing will tell.

Conclusions:

1. All subjects exercising at 80-80% $\dot{V}O_{2\,max}$ intense exercise rate overbreathed the PAPR to some extent.
2. If the entire facepiece volume protects against breathing contaminated air, then this respirator provides adequate protection. If air leakage is through some preferential route, then the level of protection is questionable.

APPENDIX 4

Inhalation Flow Rates During Strenuous Exercise

Arthur T. Johnson
Professor

Frank C. Koh
Faculty Research Assistant

William H. Scott, Jr.
Faculty Research Assistant

Kathryn R. M. Mackey
Faculty Research Assistant

Ken Y. S. Chen
Graduate Research Assistant

Biological Resources Engineering
University of Maryland
College Park, MD 20742
USA

Timothy Rehak
General Engineer
National Institute for Occupational Safety and Health

corresponding author:
Arthur T. Johnson
Biological Resources Engineering
University of Maryland
College Park, MD 20742
tel: 1-301-405-1184
email: aj16@umail.umd.edu

Abstract

It would be helpful if peak inhalation flow rates were characterized for respiratory design testing, and use. However, peak flow rates depend strongly on the wearer and the type of work being performed. Instantaneous inhalation rates for subjects exercising on a treadmill have been measured for the following conditions: 1) at 80-85% $\dot{V}O_2$ max without a respirator, 2) at 80-85% $\dot{V}O_2$ max while wearing a breath-responsive PAPR (blower flow rate) and 3) at 100% $\dot{V}O_2$ max without a respirator. Instantaneous inhalation flow rates were found to vary greatly among subjects and at different times for each subject. Depending upon the time that any given flow rate can be sustained, peak flow rates can vary considerably. Instantaneous flow rates were recorded and classified according to 20 L/min ranges so that the flow rate distribution could be obtained. If flow rates in the top one percentile are defined as peak flow rates, then a peak inhalation flow rate of up to 359 L/min (BTPS) was measured for condition 1. Peak instantaneous (less than 1% of flow rates) recorded flows were even higher, up to 442 L/min (BTPS). A peak blower flow rate of up to 679 L/min (BTPS) was measured for condition 2. Flow rates recorded at 100% $\dot{V}O_2$ max were generally higher than flow rates 80-85% $\dot{V}O_2$ max, although this varied somewhat among subjects. A linear relationship has been found between peak flow rate and average minute volume, which can then be used in a procedure to calculate peak flow rates expected at any given work rate.

Introduction

Wave shapes for flow rates of working humans are different from the sinusoids seen during inhalation at rest. If inhalation flow rate was sinusoidally-shaped, then there would be an easily definable relationship between average and peak flow. The pattern of flow rate is, instead, nearly trapezoidal, with a peak often occurring near the beginning or the end of the wave (Johnson, 1991; Johnson, 1993). The peak flow rate relationship varies among people and among breaths from the same person. Thus, the peak flow is not easily calculated from average flow rate.

Peak inhalation flow rates should be known for a number of reasons. First, flow rates supplied by powered-air purifying respirators (PAPRs) must be adequate to protect wearers (although flow rates alone do not guarantee protection). Especially for loose-fitting PAPRs, it is necessary to provide sufficient air to prevent breathing contaminated air. Face seal leakage for tight-fitting PAPRs is of concern when breathing flow rate exceeds blower flow rate and pressure inside the facepiece becomes negative. Leakage is especially of concern when beard stubble appears on the face of the wearer (deRoza et. al., 1986). Second, respirator filters are tested with defined flow rates. Filter break-through times, capacities, and pressure drops all depend on flow rates and flow patterns. Third, non-powered air-purifying respirators (APRs) affect both the pattern of breathing (Silverman et. al., 1951) and the average flow rate of breathing (Johnson, et. al., 1999). Fourth, many APRs incorporate the use of nose cups to minimize respirator dead volumes and reduce lens fogging. Nose cups feel uncomfortable to many wearers (Caretti, 2003), and interfere with nose breathing of others. The need for nose cups depends in part on flow rates encountered inside the facepiece. Fifth, peak flow rates and breathing patterns may be

incorporated into various respirator standards (ISO), and thus can have legal standing for certification requirements. It is important that these standards reflect the best possible scientific data available at the time.

In order to minimize possible respiratory effects of respirators, one must know how much degradation is caused by the respirator. That requires knowing the unencumbered response.

Methods

This study was performed in three distinct parts. These were:

1) Flow rates measured at 80-85% $\dot{V}O_2$ max without wearing a respirator
2) Flow rates measured at 80-85% $\dot{V}O_2$ max while wearing an SE-400 breath-responsive PAPR (SEA, Branford, CT).
3) Flow rates measured at the conclusion of $\dot{V}O_2$ max tests without wearing a respirator

The numbers of subjects participating in each of these parts differed and appear in Table 1. The PAPR comparison group appearing in Table 1 are those subjects who participated in both parts 1) and 2) of this study. All testing protocols were approved by the University of Maryland Institutional Review Board.

Orientation

An investigator met with the prospective participant to explain test procedures and methods. The participant was then provided with an informed consent document. A brief medical history form, and a Physical Activity Readiness Questionnaire (PAR-Q) (BCMH, 1978; Thomas et al., 1992) were both used to determine whether vigorous activity was appropriate.

Subjects selected for this study were a mix of paid and unpaid volunteers who gave written consent for their participation. A Spielberger State-Trait Anxiety Inventory (STAI) Test (Spielberger et al., 1970) was given to all volunteers to measure their anxiety levels, known to influence responses to respirator use (Johnson et al., 1995). The STAI test consists of a series of written multiple choice questions for which the respondent assesses her/his feelings. Test scores less than 30-35 are considered to be nonanxious; those above reflect higher levels of anxiety.

Calibration

All equipment was carefully calibrated before each test. Flow rates were calibrated by first determining any zero offsets in the system. With no flow applied, the output signal from the data acquisition system was accumulated for 30 seconds and then divided by this time to obtain an average zero offset value. The mean offset was then subtracted from subsequent readings. A three liter syringe was discharged through the pneumotach in five seconds or less, and the output signal accumulated to give a value corresponding to the syringes volume. A calibration factor was automatically calculated to give pneumotach flow rate. Because pressures were not measured, no pressure calibration was necessary for these tests.

The pneumotach has been checked periodically for a linear flow-pressure characteristic, and has been found to be linear. Thus, calibration at one flow rate is all that is needed to measure a range of flow rates.

The mass spectrometer was calibrated with test gases of know composition (4% CO_2, 16% O_2). This calibration was performed at daily intervals. A quick check of atmospheric gas concentrations was also performed daily.

Flow rates with the SE-400 breathing-responsive PAPR were measured with a custom flow measuring system provided by the manufacturer. The flow-sensing portion of this system was incorporated within the respirator and was not directly accessible to laboratory personnel. The system had been calibrated by the manufacturer within a few months of this use.

Maximum Oxygen Consumption Pre-Test

A maximal oxygen consumption test was performed on all prospective participants using a Quinton (Bothell, WA) motorized treadmill. Participants were asked to warm-up and stretch for approximately 5-10 minutes prior to the start of the test. After the warm-up the participants breathed through a Hans Rudolph (Kansas City, MO) two-way breathing valve configured with a rubber adaptable mouthpiece. This apparatus was interfaced with a standard Fleisch #4 (Phipps and Bird; Richmond, VA) pneumotach, with a linear range up to at least 800 L/min, and Perkin Elmer (St. Louis, MO) Model 1100 mass spectrometer to monitor continuous expired airflow and oxygen consumption. Heart rate measurement was assessed using a standard ECG 3-lead electrode configuration with the leads connected to a Hewlett Packard (Siemens; Andover, MA) Patient Monitoring System. The initial work rate was established at a speed and grade designed to elicit 70% of the participant's age-predicted maximal heart rate. The work rate (speed and grade) was adjusted every third minute until the participant experienced volitional fatigue, failed to display a rise in oxygen consumption (150 ml O_2) in accordance with the increase in work rate, or exhibited cardiovascular responses that contraindicated further assessment. Most subjects completed the $\dot{V}O_2$ max test in about 9-15 minutes.

Testing

80-85% $\dot{V}O_2$ max Testing, No Respirator

Sessions were conducted at 80-85% of the participant's maximal aerobic capacity using the motorized treadmill. One session utilized the Hans-Rudolph two-way breathing valve configured with a rubber adaptable mouthpiece and attached to a Fleisch #4 pneumotach (with an extremely low 0.1 cm $H_2O \cdot$ sec/L pneumotach (only) resistance) to measure inspiratory flow rates. The data were logged at 50 Hz using a DAS-8 (Metrabyte-Krithley; Tawnton, MA) Validyne (Northridge, CA) DP15 differential pressure transducer, 12 bit analog-to-digital converter board installed in a PC, and custom software developed specifically for our laboratory (Johnson and Dooly, 1994).

Each participant was asked to warm-up and stretch for approximately 5-10 minutes prior to the start of the session. The treadmill speed and grade were set at a work rate eliciting approximately 70% of the individual's age-predicted maximal heart rate, as determined from the $\dot{V}O_2$ max test. This work rate was slowly increased to the predetermined speed and grade corresponding to 80-85% of the participant's maximal aerobic capacity. The participant was then asked to exercise at this intensity for 6 minutes. Flow rate data were used for the entire last three minutes of each of the 80-85% $\dot{V}O_2$ max tests, when steady-state was reached. All test sessions, including the $\dot{V}O_2$ max test, included a five-minute cool down period of walking on the treadmill.

80-85% $\dot{V}O_2$ max Testing, Breath Responsive PAPR

Testing was conducted similarly to the 80-85% $\dot{V}O_2$ max sessions with no respirator except that subjects wore an SE-400 (SEA; Branford, CT) breath responsive tight-fitting full-

facepiece PAPR. Flow rate data were collected using a custom-built SEA data acquisition system at a rate of 50H_z. Flow rates were measured downstream from the PAPR blower and utilized a combination of pressure drops across the filter and inhalation valve. The system had been calibrated by the manufacturer within 6 months of this test. It was not practical to calibrate the system in our laboratory. This system measured air supplied to the PAPR facepiece, and were expected to be somewhat higher than subject inspiratory flow rates. Subjects walked for 6 minutes, with the last 3 minutes of data, assumed to be at steady-state, analyzed for instaneous flow rates.

100% $\dot{V}O_2$ max Test

For a subset of all the subjects who underwent $\dot{V}O_2$ max testing, inhalation flow rates were recorded during the final 30 seconds of the test. Inhalation and exhalation flows were separated using a Hans-Rudolph one-way breathing valve. Inhalation flows were measured with a Fleisch #4 pneumotach and Validyne DP-15 differential pressure transducer system. Data were logged into a computer at a rate of 50 H_z.

Data Analysis

Inhalation flow rates were obtained through a Hans-Rudolph two-way valve that should separate inhalation from exhalation flows. It was noticed, however, that data indicated some exhalation flows were being recorded (Figure 1a). These findings could be due to either: 1) a leaky valve allowing exhalation flow to pass through the pneumotach on the inhalation side of the valve, or 2) an uncompensated zero offset in the measurement system. Peak inhalation flows for the first instance would be correct as they stood, but peak inhalation flow rates would have to be corrected for the zero offset if the second were true.

To determine the cause of the problem, several volunteer subjects from our laboratory were asked to walk on the treadmill with two flow measurement conditions: 1) the two-way valve in place in the breathing circuit and the pneumotach configured to measure only inhalation flow rates and 2) no valve was used; only hoses conducted air from the mouth to the pneumotach. Results from one of these tests can be seen in Figure 2. Peak flow rates for the exercising subject gradually increased with time during the periods when the valve was not in place. This was interpreted as a response to the dead volume present in the tubing. Without an exhalation valve to separate expired air from inspired air, exhaled carbon dioxide was recycled into inspired air and this stimulated deeper breathing in the subject. Because this gradually increasing flow rate behavior was not seen in recordings of flow rates for the periods when breathing through the two-way valve, nor for the other subjects performing the main part of this study, it was concluded that the problem was a zero offset that needed to be corrected.

Data were subjected to an automated procedure to estimate the correct zero value. On rare occasions the offset had to be determined by viewing the waveform. In this case, exponential smoothing (Bloch, 2003) was used to reduce noise in the data to make a better estimate of the offset that required correction. As shown in Figure 1 a & b, flow rate data were able to be corrected for the apparent offset, and instantaneous flow rates could then be measured. Peak flows were identified as the flow rate that appeared in each data record. Alongside the flow rate values for 80-85% $\dot{V}O_2$ max are given flow rates for the same subjects exercising at 100% $\dot{V}O_2$ max . Flow rates at 100% $\dot{V}O_2$ max are greater than those at 80-85% $\dot{V}O_2$ max. Data from the SEA flow measuring system were analysed and displayed with custom software supplied by the manufacturer. No further adjustments were made to these data.

There was no selection procedure used to separate certain flow rate data from others. All instantaneous flow rates were converted into BTPS (Body, Temperature, Standard Pressure, Saturated with Water Vapor) conditions in order to standardize them. Otherwise, inhalation data could vary with ambient conditions. All flow rate data were separated into various ranges with a computer program. The number of instances that certain breathing flow rates were present in each range was accumulated and converted into a percentage of all flow rates. Data were pooled for all subjects.

Results

Flow rate ranges at 80-85% $\dot{V}O_2$ max are given in Figure 3. In this figure are shown the percentages of flow rates that fall into the 20 L/min flow rate range appearing on the abscissa (horizontal axis) of the graph.

The flow waveshape cannot be reproduced from the data appearing in Figure 3. To illustrate this point, Figure 4 is a composite of a graph of typical flow rate data with time at the top and the corresponding flow rate ranges at the bottom for the section of data illustrated above in Figure 4. The bottom graph of flow rate ranges is given in terms of percentages in each range.

Peak flow rates vary with time for any given subject and also vary among subjects. In an attempt to assess the importance of occurrence of any particular flow rate, Table 2 lists the percentages of the total number of tested subjects who exceeded flow rates in the given ranges for three different percentages of occurrence. For instance, 13% of the subjects exhibited 300-319 L/min 3% of the time. If it is deemed important to supply enough air to the hardest-breathing 13% of the subject population, then a blower must supply at least 319 L/min 3% of the

time. This information allows the assessment of the importance of supplying air at any particular flow rate.

In Figure 5 is shown flow rate data for 10 subjects wearing the breath-responsive PAPR, and, for comparison purposes, data for the same subjects not wearing the PAPR. It can clearly be seen that measured flow rates while wearing the PAPR were consistently higher than data from unencumbered subjects. The likely reason for this is that the PAPR supplied excess air to the facepiece in order to maintain positive facepiece pressure and guard against inward leakage. Flow rates measured represent blower flow rather than respiratory flow. In order to protect the wearer of this PAPR for the same length of time as an air-purifying respirator (APR), the filter used with this PAPR must have a larger capacity than the APR filter to account for the additional accumulated flow.

This PAPR incorporated a pressure transducer and audio signal should pressure become negative. The audio alarm did not sound for most subjects; thus, positive pressure inside the facepiece was indicated. For subjects with very high peak flow rates (e.g., subject #145), the alarm sounded often, indicating that the blower could not adjust rapidly enough to peak flows.

In Table 3 are shown percentages of the entire subject population of 13 whose flow rates exhibit certain values for three different percentages of time while wearing the PAPR. Table 3 reflects what is conveyed in Figure 5; higher flow rates must be supplied by the blower in order to maintain positive pressure inside the facepiece for a certain percentage of the population for a given percentage of the time.

In Figure 6 are shown data for 9 subjects tested at 100% $\dot{V}O_2$ max. For comparison purposes, data for the same subjects exercising at 80-85% $\dot{V}O_2$ max without a respirator are given as well. It can be seen that flow rates for 100% $\dot{V}O_2$ max exceed flow rates for 80-85%

$\dot{V}O_2$ max. Table 4 depicts the same information by percentage of the population and by time of occurrence. Alongside flow rate values for 80-85% $\dot{V}O_2$ max are given flow rates for the same subjects exercising at 100% $\dot{V}O_2$ max. Flow rates at 100% $\dot{V}O_2$ max are greater than those at 80-85% $\dot{V}O_2$ max.

The relationship between peak flows (obtained from a breath-by-breath analysis of each data set) and average minute volumes is given in Figure 7. for subjects exercising on a treadmill at 80-85% $\dot{V}O_2$ max and 100% $\dot{V}O_2$ max. Peak inhalation flow rate can be seen to be linearly related to average minute volume given for BTPS conditions. Even a casual glance at the flow rates in Figure 7 will be enough to notice that they are higher than the values that appear in the Tables. That is because the flow rate values in the Figure are instantaneous peak flow rates that did not persist for even 1% of the time. The difference demonstrates that peak flow rates do not usually persist for very long.

Discussion

The data that has been measured here points out one important fact: different people generate different flow rates. There are those whose peak flows are not nearly as great as the peak flows of others. This is intersubject variability. For the data reported here, the average peak flow, as determined from a breath-by-breath scrutiny of the data, is 215 L/min with an average maximum of 269 L/min and a standard duration of 26.5 L/min (Table 5). On the other hand, each subject breathed with a range of flow rates to give a flow rate distribution. This is intrasubject variability. Each subject exhibited a different mean, maximum, and standard duration, again found in Table 5. These standard deviations may be somewhat inflated because local peaks were sometimes included as peak flows.

The trick is to combine intrasubject and intersubject variability in a way that has meaning for the entire population. The difficulty here is that values given may be much too high for the slight breathers and underestimated too much for the heavy breathers. We have attempted to face this difficulty in the way data are presented in this paper.

The values of peak flow rates can be of interest for a number of reasons, mostly discussed earlier. Although flow rates are only one contributor to respiratory protection, they can be important nevertheless. What is often overlooked, however, is their potential contribution to the subjective feeling of the respirator wearer. Feelings of anxiety and dyspnea that some wearers experience in a respirator may have something to do with breathing patterns that do not feel right because they are confined by the respirator. Over the course of a lifetime, one can become used to a certain feel of breathing: muscle tensions, blood oxygen saturation, and carbon dioxide levels are all part of a normal pattern of breathing. Change these slowly, and adjustments come easily, change these abruptly, and some sensitive people may feel uncomfortable. It is unknown at this point whether such mechanisms operate, and if they do, the degree to which a small change, such as a muscle contraction that does not result in additional flow, can contribute to a feeling of breathlessness. It had been speculated years ago (Johnson, 1991) that muscle "length-tension inappropriatness" is a contributor to dyspnea. Perhaps we will find out that the same mechanism is important for certain respirator wearers.

Although flow rate data have been recorded for many years, measurement technology has changed significantly since the middle of the twentieth century. In addition, the physical stature of workers and potential subjects has also changed in that time. Subject pools are today much more diverse, including representation from women and a mixture of races that would have been unusual fifty years ago. Hence, we are hesitant to make direct comparisons between published

reports from that time and from this paper. Two studies of peak flow rates have recently been published, however. Berndtsson (2004) reported on peak inspiratory flow rates for seven subjects exercising at work rates ranging from 50 to 200 W, wearing six different types of respiratory protective devices, and either speaking or not speaking. At the highest workload of 200 W, (corresponding to about 90% $\dot{V}O_2$ max for his subjects), the average peak inhalation flow rate obtained from his Table VII (without speech) was 321 L/min BTPS, which was comparable to the value in this study of 359 L/min at 80-85% $\dot{V}O_2$ max (Table 2, 4% of subjects (1 subject) exceeding 359 L/min 1% of the time). Values in this report might be expected to be somewhat higher than values obtained by Berndtsson because his values were obtained from subjects wearing various respirators with their accompanying filters, whereas data in this study were obtained from subjects unencumbered by respirators. Inhalation and exhalation resistances have been shown to reduce minute volumes (Johnson et al., 1999; Caretti et al., 2001), despite the statement by Berndtsson that reduction of exhalation resistance should lower respiratory minute volume.

Also, it was not stated in the Berndtsson (2004) paper how or where air flow rate measurements were made. A resistance flow measuring device was used. If flow rates were sampled digitally, as would be expected, then the rate of sampling could influence reported results because peak flows typically exist for short durations. If all respirators used in Berndtsson's study were full-facepiece air-purifying respirators, and respirators used were identified only by manufacturer and model number, then the placement of the flow meter would be much less critical than if a PAPR were used. This can be seen in Figure 5 of this paper, where flow rates measured in the path downstream from the blower in the SE-400 breath-responsive PAPR are higher than flow rates measured from subjects not wearing respirators. The difference

is that, in order to maintain positive pressure inside the facepiece, some extra flow must be provided in addition to that supplied to the wearer. The SE-400 is a very sophisticated device that would probably provide the highest levels of protection needed in certain critical situations, but the additional flow rate provided by the blower would be expected to shorten the useful filter life by some small amount.

The second report cited for comparison is by Kaufman and Hastings (2003). Forty-eight U.S. Marines performed nine different operationally-relevant physical tasks, each with a duration between 30 and 200 sec. Flow rates were measured with a turbine flow meter in series with the respirator filter and sampled at a rate of 50 Hz. Peak flow rates were selected from periods of maximum respiratory flow. They reported an average peak inspiratory flow rate of 239 L/min during testing, although the average peak flow rate capability of their subjects (measured during pulmonary function testing) was 365 L/min.

The average peak flow of 239 L/min reported by Kaufman and Hastings was considerably below the 321 L/min reported by Berndtsson and the 359 L/min reported in the present study. Conditions of the Kaufman and Hastings test were much different from the two comparison tests. First, the Kaufman and Hastings test work rate conditions were not held steady as in the other two tests. Respiratory responses usually take at least three minutes to reach steady-state, so the short periods of transition from one of their tasks to another would likely have reduced peak inspiratory flows. Second, Kaufman and Hastings used a turbine flow meter with its inherent inertia. Although they did correct for inertial effects around zero flow, it is likely that some peak flows, as quick as they are, were not detected. Third, subjects used by Kaufman and Hastings were heavier and physically more fit than subjects in the other two studies. Berndtsson reported an estimate of $\dot{V}O_2$ max for his subjects of 3.2 L/min and average

mass of 78.0 kg; Kaufman and Hastings (correcting for an error in units in their Table 3) reported an average $\dot{V}O_2$ max of 3.9 L/min (estimated from a submaximal step test) and average mass of 80.3 kg. Subjects in this study had values averaging 2.4 to 2.9 L/min and masses of 67-75 kg (Table 1). More physically fit subjects usually have better ventilation efficiency than less physically fit subjects, so peak inhalation flow rates, although perhaps applicable to U.S. Marines performing operational tasks, may not be quite as representative of responses of the average worker. Lastly, the forty-eight subjects tested by Kaufman and Hastings, because of the relatively large number, could possibly be more representative of the population from which they were drawn than the seven subjects tested by Berndtsson and the various numbers of subjects tested in this study.

Caretti (2003B) showed a linear relationship between peak inhalation flow rates and average minute volumes for data appearing in the literature. The best-fit line,

Peak Flow (L/min) = 2.346 Minute Volume (L/min) + 20.828,

was very well determined, with $R^2 = 0.9867$. Data in the present study do not exactly fit Caretti's regression line. The R^2 value here is somewhat lower, but the slopes of the lines are similar. The lines are nearly parallel, with a difference in zero intercept. This is not too surprising due to the factors mentioned at the beginning of this discussion. Caretti analysed historical data, some up to 50 years old. As Caretti has noted, peak flow rates can be anticipated through the process of: 1) converting physical work rate into physiological work rate, 2) converting physiological work rate into oxygen demand, 3) determining corresponding minute ventilation, and 4) determining peak flow rates.

The close relationships between average minute volume and maximum inspiratory flow rate, and between average minute volume and average inspiratory flow rate can be used to

advantage. Certainly for many purposes, further experimentation intended only to measure maximum and average inspiratory flow rates during strenuous exercise is unnecessary. Maximum and average flow rate can be calculated in the following manner:

1. Beginning with the work rate level, determine oxygen consumption. This can be determined by (Johnson, 1991):

$$\dot{V}O_2 = 0.00297\ \dot{M} \qquad (1)$$

where $\dot{V}O_2$ = rate of oxygen consumption, L/min

$\dot{M}$ = work rate, $N \cdot$ m/sec or Watts

2. Average respiratory minute volume can be calculated for average males, accounting for the hyperventilation above the ventilation threshold, by (Johnson, 1993):

$$\dot{V}_{avg} = 22.34\ \dot{V}O_2 + 1.53 \qquad (2)$$

$$\dot{V}_{avg} \leq 1.55 \text{ L/min}$$

$$\dot{V}_{avg} = 22.34\ \dot{V}O_2 - 5.03 + 11.51/(3.3 - \dot{V}O_2) \qquad (3)$$

$$\dot{V}_{avg} > 1.55 \text{ L/min}$$

where $\dot{V}_{avg}$ = average minute volume, L/min

For highly-trained and larger individuals, these values would be increased. For smaller or more sedentary individuals, $\dot{V}_{avg}$ would be lower.

3. Flow rates while breathing through respirator resistances have been found to be lower than unencumbered flow rates (Johnson, et al., 1999). Adjust flow rates for the effects of respirator inspiratory resistance:

$$\dot{V}_R = \dot{V}_{avg} - 4.12\ R \qquad (4)$$

where $\dot{V}_R$ = average minute volume adjusted for inspiratory resistance, L/min

R = inspiratory resistance of respiratory apparatus, cm $H_2O \cdot sec/L$

4. Peak inspiratory flow rate can be calculated from the results we have obtained here:

$$\dot{V}_{peak} = 2.746\ \dot{V}_{avg} + 18.895 \qquad (5)$$

where $\dot{V}_{peak}$ = peak inspiratory flow rate, L/min

5. Flow rates may be adjusted for ambient conditions. Our results have been given for BTPS conditions. Inspired air is not at BTPS, but rather is at ambient conditions. The conversion is (Johnson, 1991):

$$\dot{V}_{amb} = \dot{V}_{BTPS}\left(\frac{273+\theta}{310}\right)\left(\frac{p - 6.28}{p - pH_2O}\right) \qquad (6)$$

where $\dot{V}_{amb}$ = flow rates at ambient conditions, L/min

$\dot{V}_{BTPS}$ = flow rates at BTPS conditions, L/min

θ = temperature of ambient air, °C

p = total ambient pressure, kN/m^2 = 101.3 kN/m^3 normally

pH_2O = partial pressure of water vapor in the ambient air, kN/m^2, which must be measured or estimated from a psychrometric chart.

The fact that there is a definite relationship between peak flow and average flow indicates a similarity among flow waveshapes from all subjects. If this were not so, the data would be much more scattered and the regression line would have a much lower regression coefficient.

For example, peak-to-average values for square waves are 1.0, for half sine waves are $\pi/2$, for triangular waves are 2, and for trapezoidal waves are between 1 and 2, depending on the ratios of the maximum and minimum heights. If the peak-to-average ratio were random, then no statement could be made about the waveshape. However, there was a definite peak-to-average ratio of 2.75 found for this data, and the flow waveshapes shown in Figures 1 and 4 are typically seen for subjects breathing hard. Thus, it is reasonable to conclude that breathing flow waveshapes during heavy exertion are universally determined by respiratory mechanical properties that were nearly the same for all our subjects.

One must be somewhat careful because minute volume is conventionally measured in terms of BTPS conditions (although often this is not designated), whereas the rate of oxygen use is measured at STPD conditions (Johnson, 1991). Although the above calculations are valid for the average young male adult, the results can be adjusted for other types of respirator wearers.

There are a number of uncertainties regarding respiratory flow rates that make difficult the interpretation of published experimental results. First among these is what is meant by minute volume, and, relatedly, by average flow rate. Minute volume was originally defined as the volume of air inspired per minute, and was equal to the inspired tidal volume multiplied by the respiration rate (Ganong, 1963). However, it is often more convenient to measure exhaled flows, so many minute volume measurements are made during exhalation. Exhalation volumes can often exceed inhalation volumes by 20% or more, depending on temperature and humidity conditions of measurement (Johnson, 1991).

Thereafter, minute volume has often been used synonymously with average flow rate, incurring even more uncertainty. The period of time for average flow rate is not specified, and is usually longer than the one minute duration for minute volume. Also, because flow rate is

bidirectional, the average flow rate for a whole breath (volume inhaled or exhaled divided by the entire breath interval) is different from the average flow rate for either inhalation or exhalation. Average flow rate is sometimes taken to be the accumulated exhaled volume over a long period of time (say, five or fifteen minutes). Again, it is common to call this minute volume.

Reports in the literature are often not clear on the basis for these flow rates. Are they given in STPD, BTPS, or ambient conditions? Although this is sometimes made clear, this is not always the case.

The result of all this is that precise measurements of respiratory flow rates may be made, but, unless it is exactly clear what is being reported, there is a great deal of uncertainty regarding the use of those measurements. Add to that the natural variation within the population and different responses obtained during different activities (breathing during heavy lifting, for instance, is different from breathing during running), and one can only say that there will be design trade-offs for respiratory protective devices. If a device were to protect 100% of the population 100% of the time, the device might be either too expensive, too heavy, or have a useful life too short to be practical. On the other hand, a device used by a small percentage of the population 100% of the time might be necessary for specific uses where uncertain, but potentially immediately dangerous to life or health (IDLH) contamination exists. Different respirators for different applications may be required to meet different respiratory demands.

This study was performed in the laboratory under controlled conditions. Subjects were young, healthy, and walked on a treadmill in a benign environment that was not likely to cause heat stress, anxiety, or sudden changes. So, how applicable are these results to workers who may be older, performing different tasks in harsher environments, and who may have to react to rapid changes in conditions? Despite the realistic nature of the tasks performed in the Kaufman and

Hastings study, their study was still a simulation, as are all of these studies, and it is difficult to know exactly what physiological responses would be obtained from people in real situations. It is likely, however, that breathing flow rate data obtained from $\dot{V}O_2$ max tests would not be exceeded under any circumstances.

Now that we have some breathing flow rate data, what can be done with it? Peak flow rates do not represent a very large portion of the flow rates incurred during breathing. Because these flow rates represent only a small fraction of time for a small fraction of the population, overall protection of the wearer population is not necessarily measurably better if the peak flows are accommodated or not by the respirator. A lot depends on the type of respirator used, how it is used, and how it is worn. It has been shown that respirator resistance leads to hypoventilation (Johnson et al., 1999), so peak flows are reduced accordingly. If a small amount of contaminated air enters the facepiece through face seal leakage or through momentary breakthrough of the filter, the wearer's health is not necessarily going to be compromised. Only in the most dangerous situations will the failure to supply necessary peak respiratory flow be critical. Sometimes these situations can be controlled and sometimes they can't. If they can't then the choice of a respirator and filter must be made very carefully.

Conclusions:

1. Peak flow rates vary greatly among subjects. Peak flow rates at 80-85% $\dot{V}O_2$ max can reach 359 L/min.
2. Peak flow rates for 100% $\dot{V}O_2$ max exceed those measured for 80-85% $\dot{V}O_2$ max.
3. Measured flow rates for the pressure-demand PAPR are higher than breathing flow rates.

4. Estimated peak flow rates can be calculated for various strenuous work conditions.

Funding source

This work is funded in part by the National Institute for Occupational Safety and Health (NIOSH Contract 200-2002-00531). The results published herein are solely the responsibility of the authors.

References

Berndtsson, G.: Peak Inhalation Air Flow and Minute Volumes Measured in a Bicycle Ergometer Test, *J. ISRP* 21:21-30 (2004).

Bloch, S.: *Excel for Engineers and Scientists*. New York, John Wiley and Sons (2003).

BCMH: PAR-Q Validation Report, British Columbia Ministry of Health (1978).

Caretti, D. M.: Influence of Respirator Design on Subjective Comfort, *J. ISRP* 20: 13 – 25 (2003A).

Caretti, D.: Work Rates and Anticipated Ventilatory Parameters , working paper U.S. Technical Advisory Group (TAG) Working Group 1, Project Group 5 (Human Factors), Edgewood Chemical Biological Center (2003B) Abderdeen Proving Ground, MD 21010.

Caretti, D. M., W. H. Scott, A. T. Johnson, K. M. Coyne, and F. Koh: Work Performance When Breathing Through Different Respirator Exhalation Resistances, *Amer. Indus. Hyg. Assoc. J.* 62:411 – 415 (2001).

Da Roza, R. A., C. A. Cadena-Fix, and J. E. Kramer: Powered Air- Purifying Respirator Study Final Report, UCRL-53757, Lawrence Livermore National Laboratory, Livermore, CA (1986).

Ganong, W. F.: *Review of Medical Physiology*: Lange Medical Publishers, Lost Altos, CA, p. 488 (1963).

ISO/TC94/SC15 "Personal Safety-Protective Clothing and Equipment—Respiratory Protective Devices" International Respirator Standard for All Aspects of Respirator Use and Testing.

Johnson, A. T.: *Biomechanics and Exercise Physiology* New York: John Wiley and Sons, pp. 265-267 (1991).

Johnson, A. T.: How Much Work is Expended for Respiration? *Frontiers Med. Biol. Engr.* 5: 265-287 (1993).

Johnson, A. T., and C. R. Dooly: System to Obtain Exercise Respiratory Flow Waveforms, *Comput. Meth. Programs in Biomed.* 42:27-32 (1994).

Johnson, A. T., C. R. Dooly, C. A. Blanchard, and E. Y. Brown: Influence of Anxiety Level on Work Performance With and Without a Respirator Mask, *Amer. Indus. Hyg. Assoc. J.* 56:858-865.

Johnson, A. T., W. H. Scott, C. G. Lausted, M. B. Benjamin, K. M. Coyne, M. S. Sahota, and M. M. Johnson: Effect of Respirator Inspiratory Resistance Level on Constant Load Treadmill Work Performance, *Amer. Indus. Hyg. Assoc. J.* 60: 474-479 (1999).

Kaufman, J. W., and S. Hastings: Respiratory Demand in Individuals Performing Rigorous Physical Tasks in Chemical Protective Ensembles, NAWCADPAX/TR-2003/29, Naval Air Warfare Center Aircraft Division, Patuxent River, MD (2003).

Silverman, L., G. Lee, T. Plotkin, L. A. Sawyers, and A. R. Yancey: Air Flow Measurements on Human Subjects With and Without Respiratory Resistance at Several Work Rates, *Ind. Hyg. Occ. Med.* 3:461-478 (1951).

Spielberger, C., R. Gorsuch, and R. Lushene, *STAI Manual*. Palo Alto: Consulting Psychologist Press (1970).

Thomas, S., J. Reading, R. J. Shephard: Revision of the Physical Activity Readiness Questionnaire (PAR-Q). *Can. J. Spt. Sci.* 17(4): 338-345 (1992).

Table 1. Participant Characteristics

Demographic	80-85% $\dot{V}O_2$ max no respirator	80-85% $\dot{V}O_2$ max PAPR	80-85% $\dot{V}O_2$ max (PAPR Comparison)	100% $\dot{V}O_2$ max no respirator
Number (Sexes)	24 (14M, 10F)	13 (6M, 7F)	10 (5M, 5F)	9 (4M, 5F)
Age (years)	23.3 ± 4.6 (19-35)	24.1 ± 5.9 (19-35)	24.6 ± 5.9 (19.35)	23.3 ± 2.8 (19-28)
Mass (kg)	67.1 ± 10.1 (44-91)	67.1 ± 12.4 (591)	67.7 ± 12.9 (54-91)	66.0 ± 9.1 (49-74)
Height (cm)	171 ± 8.6 (160-183)	169 ± 9.0 (157-183)	169 ± 9.4 (160-183)	172 ± 7.6 (163-183)
$\dot{V}O_2$ max (L/min)	2.7 ± 0.7 (1.5 – 4.3)	2.9 ± 0.8 (1.5 – 4.3)	2.9 ± 0.9 (1.5 – 4.3)	2.4 ± 0.6 (1.5 – 3.5)
HR max (b/min)	195 ± 11.1 (168-211)	193.4 ± 9.9 (168-203)	194 ± 10.4 (168-203)	197 ± 13.8 (186-211)
Trait Anxiety (STAI)	33.4 ± 9.5 (20-52)	35.5 ± 10.2 (25-52)	33.9 ± 9.3 (25-52)	32.2 ± 10.7 (20-52)

Values given are means ± std dev. Ranges are given in parentheses.

Table 2. Percentages of 23 subjects who Exhibited Indicated Flow Rate Ranges. 80-85% $\dot{V}O_2$ max, no respirator condition

Flow Rate	Percentage of the Time		
L/min BTPS	5%	3%	1%
0-19	100.0	100.0	100.0
20-39	100.0	100.0	100.0
40-59	100.0	100.0	100.0
60-79	100.0	100.0	100.0
80-99	100.0	100.0	100.0
100-119	100.0	100.0	100.0
120-139	100.0	100.0	100.0
140-159	91.3	91.3	95.7
160-179	87.0	87.0	91.3
180-199	69.6	78.3	82.6
200-219	60.9	65.2	69.6
220-239	34.8	39.1	52.2
240-259	26.1	34.8	34.8
260-279	17.4	21.7	26.1
280-299	13.0	17.4	17.4
300-319	13.0	13.0	13.0
320-339	8.7	13.0	13.0
340-359	0.0	4.3	13.0
360-379	0.0	0.0	4.3

380-389	0.0	0.0	0.0

Table 3. Percentages of 13 Subjects Who Exhibited Indicated Blower Flow Rate Ranges. Breath-Responsive demand PAPR condition 80-85% $\dot{V}O_2$ max,

Flow Rate	Percentage of the Time		
L/min BTPS	5%	3%	1%
0-19	100.0	100.0	100.0
20-39	100.0	100.0	100.0
40-59	100.0	100.0	100.0
60-79	100.0	100.0	100.0
80-99	100.0	100.0	100.0
100-119	100.0	100.0	100.0
120-139	100.0	100.0	100.0
140-159	100.0	100.0	100.0
160-179	100.0	100.0	100.0
180-199	100.0	100.0	100.0
200-219	100.0	100.0	100.0
220-239	100.0	100.0	100.0
240-259	92.3	100.0	100.0
260-279	92.3	92.3	92.3
280-299	46.2	69.2	76.9
300-319	38.5	38.5	46.2
320-339	38.5	38.5	38.5
340-359	38.5	38.5	38.5

360-379	15.4	30.8	38.5
380-399	15.4	15.4	30.8
400-419	15.4	15.4	15.4
420-439	7.7	15.4	15.4
440-459	7.7	7.7	15.4
460-479	7.7	7.7	7.7
480-499	7.7	7.7	7.7
500-519	7.7	7.7	7.7
520-539	7.7	7.7	7.7
540-559	7.7	7.7	7.7
560-579	7.7	7.7	7.7
580-599	7.7	7.7	7.7
600-619	0.0	7.7	7.7
620-639	0.0	7.7	7.7
640-659	0.0	0.0	7.7
660-679	0.0	0.0	7.7
680-699	0.0	0.0	0.0
700-719	0.0	0.0	0.0
720-739	0.0	0.0	0.0

Table 4. Percentages of 9 Subjects Who Exhibited Indicated Inhaled Flow Rate Range: Comparing 80-85% $\dot{V}O_2$ max and 100% $\dot{V}O_2$ max, no respirator condition.

	100% $\dot{V}O_2$ max			80-85% $\dot{V}O_2$ max		
Flow Rate	Percentage of the Time			Percentage of the Time		
L/min BTPS	5%	3%	1%	5%	3%	1%
0-19	100.0	100.0	100.0	100.0	100.0	100.0
20-39	100.0	100.0	100.0	100.0	100.0	100.0
40-59	100.0	100.0	100.0	100.0	100.0	100.0
60-79	100.0	100.0	100.0	100.0	100.0	100.0
80-99	100.0	100.0	100.0	100.0	100.0	100.0
100-119	100.0	100.0	100.0	100.0	100.0	100.0
120-139	100.0	100.0	100.0	100.0	100.0	100.0
140-159	100.0	100.0	100.0	88.9	88.9	100.0
160-179	100.0	100.0	100.0	88.9	88.9	88.9
180-199	100.0	100.0	100.0	66.7	77.8	77.7
200-219	66.7	77.8	100.0	55.6	55.6	77.8
220-239	66.7	66.7	66.7	11.0	11.1	66.7
240-259	55.6	55.6	66.7	11.0	11.1	44.4
260-279	33.3	44.4	44.4	11.0	11.0	11.0
280-299	11.1	11.1	22.2	0.0	11.0	11.0
300-319	11.1	11.1	11.1	0.0	0.0	0.0
320-339	11.1	11.1	11.1	0.0	0.0	0.0

340-359	0.0	0.0	11.1	0.0	0.0	0.0
360-379	0.0	0.0	0.0	0.0	0.0	0.0

Table 5. Peak Flow Statistics for Each Subject Based on a Breath-By-Breath Analysis

Subject	Mean (L/min)	Std. Dev. (L/min)	Max (L/min)
145	306	44.5	442
223	185	22.4	228
265	149	17.8	197
290	190	23.7	247
292	202	27.6	269
302	140	16.8	171
304	312	34.8	383
306	260	30.7	313
325	235	27.2	276
328	199	23.8	253
329	177	20.6	207
330	121	14.7	151
340	241	30.9	293
344	151	18.6	179
351	122	15.2	192
353	238	29.3	281
358	255	33.8	310
365	271	30.9	318

366	236	29.7	293
376	201	26.3	302
380	207	24.3	241
381	189	24.4	231
382	248	30.5	248
average	215	26.5	269

Captions:

Figure 1. Inhalation flow rate waveflows a) before offset correction, and b) after offset correction. Inhalation flow rates are given as negative values.

Figure 2. Flow rate tracings to test for the cause of the offset. During periods with the two-way valve in place, only inhalation flow rates were measured. With the valve replaced by a hose, exhalation flow rate was measured in addition to inhalation flow rate. The larger inhalation flow rates measured without the two-way valve were attributed to CO_2 stimulation of breathing. Inhalation flow rates are given as negative values.

Figure 3. Flow rate percentages exhibited by 24 subjects working at 80-85% $\dot{V}O_2$ max without wearing a respirator. A flow rate in the range of 360-379 L/min is discernable from the graph.

Figure 4. Composite of flow rate with time as measured on one subject (a) contrasted with the percentage of flow rates in range groups (b). The flow waveform cannot be inferred from the percentages of flows.

Figure 5. Flow rate percentages for ten subjects wearing the SE-400 breathing demand PAPR (darker bars) compared to data from the same ten subjects without wearing a respirator (lighter bars). Flow rates are higher with the PAPR.

Figure 6. Flow rate percentages for nine subjects at 100% $\dot{V}O_2$ max when not wearing a respirator (light bars). For comparison, data from the same subjects at 80-85% $\dot{V}O_2$ max are plotted as well (darker bars). Flow rates at 100% $\dot{V}O_2$ max exceed flow rates at 80-85% $\dot{V}O_2$ max.

Figure 7. Maximum recorded flow rate for each subject related to average minute volume for subjects at 80-85% $\dot{V}O_2$ max (diamonds) and 100% $\dot{V}O_2$ max (squares). The presence of a strong predictive relationship between these two variables indicates a similarity of breathing waveshapes among the subjects. Peak flow rates persist for a very short time.

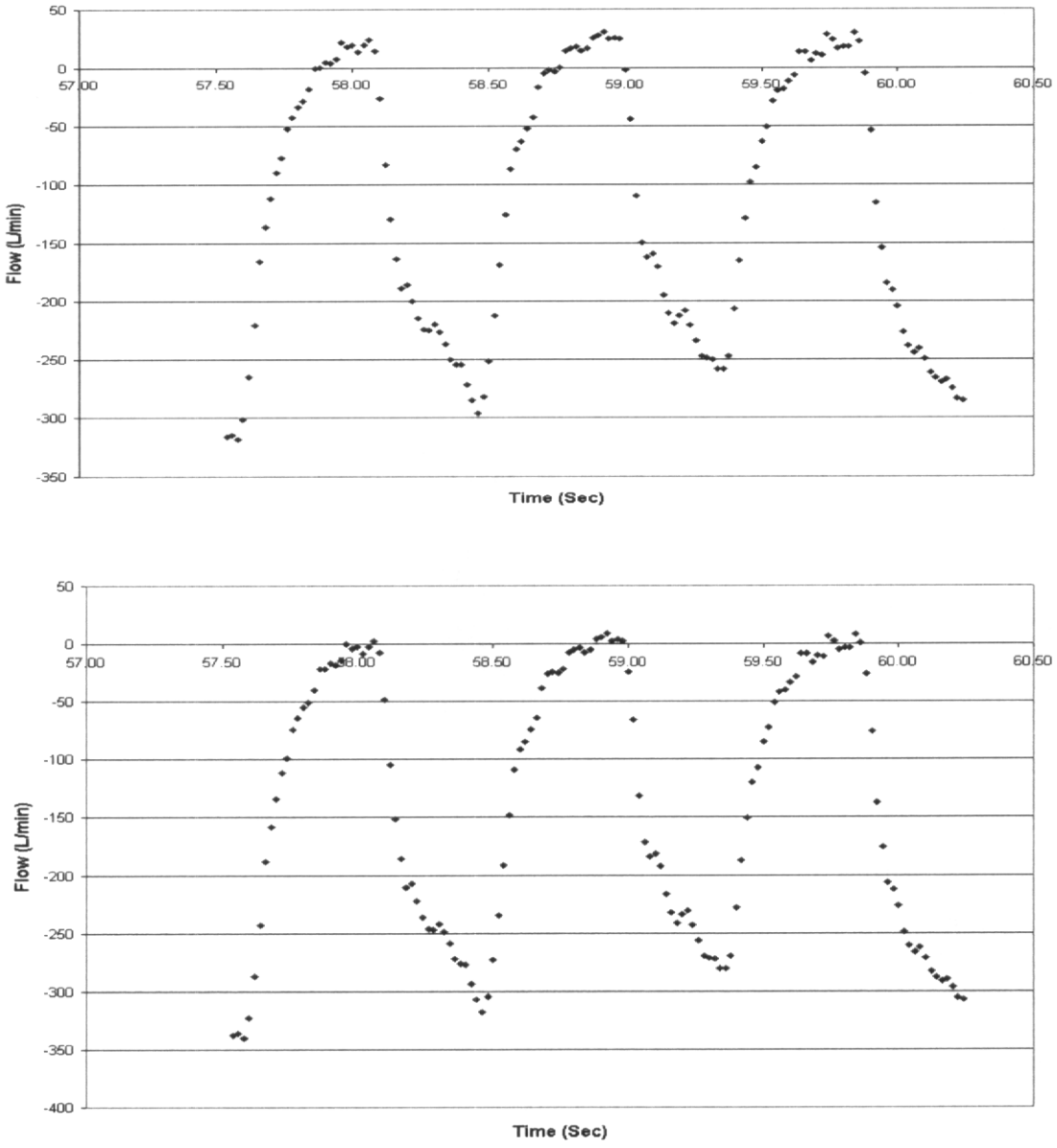

Figure 1. Inhalation flow rate waveflows a) before offset correction, and b) after offset correction. Inhalation flow rates are given as negative values.

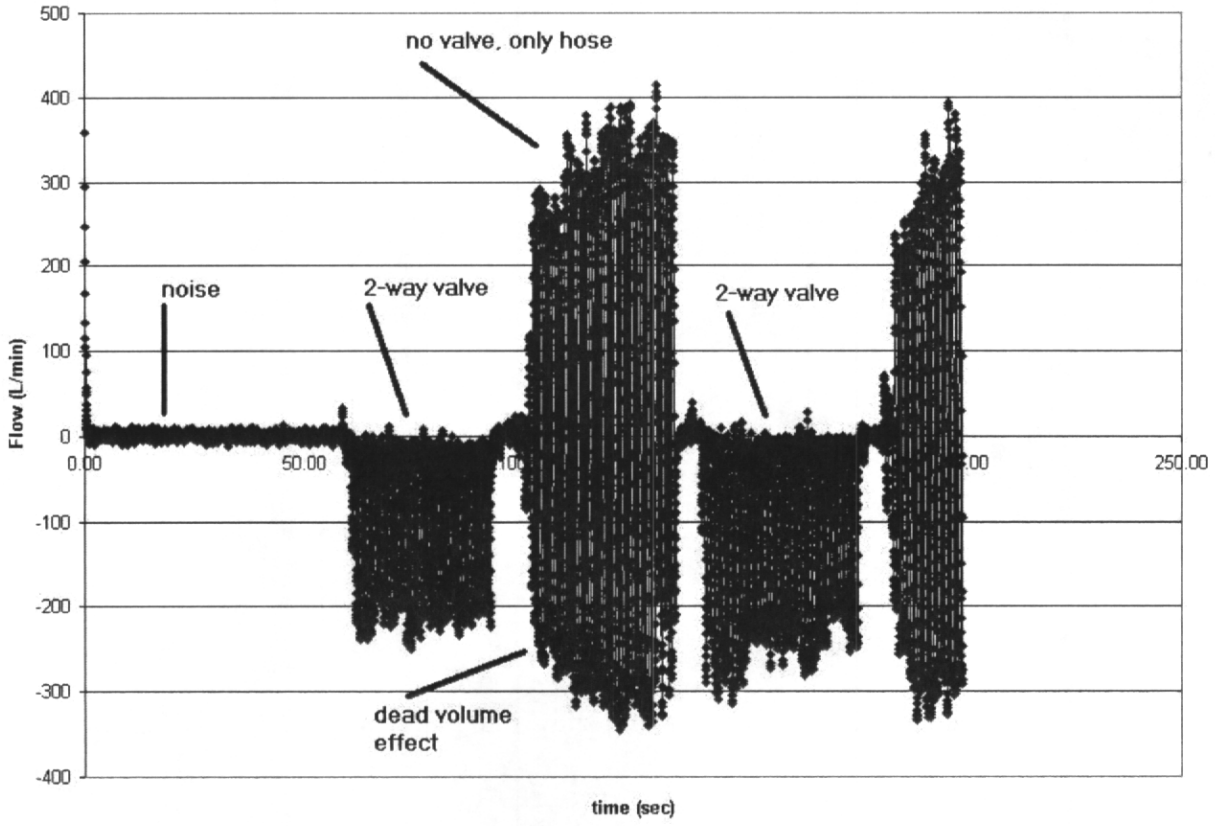

Figure 2. Flow rate tracings to test for the cause of the offset. During periods with the two-way valve in place, only inhalation flow rates were measured. With the valve replaced by a hose, exhalation flow rate was measured in addition to inhalation flow rate. The larger inhalation flow rates measured without the two-way valve were attributed to CO_2 stimulation of breathing. Inhalation flow rates are given as negative values.

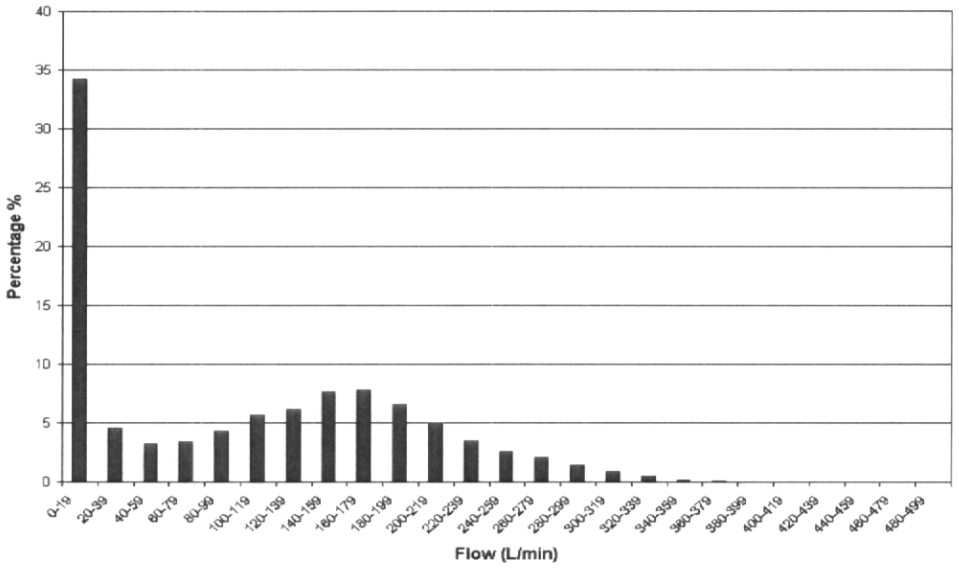

Figure 3. Flow rate percentages exhibited by 24 subjects working at 80-85% $\dot{V}O_2$ max without wearing a respirator. A flow rate in the range of 360-379 L/min is discernable from the graph.

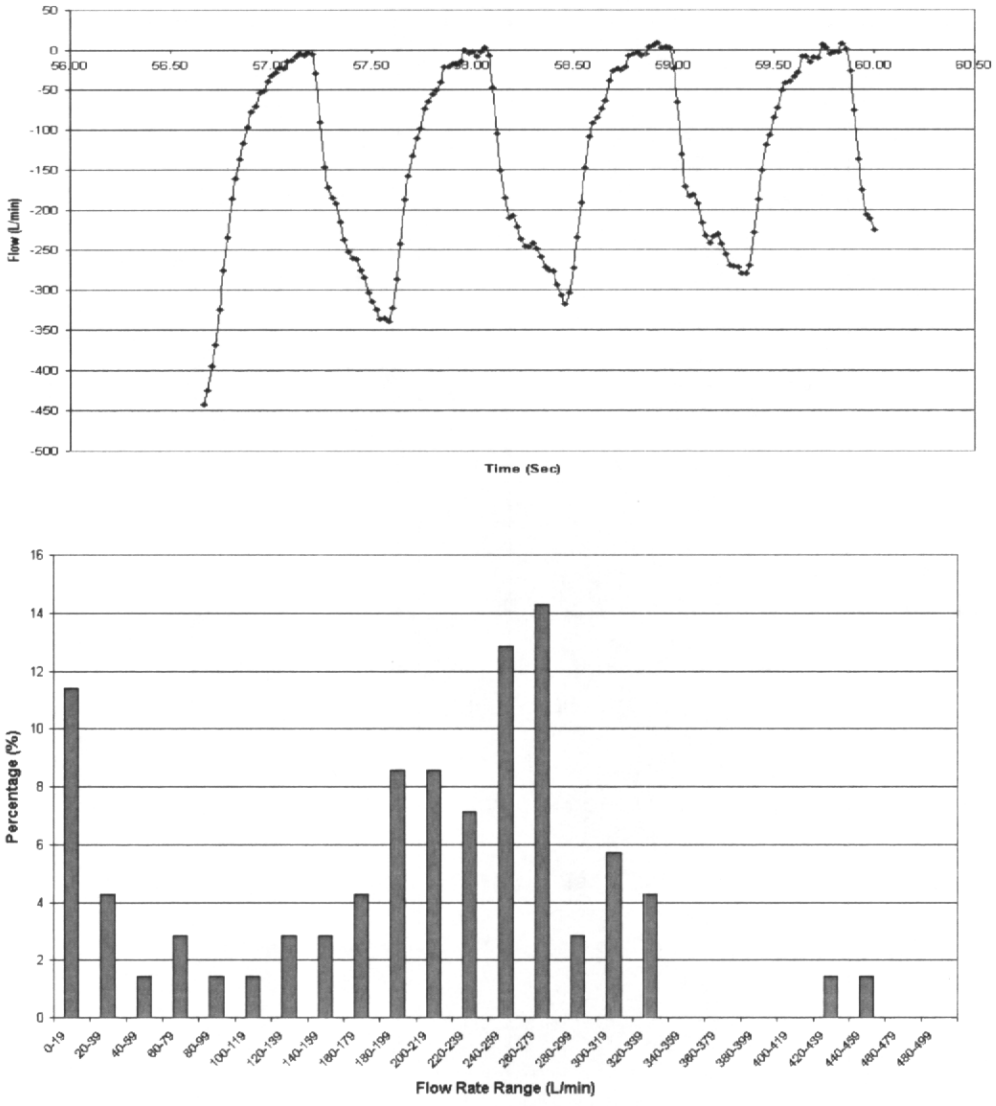

Figure 4. Composite of flow rate with time as measured on one subject (a) contrasted with the percentage of flow rates in range groups (b). The flow waveform cannot be inferred from the percentages of flows.

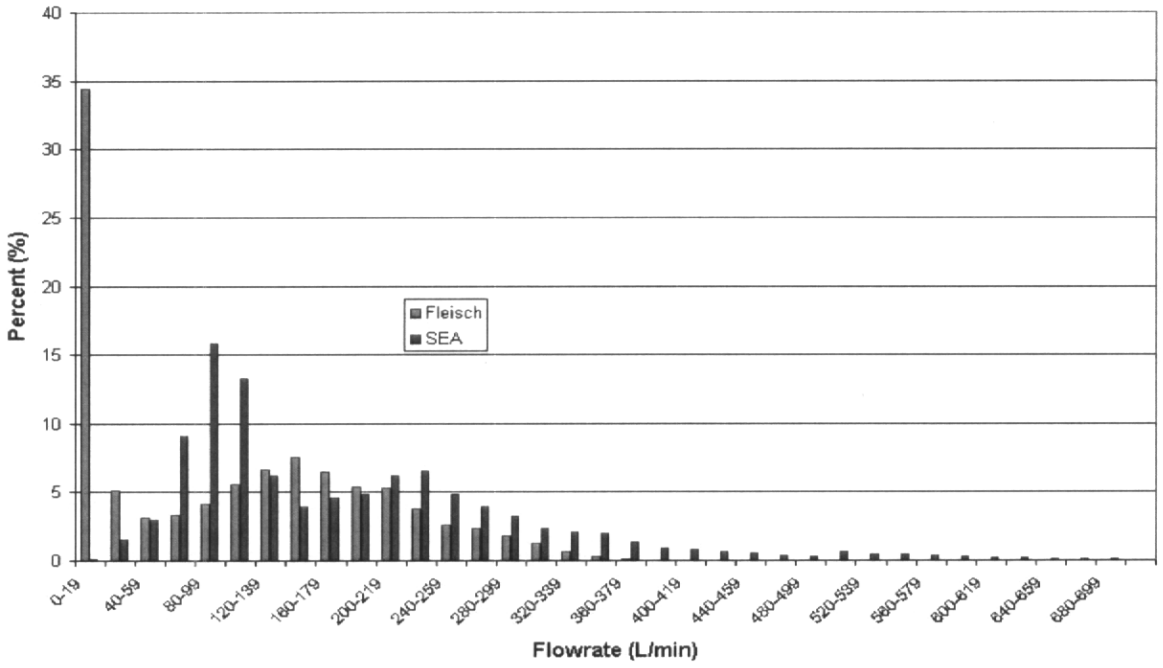

Figure 5. Flow rate percentages for ten subjects wearing the SE-400 breathing demand PAPR (darker bars) compared to data from the same ten subjects without wearing a respirator (lighter bars). Flow rates are higher with the PAPR.

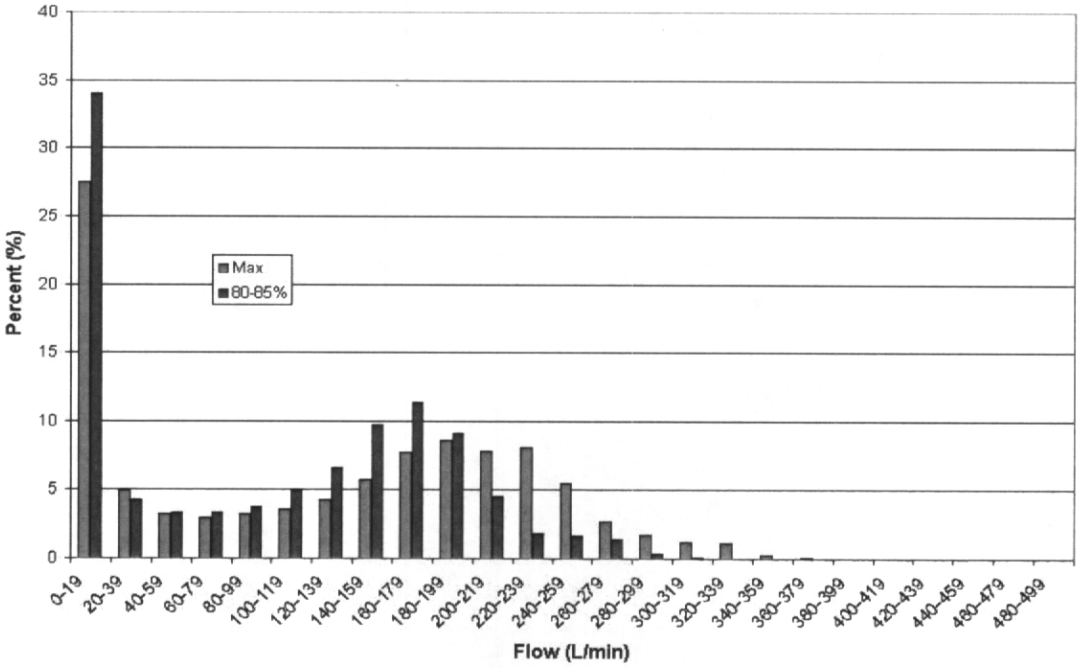

Figure 6. Flow rate percentages for nine subjects at 100% $\dot{V}O_2$ max when not wearing a respirator (light bars). For comparison, data from the same subjects at 80-85% $\dot{V}O_2$ max are plotted as well (darker bars). Flow rates at 100% $\dot{V}O_2$ max exceed flow rates at 80-85% $\dot{V}O_2$ max.

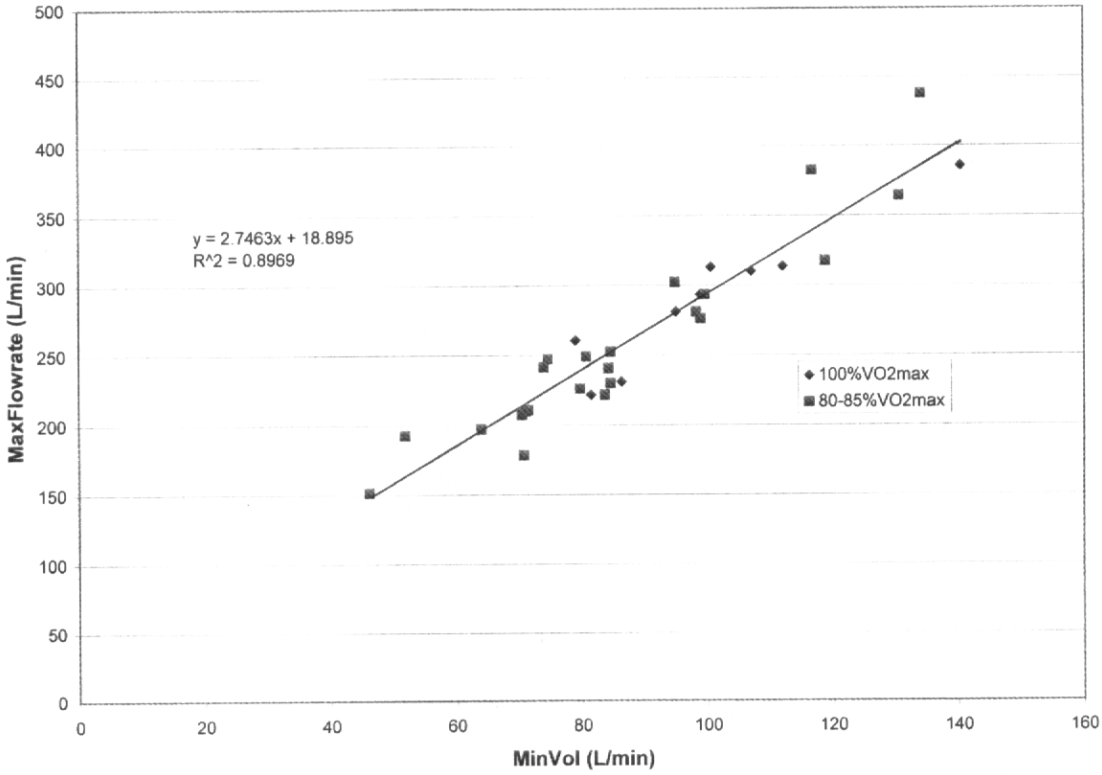

Figure 7. Maximum recorded flow rate for each subject related to average minute volume for subjects at 80-85% $\dot{V}O_2$ max (squares) and 100% $\dot{V}O_2$ max (diamonds). The presence of a strong predictive relationship between these two variables indicates a similarity of breathing waveshapes among the subjects. Peak flow rates persist for a very short time.

APPENDIX 5

Effects PAPR Helmet Weight on Voluntary Performance Time
at 80-85% of Maximal Aerobic Capacity

Arthur T. Johnson
Professor
William H. Scott
Faculty Research Assistant
Frank C. Koh
Faculty Research Assistant
Erica B. Francis
Graduate Research Assistant
Erika R. Lopresti
Graduate Research Assistant
Stephanie J. Phelps
Graduate Research Assistant

Biological Resources Engineering
University of Maryland
College Park, MD 20742
USA

Contact Information
Arthur T. Johnson
Biological Resources Engineering
University of Maryland
College Park, MD 20742
tel: 1-301-405-1184

FAX: 301-314-9023

email: artjohns@umd.edu

Abstract:

Powered Air Purifying Respirators (PAPRs) sometimes locate weights of blower, batteries, and filter on the head. When recommending that more powerful equipment be used, the result is usually more mass carried on the head. To date, none have determined the performance time penalty caused by extra mass even though there are many reports to determine the metabolic effects of added weight on the head. This study was performed to evaluate possible work performance time using several helmet weights at 80-85% $\dot{V}O_2$max . Nine subjects were tested with four weighted helmets of 0.54, 1.03, 1.85, and 3.36 kg. This study showed that performance time in minutes was linearly related to helmet mass:

$$t_{perf} = 20.25 - 2.552*kg$$

Each additional kilogram of mass resulted in 2.5 minutes less time. The comfort of the helmet also decreased as mass increased.

key words: respirator mask, ergonomics, work capacity, load

Introduction

Protective helmets are usually light weight (about 300g) and strong enough to provide head protection against dropped objects. When combined with protection against other health and safety risks (for example, respiration, vision, and hearing), the weight carried on the head can become burdensome. There are commercially-available powered air-purifying respirators (PAPRs) that locate the filter, blower, and battery in the helmet, thus placing the weight of these components on the head. Despite the fact that light loads placed on the head, high on the back, or otherwise distributed around the center of mass of the body, are carried relatively efficiently (Martin, 1985; Soule and Goldman, 1969), the extra weight does require additional energy expenditure. If an attempt is made to improve helmet PAPR respiratory protection, the additional hardware weight is likely to have some effect on work performance while wearing the device. The intent of this study was to determine how much penalty was to be paid for the recommendation of improved respiratory protection when the filters, blowers, and batteries are located in the helmet.

High work rates of about 80-85 percent of maximal aerobic capacity have been found to be the most sensitive range to test the respiratory burden of respirator masks (Johnson, 1991). Because the basic concept related to this study is a trade-off between the potential beneficial effects of increased blower flow rate and the burden of additional weight needed to power the blower, this study was conducted at the same high work rate that is used for respiratory testing of respirator masks.

Methods

Nine volunteers agreed to take part in this investigation. Of these, six were males and three were females. Their ages ranged from 20 to 42, with average of 24.8 years and 7.8 years standard deviation. Their heights averaged 168 cm ± 12 cm (std. dev.) with a 138-178 cm range. Their masses averaged 71.3 kg ± 13.6 kg, with range of 52.3 to 93.2. Their maximum oxygen uptakes averaged 3.01 L/min ± 1.02, with range of 1.91-4.87 L/min. They can be described as young, healthy, and reasonably fit. They also had little or no previous experience with occupational helmet wear.

Participants were asked to report to the laboratory on five separate occasions to perform one maximal aerobic capacity test and four weighted-helmet sessions at 80-85% of maximal aerobic capacity. The test protocol was approved by the University of Maryland Institutional Review Board.

Maximal Oxygen Consumption

A Quinton (Bothell, WA) motorized treadmill was used to determine subject maximal aerobic capacity. The participant was allowed to warm-up at approximately 60% of his or her age-predicted maximal heart rate response. A brief stretching period was permitted immediately following the completion of the warm-up phase. Next, the participant was asked to wear a Hans Rudolph (Kansas City, MO) mask configured with a one-way breathing valve. This configuration permitted the collection of expiratory air, which was directed to a mixing chamber using a flexible airflow tube. A Fleisch pneumotach (Phipps and Bird; Richmond, VA) was used to measure expired airflow and a mass spectrometer (Perkin-Elmer 1100; St. Louis, MO) analysed expiratory gas

concentrations. A computer determined oxygen consumption based on flow and gas concentration values.

Prior to the start of the experiment, a maximal oxygen consumption test ($\dot{V}O_2$max test) was performed on each subject using a Quinton (Bothell, WA) motorized treadmill and a modified Bruce incremental treadmill exercise protocol. Subjects were asked to warm-up and stretch for approximately 5-10 minutes prior to the start of the test, and were then equipped with a Hans Rudolph (Kansas city, MO) one-way breathing valve configured with a rubber adaptable mouthpiece. This apparatus was interfaced with a standard Fleisch (Phillips and Bird, Richmond, VA) pneumotach and Perkin Elmer (Pomona, CA) model 1100 mass spectrometer to monitor continuous expired airflow.

The initial work rate was established at a speed and grade designed to elicit 60% of the participant's age-predicted maximal heart rate. The work rate was adjusted by increasing the treadmill grade (1-2%) and speed (0.09 to 0.13 m/sec) every third minute until the participant experienced volitional fatigue, failed to display a rise in oxygen consumption rate of 150 mL O_2/min or more in accordance with the increase in work rate, or exhibited cardiovascular responses that contraindicated further assessment.

Helmet-Weight Sessions

Participants were asked to report to the lab on four separate occasions to exercise at 80-85% of maximal capacity while wearing a typical construction helmet (Model V-GARD; MSA, Pittsburgh, PA) modified with lead weights for helmet plus weight totals of 0.54, 1.03, 1.85, or 3.36 kg (Figure 1). The weights were located inside the helmets to minimize the possibility that the subjects could immediately recognize the treatment

levels and adjust their efforts accordingly. All participants were asked to warm-up for approximately 5 minutes on the treadmill at 60% of his or her age-predicted maximal heart rate before they were given a weighted helmet. The order of the weights was randomized, and subjects could not tell the sizes of the weights from visual cues external to the helmets to minimize the possibility that the subjects could immediately recognize the treatment levels and adjust their efforts accordingly. A strap around the chin was used to help keep the helmets in place on their heads. Next, the participant was asked to begin walking on the motorized treadmill programmed at a work rate corresponding to the warm-up exercise intensity. The treadmill was adjusted to the appropriate exercise intensity (80-85% maximal oxygen consumption) during a 90 second ramping phase. Treadmill speed and grade to elicit 80-85% $\dot{V}O_2$max were determined during the $\dot{V}O_2$max test. Thereafter, treadmill speed and grade remained the same for each subject through the different treatments. Participants were asked to exercise at this intensity until they experienced volitional fatigue or were no longer able to tolerate the helmet. Heart rate was continuously tracked during the session using a Hewlett Packard (Siemens, Andover, MA) Patient Monitoring System. Participants were asked to provide numerical subjective feedback on physical exertion and helmet comfort (appendix) every two minutes while performing the exercise task. The Borg Rating of Perceived Exertion Scale (6-20) was also periodically administered.

Performance time data were analyzed with standard analysis of variance (ANOVA) procedures. The level of statistical significance was set at p=0.05 (probability of a Type I error is one out of 20). Pairs of means were tested with the Student's t-test.

Linear regression was used to obtain the quantitative information that was the objective of this study.

Although it is not expected that helmet-placed hardware would ever be as heavy as the weights used in this study, a wide range of weights was used in order to give the best chance to separate weight effects from experimental variability. The applicable range of any conclusions drawn from these data would be wide enough to accommodate any realistic helmet weights commercially used.

Results

In Figure 2 can be seen the decrease in performance times for the four weighted helmets. A linear least square regression line to describe the data was:

$$\text{time} = 20.25 - 2.552 * \text{kg} \qquad (1)$$

Thus, each additional kilogram mass on the head could be expected to result in 2.5 min performance penalty at this rate of work.

An Analysis of Variance indicated that the different weighted helmet treatments affected performance times at a probability level of $p = 0.07$. This result did not meet the established level for statistical significance, but did show a tendency for different helmet weights to affect performance time. When performance times for pairs of means were tested with one-tailed t-tests, the only two that failed to achieve statistical significance of $p = 0.05$ were performance times with the two lightest weights, and the two heaviest weights. The other four paired comparisons were statistically significant.

A summary of test results appears in Table I. Helmet comfort degraded monotonically during the test for each helmet condition. Helmet comfort scale values

taken four minutes into the test, when all subjects were still participating, show that helmet comfort degraded from an average of 6.1 (fairly comfortable) for the lightest helmet to 1.2 (very uncomfortable) for the heaviest. Helmet comfort values taken when subjects voluntarily terminated their tests ranged from 4.4 (neutral) for the lightest helmet to 1.4 (very uncomfortable) for the heaviest. An ANOVA relating helmet comfort at four minutes to helmet weight indicated that the effects were statistically highly significant ($p = 0.000007$). Paired t-tests indicated that all paired comparisons were statistically significant ($p \leq 0.05$). Termination helmet comfort values were also statistically significant ($p = 0.05$) but the only statistically significant paired comparisons were those involving the lightest helmet with each of the others.

One observation that could have some importance is that the helmets, especially the heaviest, often slipped to one side of the head or the other during testing. Thus, the chin strap was necessary to assure that the helmets stayed on the heads. Helmet slippage however, may have contributed to lower comfort values.

Ratings of Perceived Exertion (RPE) at four minutes were nearly indistinguishable for all helmet conditions. The same was true for termination values. Normally, if there was an RPE difference to be seen, it would have been seen before termination. Equal values at termination indicate equal effort by subjects, and values are usually close to maximum (18-20). These values indicate that helmets had little effect on the effort invested by the subjects.

Discussion

Data from this simple test has provided the information needed to make recommendations to improve protection of wearers of multifunction PAPRs. For instance, one commercially-available multifunction PAPR is the Centurion MAX (Martindale Protection, Norfolk, UK) worn voluntarily by some U.S. coal miners. This PAPR includes a helmet, eye-protection visor, hearing protection, and respiratory protection against dust. A blower, battery, and filter are located in the helmet. This entire apparatus weights 1.7 kg. Our data would indicate that the penalty for working intensely while wearing the Centurion MAX is about 4 min. If additional respiratory protection were to be added, increasing the size and weight of the blower, battery, and filter, then an additional performance penalty of about 2.5 min. could be expected for each one kilogram increment in mass. Given that people would be expected to be able to work at 80-85% $\dot{V}O_2$max for 15-25 minutes, this additional time penalty can be significant.

This study was conducted at an exercise rate (90-85% $\dot{V}O_2$max) that is normally used in our laboratory for respiratory stress (Johnson, 1991; Johnson et al., 2005A). Work at this intensity cannot be sustained for a very long time, and thus is not representative of average work activities. Work rates can, however, peak this high during periods of high exertion, and these are often critical to work performance or even survival. Immediately coming to mind are fire fighting and military operations. There are times, as well, that miners or construction workers must work very hard. It is during these periods of intense activity that weight of equipment located on the helmet can be important.

Although the rate of work used in this study was high, it is at this high rate of work that additional respiratory protection would be most needed. Previous studies have shown that peak inspiratory flow rates at 80-85% $\dot{V}O_2$max can be expected to be up to 440 L/min (Johnson et al., 2005A). The Centurion MAX has been found to deliver about 110 L/min (Mackey et al., 2005), producing a shortfall of about 330 L/min. The result is that unfiltered air is supplied to the wearer from outside the visor.

It is always instructive to compare one's test results against others in the literature. Carrying weights, including on the head, has been the subject of many previous studies. These, however, have been concerned mostly with metabolic effects and not with performance times. Human load carrying is important for certain underdeveloped regions of the world (Heglund et al., 1995; Maloiy et al., 1986; Charteris et al., 1989; Datta et al., 1975; Malville et al., 2001) and the military (Stevenson et al., 2004; Reid et al., 2004; Knapik et al., 2004; Stauffer et al., 1987). As long as the weight is carried such that force it represents falls within the center of mass of the body, most investigators have found no additional metabolic penalty of the load other than the actual cost of the load (Maloiy et al., 1986; Soule and Goldman, 1969); that is, a load representing 20% of body weight increased the rate of energy consumption by 20%. Carrying loads outside the body center of mass was accompanied by increased cost (Abe, et al., 2004).

Under certain circumstances, however, an increase in load carried was not accompanied by increased oxygen consumption. Certain African women who carry loads routinely on their heads have apparently developed biomechanical adjustments that allow them to carry up to 20% of their body weights without additional energy cost (Heglund et

al., 1995; Maloiy et al., 1986; Charteris et al., 1989). For loads greater than 20% of body mass, the first 20% can be subtracted from the load cost. There also appears to be an interaction between load carried and walking speed (Abe et al, 2004; Griffin et al., 2003).

Although results in Figure 2 might suggest a nonlinear relationship between helmet weight and mean performance times, a simple linear relationship was used because of several reasons. First, the large variances of the results, and, second, the small number of conditions make it hard to justify more complex mathematical treatment. Increases in oxygen consumption accompanying greater carried weights would, perhaps, be reason to fit the data with a hyperbolic relationship, but, again, such an expression would be highly speculative.

If the regression line in Figure 2 is extrapolated back to zero mass carried, then unencumbered performance time would have been about 20.3 min. The heaviest helmet reduced performance time to 12.2 min, a 60% decrease. Because the previous references related to energy expenditure and not the maximum time that the load could be carried, there is no real comparison that can be made.

To investigate this issue quantitatively, we can use the Kamon formula that relates time to exhaustion to relative oxygen consumption (Johnson, 1991):

$$t_{exh} = 120\left(\frac{\dot{V}O_2 max}{\dot{V}O_2}\right) - 117 \qquad (2)$$

where t_{exh} is in minutes.

Average $\dot{V}O_2$ max for our subjects was 3.01 L/min, and unencumbered subjects would perform (t_{exh}) for 20.3 min (extrapolated). Thus, the estimated average oxygen consumption ($\dot{V}O_2$) for the unencumbered condition calculates to be 2.63 L/min. This

turns out to be 2.63/3.01 = 87% $\dot{V}O_2max$, which is nearly equal to the target work rate of 80-85% $\dot{V}O_2max$.

Obviously, subjects in this study did not react as those African women. The heaviest weighted helmet was 3.36 kg, or 5% of average body mass. Adding 5% to the estimate of the unencumbered oxygen consumption gives (2.63)(1.05) = 2.76 L/min for the heaviest helmet. Plugging this back into the Kamon formula gives a performance time (t_{exh}) of 13.8 min. The actual average performance time for this condition was 12.2 min. There is an apparent (13.8 – 12.2/13.8) = 11% performance time penalty for carrying the heaviest weight on the head compared to the predicted value. The oxygen consumption value that gives a performance time of 12.2 min is 2.80 L/min, or a (2.80 – 2.63)/2.80 = 6% increase in oxygen consumption for a 5% increase in mass carried. Results of these calculations are encouraging because the values are reasonable.

Conclusion:

Voluntary performance time decreased as the mass held on the head increased. Each additional kilogram mass decreased average performance time by about 2.5 min.

Funding Source

This work was funded in part by the National Institute for Occupational Safety and Health (NIOSH Contract 200-2002-00531).

Appendix: Helmet Comfort Scale (Johnson et al., 2005B)

10	very, very comfortable
8	very comfortable
6	fairly comfortable
4	fairly uncomfortable
2	very uncomfortable
0	very, very uncomfortable

References

Abe, D., Yanagawa, K, Niihata, S., 2004. Effects of load carriage, load position, and walking speed on energy cost of walking, Appl. Ergon. 35(4), 329-335.

Charteris, J., Scott, P. A., and Nottrodt, J. W., 1989. Metabolic and kinematic responses of African women headload carriers under controlled conditions of load and speed. Ergonomics, 32(12): 1539-1550.

Datta, S. R., Chatterjee, B. B., Roy, B. N., 1975. Maximum permissible weight to be carried on the head by a male worker from eastern India, J. Appl. Physiol. 38(1): 132-135.

Engels, H. J., Smith, C. R., Wirth, J.C., 1995. Metabolic and hemodynamic responses to walking with shoulder-worn exercise weights: a brief report, Clin. J. Sport Med. 5 (3), 171-174.

Falola, J. M., Delpech, N., Brisswalter, J. 2000. Optimization characteristics of walking with and without a load on the trunk of the body, Percept. Mot. Skills 91(1), 261-272.

Griffen, T. M., Roberts, T. J., Kram, R. 2003. Metabolic cost of generating muscular forces in human walking: insights from load-carrying and speed experiments, J. Appl. Physiol. 95(1), 172-183.

Heglund, N. C., Willems, P. A., Penta, M., Cavagna, G. A. 1995. Energy-saving gait mechanics with head-supported loads, Nature 375(6526), 52-54.

Johnson, A. T., 1991. *Biomechanics and Exercise Physiology*, Wiley, New York, available at www.bre.umd.edu/johnson.htm.

Johnson, A. T., Koh, F. C., Scott, W. H., Mackey K. M.. Chiou, K. Y. S., and Rehak, T. 2005A. Inhalation flow rates during strenuous exercise, J. ISRP 22:79-96.

Johnson, A. T., Scott, W. H., Phelps, S. J., Caretti, D. M., and Koh, F. C. 2005B. How is respiratory comfort affected by respiratory resistance? J. ISRP. 22::38-46.

Knapik, J. J., Reynolds, K. L., Harman, E. 2004. Soldier load carriage: historical, physiological, biomechanical, and medical aspects, Mil. Med. 169(1), 45-56.

Mackey, K. R. M., Johnson, A. T., Scott, W. H., Koh, F. C. 2005. Overbreathing a loose-fitting PAPR, J. ISRP 22:1-10.

Maloiy, G. M., Heglund, N. C., Prager, L. M., Cavagna, G. A., Taylor, C. R. 1986. Energetic cost of carrying loads: have African women discovered an economic way?, Nature 319(6055): 688-689.

Malville, N. J., Byrnes, W. C., Lim, H. A., Basnyat, R. 2001. Commercial porters of eastern Napal: health status, physical work capacity, and energy expenditure, Am. J. Hum. Biol. 13(1), 44-56.

Martin, P. E., 1985. Mechanical and physiological responses to lower extremity loading during running, Med. Sci. Sports Exer., 17, 427-433.

Reid, S. A., Stevenson, J. M., Whiteside, R. A. 2004. Biomechanical assessment of lateral stiffness elements in the suspension system of a backpack, Ergonomics 47(12), 1272-1281.

Soule, R. G., Goldman, R. F. 1969. Energy cost of loads carried on the head, hands, or feet, J. Appl. Physiol. 27, 687-690.

Stauffer, R. W., McCarter, M., Campbell, J. L, Wheeler, L. F. Jr. 1987. Comparison of metabolic responses of United States military academy men and women in acute military load bearing, Aviat Space Environ. Med. 58(1): 1047-1056.

Stevenson, J. M., Bryant, J. T., Reid, S. A., Pelot, R. P., Morin, E. L., Bossi, L. L. 2004. Development and assessment of the Canadian personal load carriage system using objective biomechanical measures, Ergonomics 47(12): 1255-1271.

Figure Captions

Figure 1. Photograph showing the inside of one of the helmets used in this study. Additional weight was affixed on the inside of the helmet where subjects could not immediately see which weight was being tested. The lead weight was enclosed in plastic and held in place with a bolt through the helmet.

Figure 2. Average Performance Times for Four Different Helmet Weights

Table I: Summary of Test Results

	Helmet Weight (kg)			
	0.54	1.03	1.85	3.36
Performance Time	17.9	20.2	13.5	12.2
(min)	±6.5	±10.1	±5.4	±4.5
RPE (4 min)	14.3	14.1	15.3	15.2
	±1.3	±1.3	±1.5	±1.6
RPE (termination)	19.2	19.1	18.9	18.2
	±0.67	±0.78	±1.2	±1.3
Helmet Comfort	6.1	4.9	3.6	1.2
(4 min)	±1.8	±1.5	±2.1	±1.3
Helmet Comfort	4.4	3.0	1.7	1.4
(termination)	±3.0	±2.4	±1.6	±2.6

Values given are means ± std dev. All values were obtained from nine subjects.

Figure 1. Photograph showing the inside of one of the helmets used in this study. Additional weight was affixed on the inside of the helmet where subjects could not immediately see which weight was being tested. The lead weight was enclosed in plastic and held in place with a bolt through the helmet.

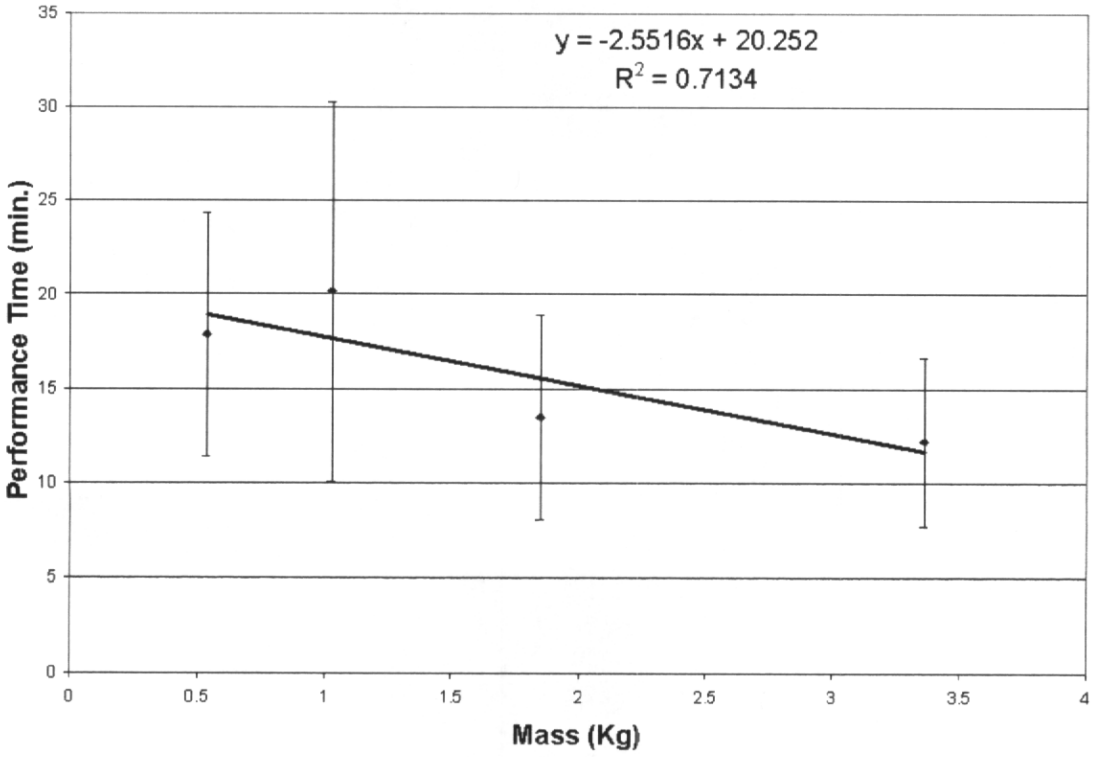

Figure 2. Average Performance Times for Four Different Helmet Weights

APPENDIX 6

Flow Visualization in a Loose-Fitting PAPR

Frank C. Koh
Faculty Research Assistant

Arthur T. Johnson
Professor
Fischell Department of Bioengineering
University of Maryland
College Park, MD 20742

Timothy R. Rehak
General Engineer
National Personal Protection Technology Laboratory
National Institute for Occupational Safety and Health
Pittsburgh, PA

Corresponding author:
Arthur T. Johnson
Fischell Department of Bioengineering
University of Maryland
College Park, MD 20742
tel: 301-405-1184
email: artjohns@umd.edu

Abstract

Two loose-fitting powered air-purifying respirators were challenged with a glycerol fog to determine flow pathways and amounts within the face pieces. Fog was drawn from the environment around the respirator by either a steady vacuum (to determine flow pathways) or a breathing machine (to determine inhaled amounts). Movement of the fog within the face piece was captured by digital video and examined frame-by-frame. It was found that the loose-fitting PAPR without a scarf offered no protection against the fog, whereas the PAPR with a scarf allowed up to 1.4 L of inhaled breath before the fog reached the mouth. Tilting the head affected the amount of protection given by the PAPR. It was concluded that this PAPR could offer some protection to the wearer in a nonthreatening contaminant situation.

Introduction

Loose fitting powered air-purifying respirators (PAPRs) have the advantages that they never restrict breathing of the wearer, and they can accommodate items, such as normal eyeglasses, worn on the face. Air drawn by a blower through a filter is blown across the face and intersects the normal path for breathed air to enter the mouth. Thus, under quiet circumstances, the air that is inhaled should be filtered air. When exertion increases and breaths become deeper, however, there is little to impede contaminated air from mixing with the filtered air. Most loose-fitting PAPRs incorporate a face shield and some have a cloth scarf spanning the gap between the face shield and face or neck to block contaminated air from entering the vicinity of the mouth.

Mackey et al. (2005) published a report about overbreathing a multifunction, loose-fitting PAPR, the Centurion MAX (Martindale Protection; Thetford, Norfolk, UK). They reported that all sixteen subjects inhaled more air than was supplied by the PAPR blower. In the same paper they also reported a measured volume inside the face shield of 1.4 L. They contended that if the whole 1.4 L was protective, then the problem of overbreathing would be minimal. This condition would have required diffuse, nonpreferential flow of outside air into the face piece.

The Racal Air-Mate 3 (Frederick, MD) loose-fitting PAPR is no longer commercially available, but differs from the Centurion MAX in that there is no scarf and ear muffs. Thus, a difference in the amount of outside air, and the pathway taken by that air could be anticipated when comparing these two PAPRs.

Visualization of flow pathways requires generation of visible fine particles and introducing them in the air outside the face piece. The paths taken by these particles

must then be able to be seen as they cross the face enroute to the mouth. Fortunately, the face shields for these two PAPRs are transparent.

Several different particle generation schemes were considered. One that was attempted and failed was to introduce cold, moist outside air into warm, moist air resident inside the face shield. The expected fog never formed. Another scheme was to burn incense candles and hold them near the PAPR periphery. This method was successful in that the smoke could be seen entering the face piece and flowing to the mouth. However, it had the disadvantage that points of entry of smoke into the face piece were not spontaneous, but depended upon where the candle was held. Aerosolized mineral oil was also attempted. The particles generated by the oil was dense and diffuse. This method had much to recommend it, but left an oily residue on all surfaces contacted by the smoke. Eventually, a glycerol fog was generated with a machine designated for theatrical use.

The objective of this paper is to report on the results of flow visualization in two loose-fitting PAPRs. From these results, conclusions may be drawn about the protection afforded by the dead volume within the face shield.

Methods

These tests were all conducted with the Centurion MAX and Racal AirMate 3 respirators mounted on a medium-sized head form (Krug Life Sciences; Houston, TX). The head form was covered with black electric tape to increase visibility of the fog and not damage the original head form surface. A green light emitting diode (LED) was attached to the upper lip of the head form with the electrical wiring tucked under the

black electric tape. This LED helped determine timing of the video frames during data analysis. A one inch long thin string/wick taped to the base of the bottom lip of the head form mouth fluttered in the direction of the breathing phase and helped identify inhalation or exhalation. The LED and string is shown in Figure 1.

Video images of the visualized flow inside the face piece were recorded digitally with a Sony (Tokyo, Japan) DCR-HC90 AVI-protocol camera with 3 megapixel resolution. The camera was aimed through the visor (face shield) of the respirator and focused on the area of the mouth. Two conventional desk lamps each with 75 watt incandescent bulbs were placed on either side of the head form above the eyebrow line and directed onto the head form through the visor. Darkening the room in which all this took place helped to minimize visor glare.

Once the respirator was placed on the head form, it remained unmoved until all tests were completed. This eliminated the possibility that differences in respirator placement would affect results.

Fog was introduced to the volume surrounding the respirator inside a portable breathing chamber (PBC) placed over the respirator and head form. The PBC has been described previously (Mackey et al., 2005), and consisted of a cylindrical plastic container with a rectangular transparent visor. In this case, the PBC visor was removed and the edges of the PBC were sealed to the respirator face shield with plastic wrap and transparent tape. This was done to keep a layer of fog from forming between the PBC visor and the respirator face shield. A 5 cm (2 inch) diameter opening at the top of the PBC and a gap around the neck at the bottom of the PBC were left open to allow outside

air to be supplied to the respirator, avoid pressure build-up within the PBC, and allow free flow of exhaled air and blower output.

The Fogstorm 1200 HD (Los Angeles, CA) generates about 200 m^3 (7000 ft^3) per minute of fog. In order to minimize the momentum of the fog that may influence the over breathed airflow pathway, a fog retention container was created. A six gallon food grade bucket acted as storage for the fog and allowed a passive flow of fog into the PBC. The bucket lid was modified with two holes. Inserted through one hole (inlet) was a 2.5 cm (1 inch) inner diameter tube that reached the bottom of the bucket. This hose connected to the fog machine and supplied smoke to the bottom of the bucket. The second hole on the lid was the outlet with 1.3 cm (0.5 inch) inner diameter. Connected to the outlet hole was a 2.5 cm inner diameter tube that was inserted into the PBC next to the head form spine. This allowed for an even distribution of fog throughout the PBC.

Two schemes of flow were used while the PAPRs were mounted on the head form. The first was steady inhalation flow caused when a vacuum line was connected to the flow pathway through the head form. This condition was used to ascertain the path taken by the fog into and inside the face piece. The PAPR blower was kept off to determine points where the fog entered the face area. The blower was then turned on, but the vacuum-induced steady flow was kept greater than blower flow to determine flow pathways inside the face piece.

The second condition was sinusoidal breathing during the time when the PAPR blower supplied air to the face area. This flow condition was used to determine the inhaled volume of air when the fog first reached the mouth. Blower flow rates were held constant. A dc power supply was set at 4.5v and ran the Centurion MAX blower at a

nominal 100 L/min. The battery terminals for the Racal AirMate 3 were not accessible, so the battery was fully charged and the blower supplied air at 211 L/min. A Krug Life Sciences (Houston, TX) breathing machine was used to provide a controllable breathing air flow to the PAPR.

Flow rates were measured with Fleisch (Phipps & Bird; Richmond, VA) pneumotachs and Validyne (Cupertino, CA) DP-15 pressure transducers. A Fleisch #3 pneumotach was used to measure the flow at the mouth of the head form, and was located upstream from, and on the distal side of, the head form. A Fleisch #4 pneumotach was used to measure PAPR blower flow rate. It was located at the inlet side of the blower and attached to the blower with a plastic adapter between the pneumotach and the inlet filter of the Centurion MAX. The pneumotach was placed in the supply hose of the Racal Air Mate 3, on the discharge side of the blower. A computer program using LabView 4 (National Instruments; Austin, TX) logged flow rate data. The electrical signal lighting the LED was also logged concurrently.

After the PAPR was fitted on the head form, the PBC was placed over the ensemble. The scarf that came with the Centurion MAX was put into place correctly: it was evenly centered, covering the gap between the face shield and chin, and had a small gap near the ear lobe and lower jaw line. It was loosely in contact with the head form beneath the chin. Fog was then introduced into the PBC. The Racal PAPR had no scarf.

Breathing machine minute volumes used were 31, 70, 89, 110, and 121 L/min. Respiration rates were held at 30 breaths/min for each minute volume. This would give tidal volumes of 1.5, 2.4, 3.0, 3.6, and 4.0 L for each condition.

It was suspected that head pitch (angle displacement up or down) and roll (angular displacement side to side) could affect preferential flow pathways. In order to test this supposition, the head form was tilted 5.9 degrees (pitch) and the side-to-side tilt (roll) was set at 4.8 degrees. Steady flow was used with the blower on to determine flow pathways inside the face piece. Pitch and roll measurements were made only with the Centurion MAX respirator.

Each image frame was frozen on the computer monitor using a program called Adobe Premiere Pro 1.5 (San Jose, CA). Close and careful scrutiny was needed to locate visually the fog on each frame. Sometimes the fog appeared as ghostly fingers (during constant flow) and other times as a wispy cloud (breathing). Pulsing of the LED visible on each frame was used to help determine corresponding times and flow rates from the breathing machine and PAPR blower.

Drawings were made of flow pathways by illustrating the sequences of fog locations on a frame-by-frame basis. Net flow rates were calculated by subtracting blower flow from breathing machine flow; this represented overbreathing air flow coming from the outside without passing through the PAPR filter. Inhaled volume was determined by accumulating breathing machine inhalation flow rate with time.

Results

Both respirators showed fog leakage under certain conditions (Figure 2). The scarf made a big difference, because fog was only apparent for the Centurion when breathing flow rate exceeded blower flow rate. The Racal device without the scarf was filled with fog under all conditions, whether the blower was operating or not, or when the

blower was operating and there was no inhalation flow rate (i.e., breath-holding). There are apparent regions of turbulence inside the face shield that tend to draw outside air into the face piece. In both instances, when fog entered beneath the face shield from the periphery, it appeared to flow to the front, hit the face shield, and curve back toward the mouth. Different layers of fog flowing in different directions were apparent simultaneously.

Flow pathways inside the Centurion were charted with the blower off and steady inhalation flow rate set at 18 L/min (Figure 3). Some leakages began at gaps between the visor scarf, and head form near the chin and under the ears. Fog flowed across the face and into the mouth. When the blower was turned on and steady inhalation flow exceeded blower flow, fog pathways were similar (Figure 4). Fog persisted within the face area as long as inhalation flow rate exceeded blower flow rate and fog was present outside the respirator.

There was a narrow two-inch strip in the center of the face from the blower outlet at the top of the forehead in the helmet of the Racal to the bottom of the chin that was free of fog when the blower was operating. Vigorous mixing of the fog leaking in from the periphery filled the remainder of the face area with fog and made further visual analysis difficult.

When the Centurion blower was operating, and the breathing machine was providing intermittent inhaled flow, fog entered the face area only when inhalation flow rate exceeded blower flow rate. Fog was expelled quickly from the face area when blower flow exceeded breathing flow (inhalation), and during exhalation. The leak points and fog pathways were similar to those depicted in Figure 4.

The accumulation of the residue drawn in by the over inhaled air, may interfere with vision. One side affect of fog entering the visor area of the PAPR was that the inside of the visor became deposited over time with food grade polyfunctional glycerol. One can imagine dusty or oily ambient conditions where this may happen while the respirator is being worn.

Of some interest is the volume of inhaled air that can be breathed before contaminated air reaches the mouth. In order to determine this volume, flow rate during each inhalation was accumulated and the volume noted when videos indicated that fog first reached the mouth. These tests were repeated for minute volumes of 31, 70, 89, 110 L/min at 30 breaths /min.

In Table I are found the results for ten determinations at each minute volume. Breathing machine inhaled volume averaged 1.4 L before the fog reached the mouth. Interestingly, this value equals the dead volume of the respirator as measured previously (Mackey et al., 2005). Whereas the fog reached the mouth for all minute volume settings, no fog entered the mouth for the smallest minute volume of 35 L/min. The volumes of contaminated air (air containing fog) inhaled into the breathing machine depended, of course, on tidal volume. These values also appear in Table I. There appeared to be no protection afforded by the dead volume of the Racal AirMate 3; fog reached the mouth and was inhaled at all minute volumes.

Head pitch and roll affected the volume inhaled before the fog reached the mouth (Table II). The leak points were similar to the steady state tests with vacuum flow greater than blower flow and the head form was level. As depicted in Table II with the breathing minute volume set at 121 L/minute and the Centurion blower flow set at 100

LPM, the head pitch changed the volume inhaled before the fog reached the mouth. Looking up by 5.9 degrees caused the fog to reach the mouth when 1.4 L was inhaled, whereas looking down by 5.9 degrees caused the fog to reach the mouth when 1.2 L was inhaled. The control condition of zero degrees showed a volume for the fog to reach the mouth to be about 1.6 L. The greatest contaminated (fog/air) volume of 1.74 L was inhaled when the head form looked down 5.9 degrees.

In Figure 5 is a composite diagram of flow rates and volumes in the Centurion MAX along with diagrams of progress of the fog within the face shield. As seen in the upper portion of the diagram, fog does not begin to enter the face piece until breathing machine flow rate exceeds blower flow rate. Fog moves toward the mouth as inhalation progresses, and eventually reaches the mouth toward the end of inhalation. The fog did not reach the mouth until after blower flow exceeded breathing machine flow. The fog inside the face piece dissipated during the exhalation portion of the cycle.

Discussion

There are two assumptions made with loose-fitting PAPRs that relate to this work. The first is that a loose-fitting PAPR with the blower operating offers respiratory protection, and the second is that once inhalation flow rate exceeds blower flow rate there is no further protection. Both proved to be incorrect in this study. The Racal AirMate 3 without a scarf to partially confine air inside the face area had fog sucked into the face area by flow turbulence. We can conclude that this respirator would offer very little protection even under conditions of light exertion and high blower flow rate. The Centurion MAX, with scarf in place, offered an average of about 1.4 L of tidal volume

before contaminated air would have been inhaled. This 1.4 L corresponds to the tidal volume present during moderate exertion, and so can be significant.

Even so, the range of measured inhaled volumes before contamination reached the mouth was 1.13 L to 1.71 L. In order to protect the head form under all measured conditions, tidal volumes of 1.13 L should not be allowed. However, we are not here to protect head forms, but to protect humans. Different humans have different facial configurations (and, presumably, respirator dead volumes) and some variability in placement of the helmet and scarf. Humans also tilt their heads and bodies, and move around. Tilting the head form was found to affect protective volume of the Centurion MAX. The conclusion from all this is that there is some protection afforded by this respirator, but that some safety factor should be applied in order to give a conservative estimate of protective dead volume. Based upon measurements made in this study, and taking into account the fact that the Centurion MAX is often used where the contaminant threat is not high, a protective dead volume of 1.0 L might be suggested.

Tight-fitting respirators can, under some conditions, be put on in contaminated atmospheres. The U. S. Army, for instance, used to train soldiers by having them remove their respirators in the presence of tear gas. The soldiers were then required to give their names, ranks, and serial numbers (always very quickly!), and then put their respirators back on. If enough air is held in the lungs during donning, then exhaled air can be used to purge the tight-fitting respirator of contamination.

There is no such possibility with a loose-fitting PAPR. The only way the dead volume of a loose-fitting respirator can be purged is with the PAPR blower. And it takes a while before the blower can remove all contamination in the PAPR dead volume.

Therefore, if the PAPR is to be put on in the presence of contaminants, the wearer should hold her or his breath while the blower removes contamination. We found that fog that entered the respirator dead space was not completely removed during the subsequent exhalation. That means that breath holding for a time period equal to several exhalations, or about 5 sec, would probably be required.

In comparing the Racal and Centurion, the benefit of some kind of face seal is very apparent. The Centurion, which contains both a loose face seal around the temporal bone and a loose seal around the mandible, limits the free motion of the contaminants from entering the visor area. However, when over breathing starts, the fog enters the visor area around the ramus and mandible. From visual observation, the fog that entered the visor due to over breathing seems to dissipate within the visor during exhalation. Whether all the fog that entered the visor was evacuated during the exhalation cycle is unknown.

One aspect about loose-fitting PAPRs that was underscored by this test is that it is difficult ahead of time to predict the contaminant threat faced by the wearer of one of them. One would think that the presence of flow from a blower would protect to some extent, but these results have shown that protection comes from enclosure of a certain volume, whether that enclosure be loose or tight. The presence of the Centurion MAX scarf makes the Centurion much more protective than the Racal, even though the Racal blower supplied a higher flow rate. Although proper placement of the scarf was not investigated, there is much more to be determined with further study. Certainly the wearer should be made aware of the importance of this piece of cloth.

A quick experiment was performed using the Centurion without its scarf. Fog reached the mouth quicker without the scarf; 1.2 L of air was inhaled before fog reached the mouth without the scarf as compared with 1.4 L with the scarf. The fog generally entered the facial volume in nearly the same place with or without the scarf.

Acknowledgement: This work was funded in part by the National Institute for Occupational Safety and Health (NIOSH) Contract 200-2002-00531.

Table I. Volume of Inhaled Air Before and After the Fog Reached the Mouth at Different Minute Volumes for the Centurion MAX Respirator. Each Value is the Result of Ten Independent Readings.

Minute Volume (L/min)	Tidal Volume (L)	Volume Inhaled Before Fog Reached Mouth (L)	Volume Inhaled After Fog Reached Mouth (L)
31	1.5	1.45 ± 0.045	0.00 ± 0.000
70	2.4	1.23 ± 0.057	0.43 ± 0.054
89	3.0	1.25 ± 0.149	0.81 ± 0.107
110	3.6	1.52 ± 0.065	1.10 ± 0.062
121	4.0	1.55 ± 0.106	1.54 ± 0.095
Avg.		1.40 ± 0.150	

Values given are means ± std. dev. Although fog reached the mouth at 31 L/min, no fog entered the mouth. The volume inhaled before fog reached the mouth and the volume inhaled after fog reached the mouth do not equal the tidal volume; the blower supplies the remaining volume difference.

Table II. Volumes of Air Before and After the Fog Reached the Mouth at Several Head Pitch and Roll Angles. Each Value is the Result of Ten Independent Readings. Breathing Minute Volume Was Set at 121 L/min with Tidal Volume of 4.0 L.

Condition	Volume Inhaled Before Fog Reached Mouth (L)	Volume Inhaled After Fog Reached Mouth (L)
Level	1.55 ± 0.106	1.54 ± 0.095
Down 5.9°	1.19 ± 0.093	1.74 ± 0.051
Up 5.9°	1.45 ± 0.256	1.55 ± 0.202
Side 4.8°	1.70 ± 0.090	1.39 ± 0.073

Values given are means ± std. dev.

Figure 1. Black head form with LED and fluttering string at the base of the bottom lip.

Figure 2. One frame of a video taken during a fog challenge test. This picture shows fog inside the face area of the Centurion MAX.

Figure 3. Fog flowed toward the mouth and circled around the eyes and curved back into the mouth when the Centurion blower was off and steady flow was set at 18 L/min.

Figure 4. Simplified diagram of fog across the face when the Centurion blower was producing 100L/min and the breathing flow was higher. Each figure depicts a different layer of fog flow within the visor and head form that was only visible when inhalation flow exceeded blower flow.

Figure 5. Flow and volume with time when the breathing machine overbreathed the Centurion MAX blower. The upper portion of the diagram represents flow rates of the breathing machine set at a minute volume of 31 L/min at 30 breaths/min. Net flow is the difference between blower flow (nominally 100 L/min) and breathing machine flow. Diagrams inserted at different points of the figure show progress of the fog towards the mouth. The lower portion of the diagram shows breathing machine accumulated inhaled volume during the same time period.

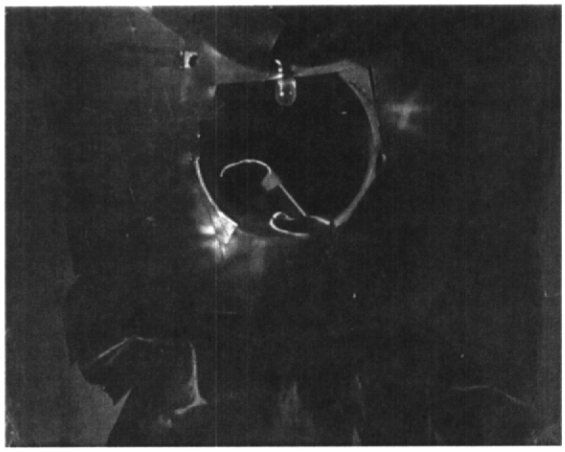

Figure 1. Black head form with LED and fluttering string at the base of the bottom lip.

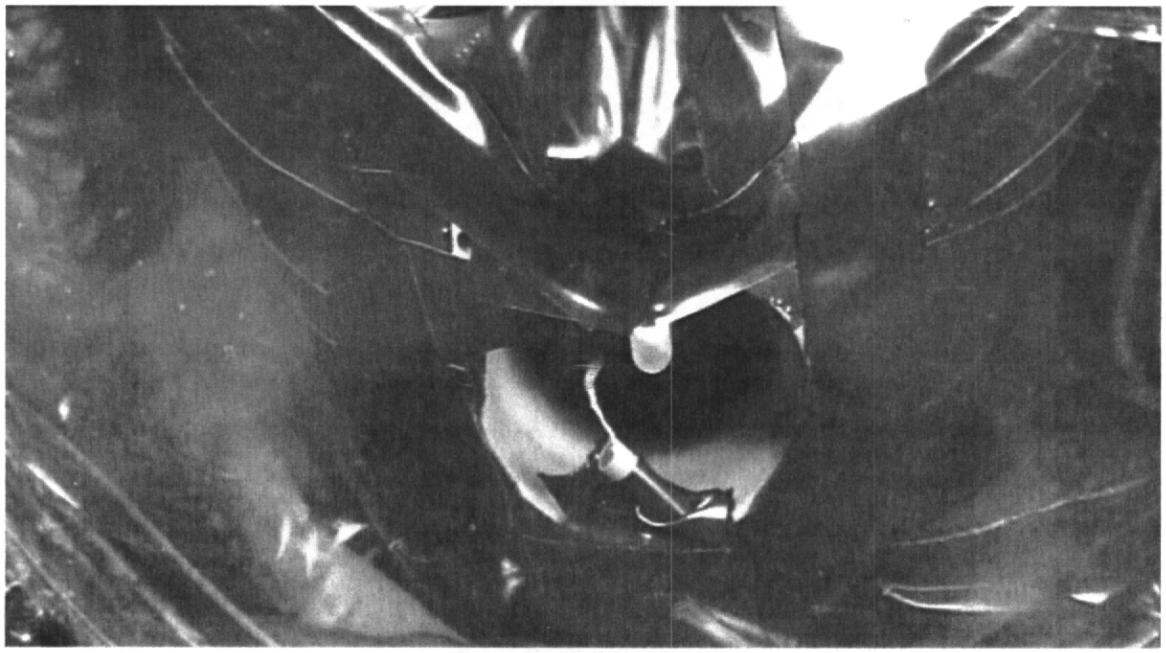

Figure 2. One frame of a video taken during a fog challenge test. This picture shows fog inside the face area of the Centurion MAX.

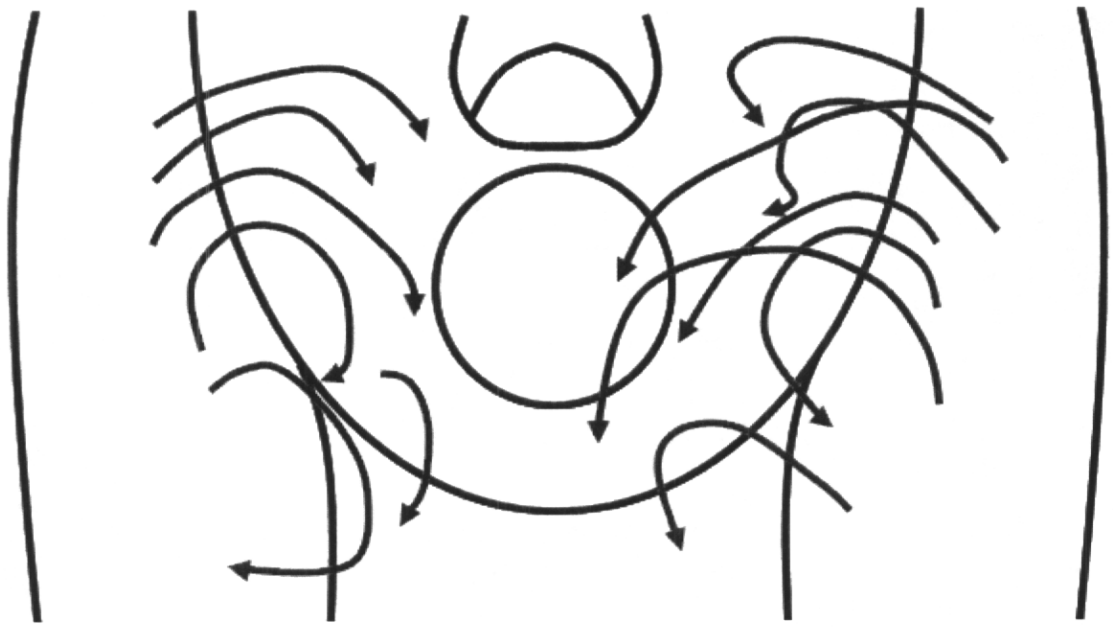

Figure 3. Fog flowed toward the mouth and circled around the eyes and curved back into the mouth when the Centurion blower was off and steady flow was set at 18 L/min.

Figure 4. Simplified diagram of fog across the face when the Centurion blower was producing 100L/min and the breathing flow was higher. Each figure depicts a different layer of fog flow within the visor and head form that was only visible when inhalation flow exceeded blower flow.

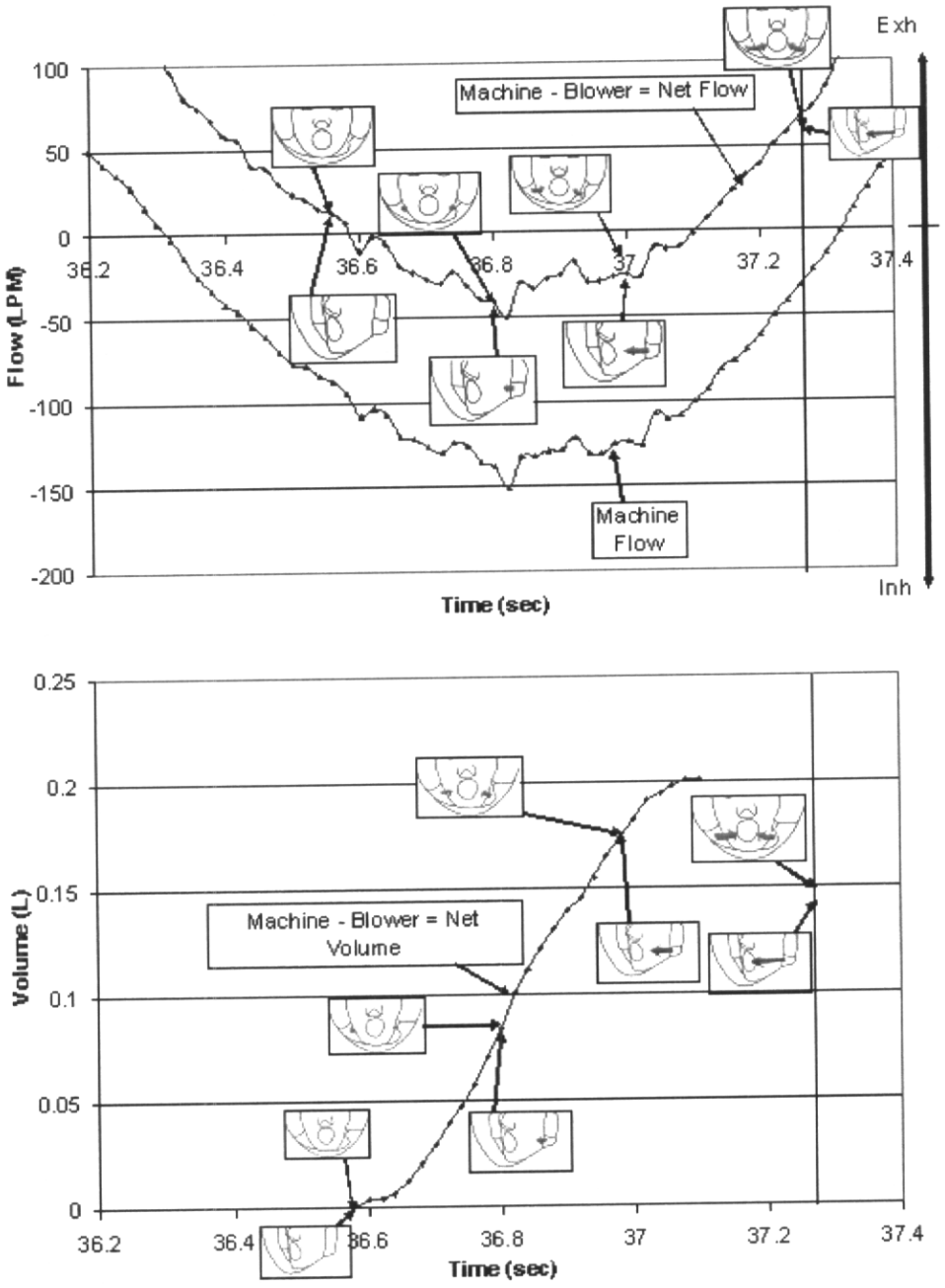

Figure 5. Flow and volume with time when the breathing machine overbreathed the Centurion MAX blower. The upper portion of the diagram represents flow rates of the breathing machine set at a minute volume of 31 L/min at 30 breaths/min. Net flow is the difference between blower flow (nominally 100 L/min) and breathing machine flow. Diagrams inserted at

different points of the figure show progress of the fog towards the mouth. The lower portion of the diagram shows breathing machine accumulated inhaled volume during the same time period.

References

Mackey, K. R. M., A. T. Johnson, W. H. Scott, and F. C. Koh, Overbreathing a Loose-Fitting PAPR, *J. ISRP* 22:1-10 (2005).

APPENDIX 7

Inward Leakage in Tight-Fitting PAPRs

Frank C. Koh
Faculty Research Assistant

Arthur T. Johnson
Professor
Fischell Department of Bioengineering
University of Maryland
College Park, MD 20742

Timothy E. Rehak
General Engineer
National Personal Protection Technology Laboratory
National Institute for Occupational Safety and Health
Pittsburgh, PA

Corresponding author:
Arthur T. Johnson
Fischell Department of Bioengineering
University of Maryland
College Park, MD 20742
tel: 301-405-1184
email: artjohns@umd.edu

Abstract

A combination of fog flow visualization and local flow measurement techniques was used to determine the inward leakage for two tight-fitting Powered Air-Purifying Respirators (PAPRs), the 3M Breathe-Easy PAPR and the SE 400 breathing demand PAPR. They were mounted on a breathing machine head form and flows were measured from the blower and into the breathing machine. Both devices leaked a little at the beginning of inhalation through their exhalation valves. In both cases, the leakage was not enough for fog to appear at the mouth of the head form. It was concluded that these devices would provide adequate protection for the wearer.

keywords: flow visualization, fog, pneumotach, respirator, protection factor.

Tight-fitting Powered Air-Purifying Respirators (PAPRs) can be used in situations where contaminated air must be filtered, yet the additional work of drawing air through the filter can be supplied by a battery-powered blower rather than the wearer's respiratory muscles. Tight-fitting PAPRs form a tight seal with the face, which should minimize exposure to contaminated air. Maintenance of a positive pressure within the facepiece portends that any face seal leakage that does occur flows outward rather than inward. Performance of work while wearing PAPRs in the heat is influenced also by the cooling flow of air across the face[1].

Despite these advantages, some doubts remain. Is the protection afforded by tight-fitting PAPR wear as good as it would seem? Is there opportunity for contamination to enter the facepiece and be inhaled by the wearer? What pathways might inward leakage, if it exists, follow?

In this study we have been motivated to explore these issues. Following the visualization of flow pathways in loose-fitting PAPRs[2], the attempt was made to detect contamination (represented by glycerol fog) within facepieces of tight-fitting PAPRs. The major hurdle to overcome is the fact that tight-fitting PAPRs almost always include visually-opaque facepieces, unlike loose-fitting PAPRs.

Methods

Two commercially-available tight-fitting PAPRs (SE 400; SEA, Meadowlands, PA; and 3M Breathe Easy; St. Paul, MN) were tested on a breathing machine head form (Krug Life Sciences; Houston, TX). The SE 400 PAPR is a breathing-demand device with a blower that adjusts to the breathing flow rates of the wearer. The 3M Breathe-

Easy PAPR has a blower that is supposed to supply a constant 114 L/min flow rate to the facepiece. The SE 400 blower was operated with a fully-charged battery; the 3M Breathe-Easy blower had accessible electrical connections and was attached to a dc power supply at 4.8 volts.

Both PAPRs were installed, in turn, on the head form and the head straps adjusted for tight, uniform fits (Figure 1). One set of measurements was made on each PAPR in this unmodified condition. Another set of measurements was made with ample modeling clay applied around the facepiece periphery to obstruct any inadvertent leaks formed at the face seal. A third set of measurements was made with clay to investigate exhalation valve leakage.

Two MedGraphics (St. Paul, MN) #5038773 pitot-tube flowmeters were used, one measuring blower flow to the facepiece and another measuring flow into the breathing machine. The difference between the two measured flow rates would be caused by leakage somewhere in the system. When inhaled flow rate exceeded blower flow rate, the leakage is inward. This difference, when integrated, gave the total volume of air leaked from the outside into the facepiece. The flow meter on the SE 400 was attached to the inlets of the filters with a custom-made adapter; the flow meter for the 3M Breathe Easy was inserted in the hose between the filter and the facepiece.

The entire breathing machine and PAPR was located inside a phone booth-sized box of dimensions 137 cm (54 in) by 76 cm (30 in) by 180 cm (71 in). The box was constructed of a wood frame with plywood walls. The upper part of the box was made from Lexan transparent plastic material in order to see what was going on inside.

Glycerol fog was formed with a Fogstorm 1200 HD (Los Angeles, CA) generator that can generate 200 m^3 fog per minute. This fog was introduced into the test chamber through a hose inserted through the side of the chamber. Fog permeated the entire atmosphere inside the chamber.

Of primary interest was the point at which fog reached the mouth. Because both PAPRs had opaque facepieces, a bronchoscope (Pentax model B011471; Asabi Optical, Tokyo, Japan) was placed inside the tube leading to the mouth of the head form, with its tip at the mouth and facing the cavity between the PAPR facepiece and the head form. The place where the bronchoscope penetrated the head form breathing tube was sealed around the bronchoscope with silicone sealant.

The bronchoscope consisted of a bundle of optical fibers that conducted light toward the tip and an image back from the tip. The image was converted into video form by a small television camera, and the resulting image displayed on a television monitor. Evidence of the presence of fog could be detected from the monitor.

Because it was difficult to adapt the bronchoscope television image to a form that permitted frame-by-frame analysis, a Sony (Tokyo, Japan) DCR-HC90 video camera with 3 megapixel resolution was used. An S-video jack on the monitor was plugged into the Sony camera and the signal was recorded digitally at 40 frames/sec.

Also included in the bronchoscope image were two light-emitting diodes (LEDs) located at the mouth of the head form. A green LED driven by a 10 Hz square-wave electrical signal was used to help synchronize recorded images. A red LED was connected to a comparator circuit that detected inhalation. In this way, image timing and

breathing phase were able to be known for sure. No accessory lighting was necessary to illuminate the dark inside of the facepiece.

Careful calibration of the flow meters was necessary because the difference in their readings was so important. Each flow meter was attached to a Validyne (Northridge, CA) DP-15 differential pressure transducer and a Validyne CD-12 demodulator transducer indicator. The transducer indicators produced an electrical voltage related to the transducer pressure. These were calibrated first with an inclined manometer; a T-connector was used to apply the same pressure simultaneously to both pressure transducers. Once the pressure transducers were calibrated and connected to the flow meters, both flow meters were calibrated with the same flow from the breathing machine. They were arranged in series with 3.8 cm (1.5 in) diameter, 38.1 cm (15 in) long pipes upstream from the flow meters, between the flow meters, and downstream from the flow meters. A Fleisch #3 (Phipps and Bird; Richmond, VA) pneumotach inside the breathing machine served as the flow reference.

For each of these tests, the Krug breathing machine was operated at 30 breaths/min and with a tidal volume of 2.25 L.

After it became apparent from the flow rate differential that there was a source of leakage into the facepiece, clay was used as an insurance seal around the facepiece periphery and the test repeated. When leakage was still detected, attention turned to the exhalation values. With modeling clay still in place, the test was again repeated, but the video camera was moved from the bronchoscope monitor and aimed at the exhalation valve so that it could detect valve actions. Duplicate green and red LEDs outside the facepiece maintained the ability to keep track of time and phase of the breathing cycle.

The exhalation valve cover from the 3M Breathe Easy was removed for better viewing. The valve cover from the SE 400 did not have to be removed, and was kept in place.

Results

Flow meter calibration required extra care. In Figure 2 is shown the relation between pressure and flow for one of the flow meters. A Pitot tube flow meter should theoretically relate pressure to the square of the flow. When negative calibration pressures were inverted, a complete parabola resulted (Figure 3). A quadratic regression equation forced through the origin gave a very high correlation coefficient. In order to check that both flow meters had identical characteristics, the two flow meters were connected in series to the breathing machine. From Figure 4, it can be seen that readings from both flow meters were nearly perfectly correlated.

In Figure 5 are shown the results from the 3M Breathe Easy without clay sealing the facepiece to the head form. On the left, the breathing machine was off (no flow) and the blower supplied a constant flow of nearly 100 L/min. At 19 seconds, the breathing machine was turned on, and both flows increased. Breathing machine flow can be seen to be greater than blower flow during inhalation. The difference represents leakage. This difference was integrated to obtain leakage volume as long as blower flow was less than breathing machine flow, and the results shown in the lower diagram of Figure 5. This shows that nearly 0.26 L of outside air leaks into the facepiece during each inhalation. This air is presumably swept from the facial volume during exhalation.

Also to be noted here is that blower flow rate was not constant. It varied during the breathing cycle, becoming about 230 L/sec during inhalation peaks and falling to

nearly zero during exhalation. The power required to move the extra air through the filters must necessarily be coming from the breathing machine.

There are a few blower negative flow values during exhalation. This means that respired air is being pushed backwards through the filters. At least part of the hose between the blower and the facepiece is also being filled with respired air. This PAPR has no check valve in the blower circuit to prevent backwards flow.

In Figure 6 are shown the same two flow measurements (top) and the same volumes (bottom) as in the previous Figure, except that the time scale has been compressed. Both blower and breathing machine were off until 10 sec., when the blower was turned on. At 20 sec the breathing machine was turned on. At about 40 sec, the blower was turned off. The same leakage volume seemed to occur whether the blower was on or off. There was more back flow of air through the filter when the blower was off.

When clay was carefully used around the mask periphery, the leakage volume decreased to about 0.21 L to 0.24 L from 0.26 to 0.29 L for each inhalation (Figure 7). Again, the leakage volume does not depend upon blower activity. The bronchoscope showed no evidence of fog reaching the mouth.

Results for the SE 400 with clay around the face seal are shown in Figure 8. The blower was turned on at 10 seconds and maintained a steady flow rate of about 25 L/min until the breathing machine was turned on at about 25 seconds. This PAPR has an active blower control that adjusts to breathing demand. For the first few breaths after the breathing machine was turned on, leakage volume was about 0.19 L. It subsequently decreased and varied throughout the range of 0.04 to 0.18 L. The leakage volume value

seemed to depend on whether the blower was actively increasing or decreasing speed, but the exact dependence was not determined. When the blower was turned off at about 75 seconds, leakage volume increased to 0.22 L. Again, the bronchoscope detected no fog at the mouth.

Leakage volumes from both PAPRs with clay sealing their peripheries seemed to indicate that inward flow was coming through the exhalation valves. Indeed, an inspection of the videos taken of both exhalation valves showed that neither valve closed instantaneously when inhalation began. The exhalation valve on the SE 400 is larger than the corresponding valve on the 3M Breathe Easy. The SE 400 valve tended to flutter, opening about three times after inhalation began. The 3M valve did not flutter, but stayed open long enough to let pass about 0.01 L of air before it closed (the range was measured at 0.00 to 0.03 L). Leakage volume for the SE 400 could not be determined because it was too difficult to see exactly when the valve was opened or completely closed.

Discussion

These results demonstrated that tight-fitting PAPRs do not exclude all contaminated air from the facepiece. However, the amounts leaked are extremely small.

Dead volumes of these masks were not measured but should fall in the range of about 0.97L, which is the measured interior volume of the similar 3M FRM40 facepiece. Measured dead volume of the FRM40 nosecup is about 0.09L. These were measured as the volumes of water filling the space between the facepiece and the head form.

What this tells us is that the leakage volumes for both respirators tested in this experiment are much less than the dead volumes of the facepieces. It would therefore be expected that contaminated air would not reach the mouth and be breathed by the wearer. This is confirmed by the lack of fog appearing at the mouth.

However, one might make the case that it is the volume inside the nose cup that matters. This is because the exhalation valve is located directly in front of the nose cup. Leakage coming through an imperfectly closed exhalation valve could probably find a direct route to the mouth. From results measured in this present study, the dead volume of the nose cup is still sufficiently large to protect the wearer. Lack of fog appearing at the mouth confirms this observation.

There were some severe constraints on the precision at which this experiment could be conducted. The opaque facepiece was the largest of these. Because the flow pathways for the fog could not be followed from the point of entry through the space in front of the face, it was not possible to say definitively where the leakage came from. The SE 400 exhalation valve fluttered whenever the breathing machine flow was higher than its blower flow. It was not enough apparent when the valve actually closed to estimate the leakage volume. This value was easier to estimate with the 3M Breathe Easy, but the 0.01 L estimated as valve leakage did not match with the 0.23 L obtained from flow meter difference. So, although we are reasonably confident in the 0.23 L leakage volume estimate, we are not so confident that we know where it comes from. Only further investigation will tell how much contamination exposure the wearer is exposed to.

The breathing demand SE 400 definitely had lower leakage volume than the 3M Breathe Easy. This volume changed as the blower adjusted to the demand. Leakage in the SE 400 was often accompanied by short bursts of its negative-pressure alarm.

We also found interesting the blower on the 3M device. It did not deliver a constant flow rate, but instead delivered an amount dependent upon the inhaled flow rate. The extra energy needed to draw extra air across the filter, blower, and tubing resistance would have to have come from the breathing machine. If a human had to supply the same amount of energy, breathing through this respirator could become very tiring. An analysis of this situation appears in Johnson et al.[3]

The fact that air could flow backwards, even by a small amount, in the tube that supplied filtered air to the facepiece means that the effective dead volume of the device would be increased because some of the exhaled carbon dioxide could be rebreathed. The amount, as measured herein, was small, and so not likely of consequence for the average wearer. Should there be less blower flow, perhaps from lower battery voltage, then the amount of rebreathed air could become more significant. It is not likely that exhaled breath moisture could reach the filter, but, if it could, filter life could be adversely affected. A simple check valve in the supply circuit could solve the problem.

There are two ways in which the breathing machine used in this experiment differed from a human. The first is that the breathing machine acted as an ideal flow source: its flow rate was largely independent of the resistance of the device attached to it, quite like a positive-displacement pump. The breathing machine develops whatever pressure it needs to draw the required flow rate, and this pressure is limited only by the mechanical strength of the machine.

A human respiratory system is different: first, the maximum pressure it can develop is very low in comparison to the mechanical strengths of steel parts; second, this pressure varies as lung volume changes[4]; third, the respiratory system has resistance and compliance elements that make it far from an ideal flow source. Consequently, one would expect a human to adjust his flow rate to the limits of the device.

The second difference between the breathing machine and a human involves the tidal volume used. A tidal volume of 2.25 L is large for a human of medium size, and is normally only reached during extreme activity. We used this large a tidal volume to make clear what results we could obtain from these two respirators. Under more normal circumstances, tidal volumes would be less and so would leakage volumes. How much less is difficult to say, especially for the breathing-demand respirator.

OSHA[5] has published a list of assigned protection factors (APFs) for sundry classes of respirators. Tight-fitting PAPRs have an assigned protection factor of 1000 unless indisputable evidence demonstrates that the protection factor is much higher. Results from this experiment do not dispute this ruling. Granted that there was a considerable amount of leakage of air into the facepiece, but the lack of fog seen at the mouth indicates that the wearer is protected adequately. Besides, the leakage that occurs probably as a result of exhalation valve dynamics is of very short duration, and may not result in a significant concentration of contaminant inside the facepiece. A very fast responding particle counter would be necessary to measure the exact contaminant concentration.

We have investigated imperfections in two powered air-purifying respirators from two reputable manufacturers. There is no reason to expect that similar types of

respirators from other manufacturers would not show similar responses. In the technological cycle of product improvement, tests such as these lead to focus on items that limit performance. From such tests come devices that are safer, and, we would hope, more compatible with those who wear them.

Acknowledgement: This work was funded in part by the National Institute for Occupational Safety and Health (NIOSH) Contract 200-2002-00531.

Figure Captions

Figure 1. Schematic diagram of the experimental arrangement with flow meters, light-emitting diodes, PAPR, head form, and bronchoscope.

Figure 2. Pressure-flow relation for one of the Medgraphics flow meters used in this study.

Figure 3. Pressure-flow reaction for the flow meter with negative pressures inverted. The result is a parabola that can be used to describe calibration results mathematically.

Figure 4. Plot of readings from the two flow meters. With an intercept of zero and a slope of one, it can be seen that both flow meters give nearly identical results. This is important when differences between the two measured flow rates are calculated.

Figure 5. Flow rates (upper) and leakage volumes (lower) are plotted with time for the 3M Breathe Easy PAPR. Volumes are accumulated when blower flows are less than breathing machine flows. No clay was used to seal the periphery.

Figure 6. Flow rates (upper) and leakage volumes (lower) for the 3M Breathe Easy PAPR shown in the previous Figure. The time scale has been compressed to show effects of blower and breathing machine activity. No clay was used to seal the periphery.

Figure 7. Results for the 3M Breathe Easy PAPR when clay was carefully used to seal the periphery. Leakage volume decreased.

Figure 8. Flow rates (upper) and leakage volumes (lower) for the SE 400 PAPR with clay sealing the periphery.

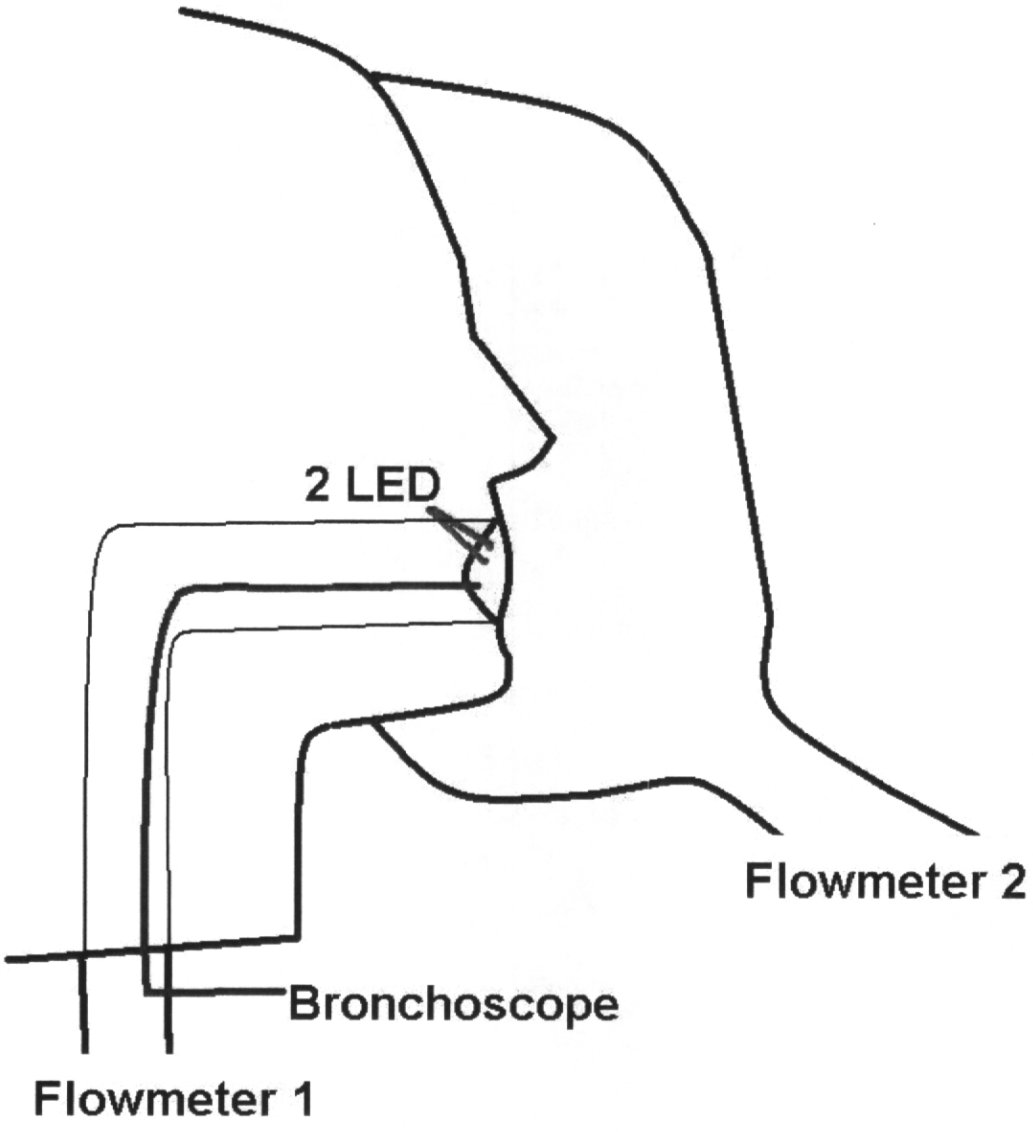

Figure 1. Schematic diagram of the experimental arrangement with flow meters, light-emitting diodes, PAPR, head form, and bronchosco

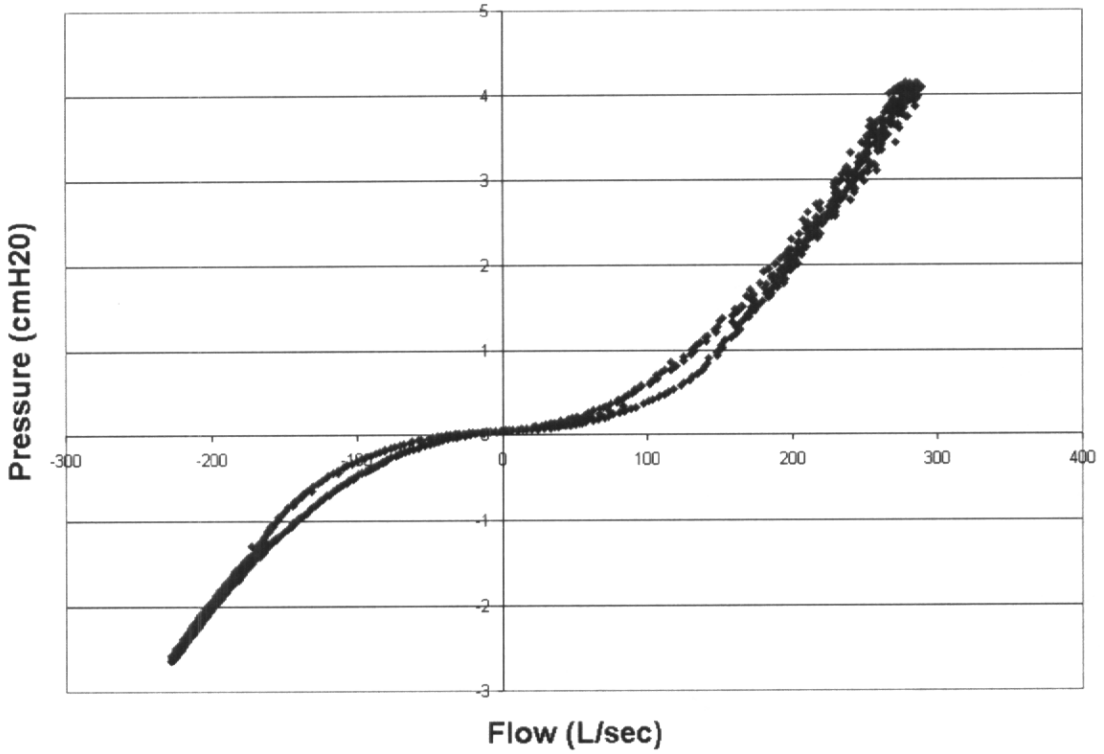

Figure 2. Pressure-flow relation for one of the Medgraphics flow meters used in this study.

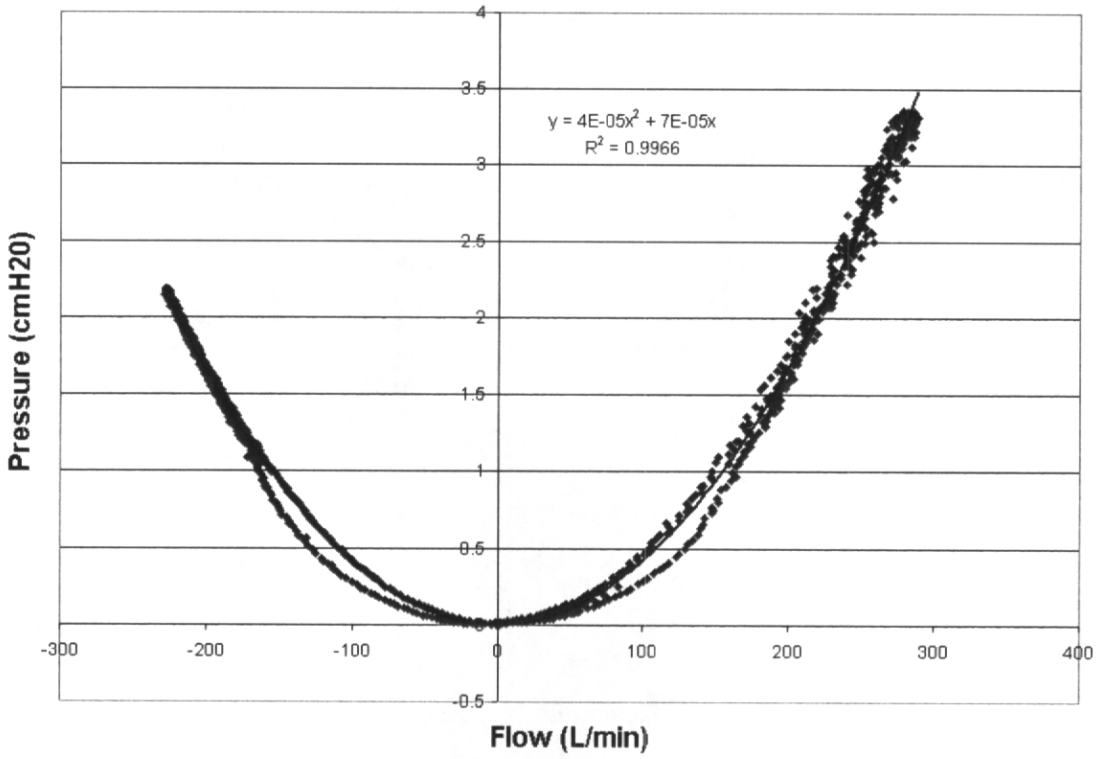

Figure 3. Pressure-flow reaction for the flow meter with negative pressures inverted. The result is a parabola that can be used to describe calibration results mathematically.

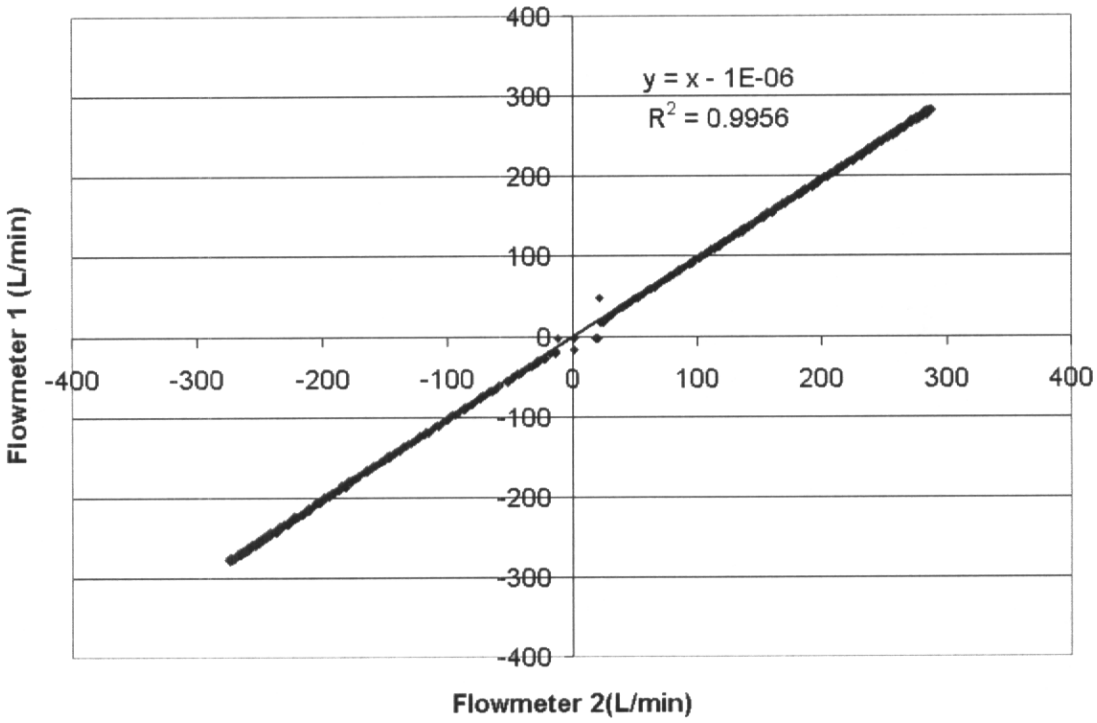

Figure 4. Plot of readings from the two flow meters. With an intercept of zero and a slope of one, it can be seen that both flow meters give nearly identical results. This is important when differences between the two measured flow rates are calculated.

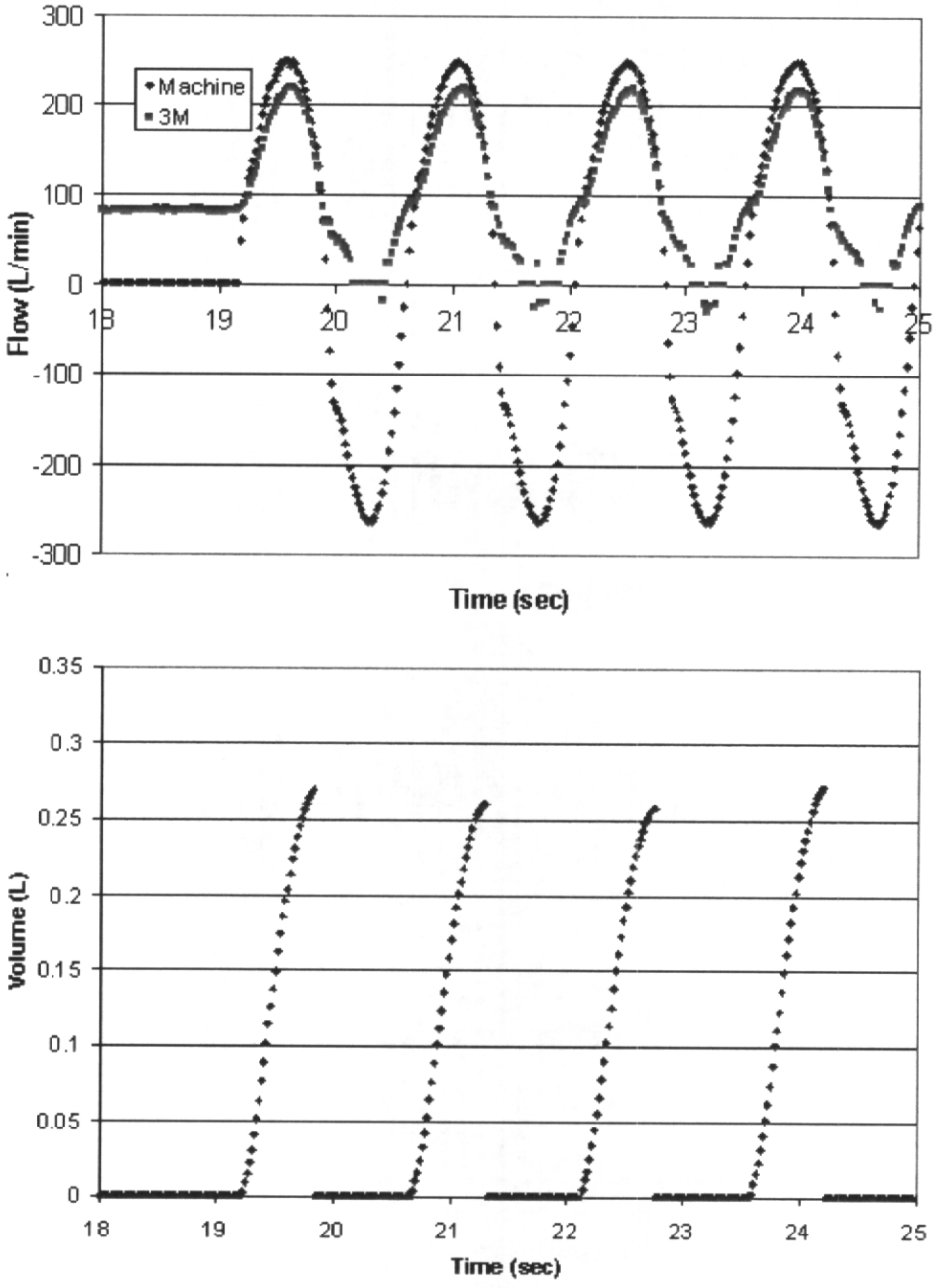

Figure 5. Flow rates (upper) and leakage volumes (lower) are plotted with time for the 3M Breathe Easy PAPR. Volumes are accumulated when blower flows are less than breathing machine flows. No clay was used to seal the periphery.

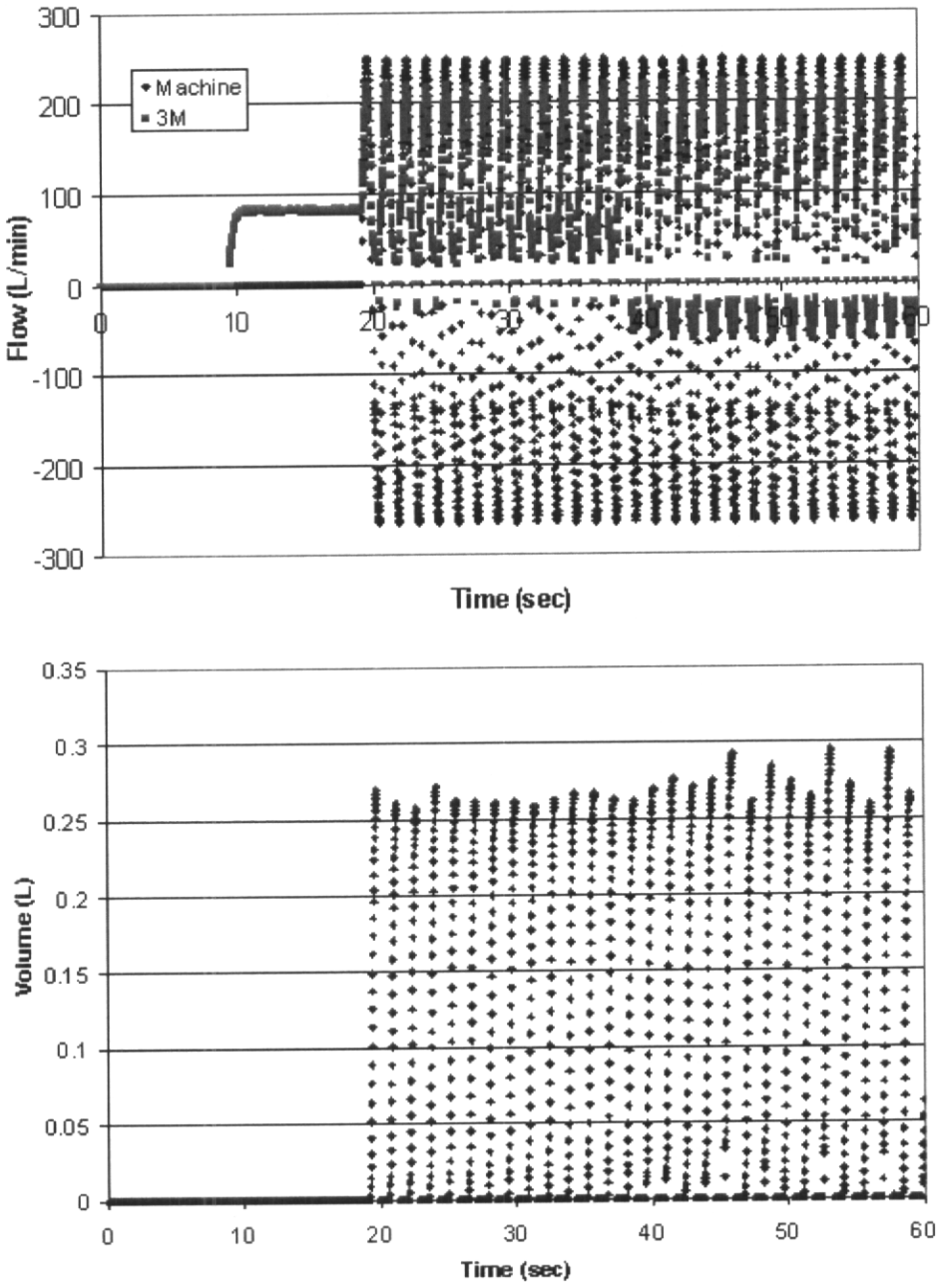

Figure 6. Flow rates (upper) and leakage volumes (lower) for the 3M Breathe Easy PAPR shown in the previous Figure. The time scale has been compressed to show effects of blower and breathing machine activity. No clay was used to seal the periphery.

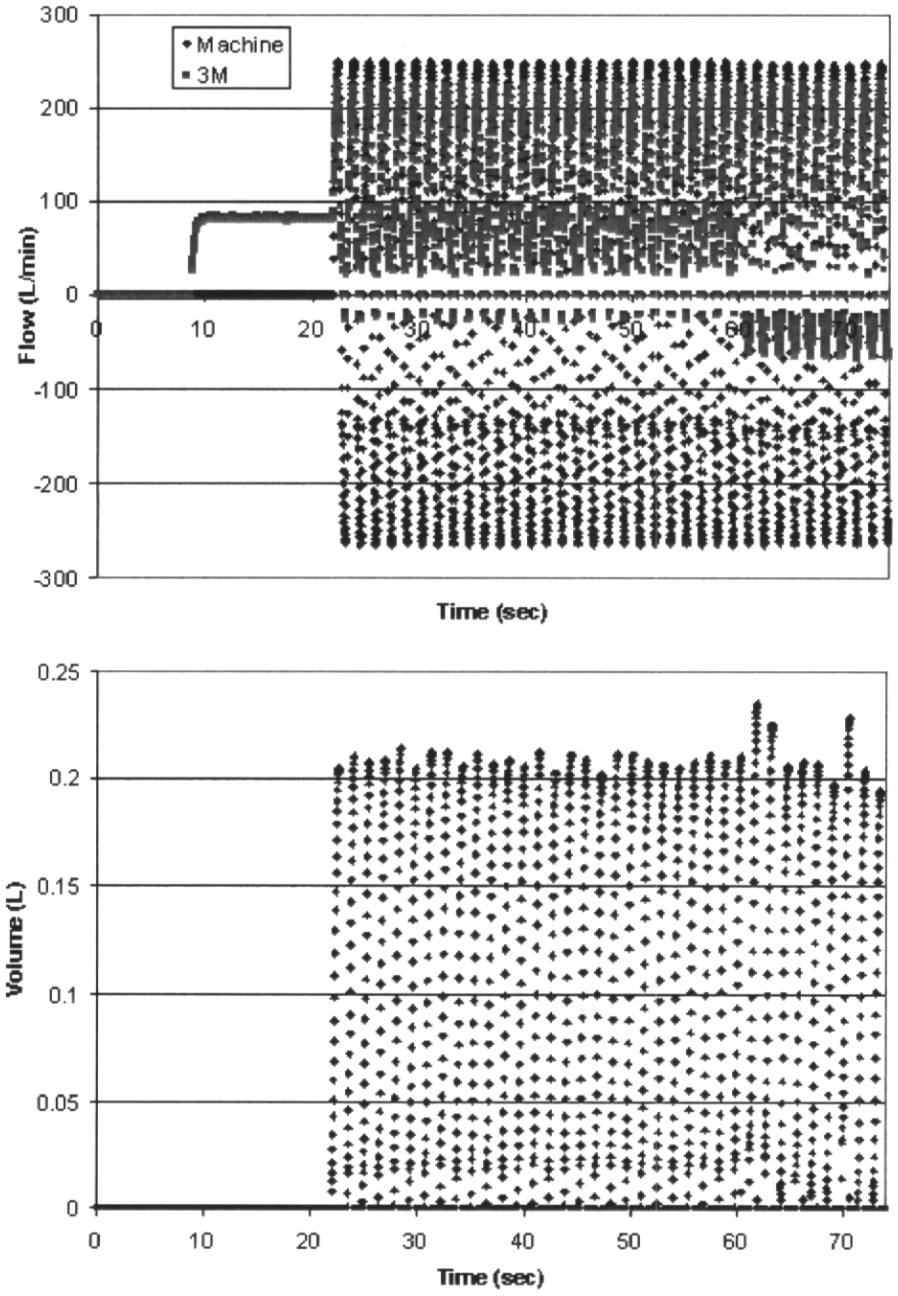

Figure 7. Results for the 3M Breathe Easy PAPR when clay was carefully used to seal the periphery. Leakage volume decreased.

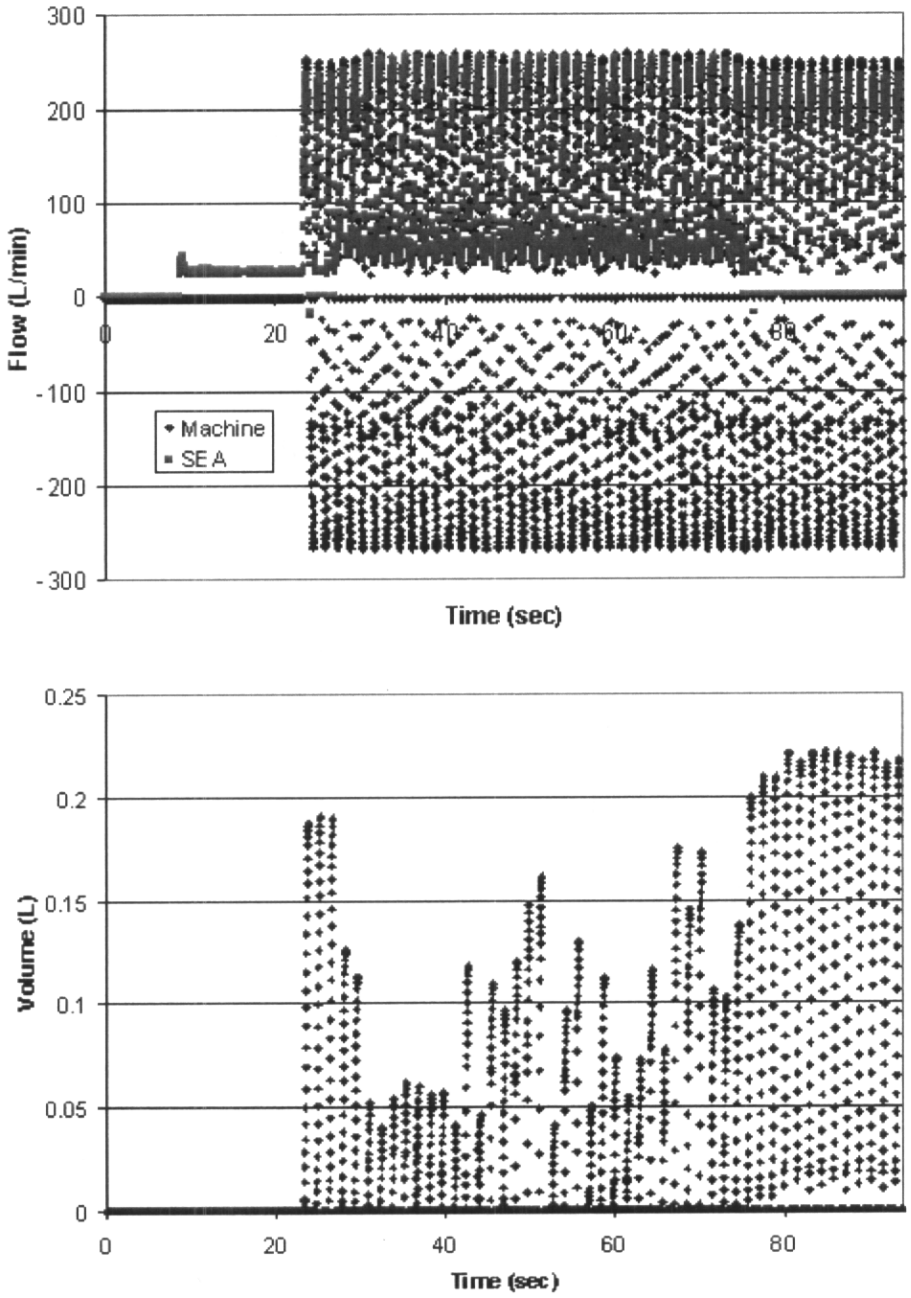

Figure 8. Flow rates (upper) and leakage volumes (lower) for the SE 400 PAPR with clay sealing the periphery.

References

1. Johnson, A. T., W. H. Scott, C. G. Lausted, and K. M. Coyne: Comparison of treadmill exercise performance times for several types of respirators, *J. ISRP* 17:19-23 (1999).

2. Koh, F. C., A. T. Johnson, and T. E. Rehak: Flow visualization in a loose-fitting PAPR, *J. ISRP* (submitted).

3. Johnson, A. T., K. R. Mackey, W. H. Scott, F. C. Koh, K. Y. H. Chiou, and S. J. Phelps: Exercise performance while wearing a tight-fitting powered air purifying respirator with limited flow, *J. Occup and Environ. Hyg* 2: 368-373 (2005).

4. Lausted, C. G., A. T. Johnson, W. H. Scott, M. M. Johnson, K. M. Coyne, and, and D.C. Coursey: Maximum static inspiratory and expiratory pressures with different lung volumes, *Biomed. Engr. Online* 5:29 (5 May) doi: 10.1186/1495-925X-5-29 (2006).

5. OSHA: Assigned protection factors; final rule – 71:50121-50192, Code of Federal Regulations, 29 CFR 1910, 1915, and 1926 (2006).

APPENDIX 8

Human Subject Testing of Leakage in a Loose-Fitting PAPR

Arthur T. Johnson
Professor

Frank C. Koh
Faculty Research Assistant
Fischell Department of Bioengineering
University of Maryland
College Park, MD 20742

Shaya Jamshidi
Graduate Research Assistant

Timothy E. Rehak
General Engineer
National Personal Protection Technology Laboratory
National Institute for Occupational Safety and Health
Pittsburgh, PA

corresponding author:
Arthur T. Johnson
Fischell Department of Engineering
University of Maryland
College Park, MD 20742
tel: 301-405-1184
email: artjohns@umd.edu

Abstract:

Leakage from loose-fitting PAPRs can compromise the safety of wearers. The Martindale Centurion MAX multifunction PAPR is a loose-fitting PAPR that also incorporates head, eye, and ear protection. This respirator is used in mines where coal dust is usually controlled by ventilation systems. Should the respirator be depended upon for significant respiratory protection?

Ten human volunteers were asked to wear the Centurion MAX inside a fog-filled chamber. Their inhalation flow rates were measured with small pitot-tube flowmeters held inside their mouths. They were video imaged while they breathed deeply, and the points at which the fog reached their mouths were determined.

Results showed that an average of 1.1 L could be inhaled before contaminated air reached the mouth. As long as the blower purges contamination from inside the face piece during exhalation, the 1.1 L acts as a buffer against contaminants leaked due to overbreathing of blower flow rate.

keywords: respirator, protection, dead volume, protection factor

Introduction

Loose fitting powered air-purifying respirators (PAPRs) have the advantages that they never restrict breathing of the wearer, and they can accommodate items, such as normal eyeglasses, worn on the face. Air drawn by a blower through a filter is blown across the face and intersects the normal path for breathed air to enter the mouth. Thus, under quiet circumstances, the air that is inhaled should be filtered air. When exertion increases and breaths become deeper, however, there is little to impede contaminated air from mixing with the filtered air. Most loose-fitting PAPRs incorporate a face shield and some have a cloth scarf spanning the gap between the face shield and face or neck to impede contaminated air from entering the vicinity of the mouth.

Mackey et al.[1] published a report about overbreathing a multifunction, loose-fitting PAPR, the Centurion MAX (Martindale Protection; Thetford, Norfolk, UK). They reported that all sixteen subjects inhaled more air than was supplied by the PAPR blower. In the same paper they also reported a measured volume inside the face shield of 1.4 L. They contended that if the whole 1.4 L was protective, then the problem of overbreathing would be minimal. This condition would have required diffuse, nonpreferential flow of outside air into the facepiece.

Experiments have been conducted on a loose-fitting PAPR mounted on a head form and challenged with generated fog .[2] The breathing machine was adjusted such that inhaled flow rate exceeded blower flow rate. It was found that the volume of air inhaled before fog reached the mouth averaged 1.4 L. The present experiment was conducted to determine if the same results can be anticipated for human wearers.

Methods

Ten young, healthy participants volunteered from the University of Maryland student body. This protocol was approved by the University of Maryland Institutional Review Board.

Subjects sat in a full body chamber constructed of plywood and Lexan plastic windows in order to see inside the chamber. Overall dimensions of the chamber were 137 cm (54 in) by 76 cm (30 in) by 180 cm (71 in). The rigid plastic window at the front of the chamber was replaced by a transparent thin plastic film normally used to reduce home window drafts. Each subject wore a Centurion MAX (Martindale Protection; Thetford, Norfolk, UK) multifunctional powered air-purifying respirator (PAPR) and leaned into the transparent film with the PAPR visor in contact with the film. Thus, it could be seen when fog that filled the chamber entered the space between the visor and the face.

Glycerol fog was produced outside the chamber with a Fogstorm (Los Angeles, CA) 1200 HD generator, and introduced into the chamber through a hose inserted into a port in the chamber wall. The fog generator was capable of producing about 200 m^3 (7000 ft^3) of fog per minute. Fog filled the chamber in a very short time, and was used as a safe and visible surrogate for contaminated air.

The aim of this research was to determine the amount of protective dead volume in the region between the face shield and the face. Hence, subjects were asked to inhale very deeply to induce fog to reach the mouth from the outside. In order to solicit a maximal inhalation and to allow dissipation of condensation that formed on the visor from the previous exhalation, each individual was instructed to exhale as completely as

possible and to hold his/her breath for 15 seconds before inhaling as deeply and quickly as possible. Filtered air from the PAPR blower was clear of fog and filled the visor space completely until the subject drew enough air from the outside by overbreathing the blower capacity. When that happened, fog could be seen entering the space behind the visor.

In order to improve fog visibility, each subject applied black face paint on their skin below the nostril, below the cheek line, and above the jaw line. A wire with two light-emitting diodes (LEDs) was draped over the ear and taped with black electrical tape near the lips to assist with video interpretation. One LED blinked at 10 Hz and the other was driven by a comparator circuit and indicated when the inhalation phase of breathing was in progress.

Measurement of flow rates was made with two MedGraphics (St. Paul, MN) pitot-tube flow meters. One was used to measure PAPR blower flow rate and was taped and sealed to the blower inlet with a flexible plastic cone. The other was cleaned and placed inside the subject's mouth with lips sealed around the pneumotach and associated tubing. Subjects wore nose clips to obstruct nasal flow. In this way, overbreathing could be detected as the difference between mouth and blower flow rates.

Calibration of the pneumotachs was extremely important because flow rate differences were to be calculated. The MedGraphics flow meters were calibrated against a Fleisch #3 pneumotach (Phipps and Bird; Richmond, VA) and then against each other by placing them in series and connecting them to a breathing machine. Flow signals were integrated to obtain volume, and this volume compared to syringe volume. Flow rate

data from one pneumotach plotted against data from the other demonstrated the two data sets to be identical statistically.

The Centurion MAX consisted of a helmet with a blower and particulate filter. A pivoted visor eye protection, and ear muff hearing protection were attached to the helmet. A scarf was worn below the chin and around the mandible just below the ears. All components of the Centurion MAX PAPR were worn by the subjects as the manufacturer had intended. The visor was preheated with a blow dryer before being put on by the subject to reduce condensation from the exhaled breath.

Video images of the fog flowing inside the PAPR were recorded digitally with a Sony (Tokyo, Japan) DCR-HC90 camera with 3 megapixel resolution.[2] The camera was aimed through the plastic film and face shield visor of the PAPR, and focused on the area of the mouth. The experiment was conducted in a darkened room with two incandescent lights aimed toward the face from outside the chamber. Proper positioning of the lights eliminated glare from the visor and face.

Each image was frozen on the computer monitor using a program called Adobe (San Jose, CA) Premiere Pro 1.5. Pulsing of the LEDs helped to determine timing and respiratory cycle phase. Overbreathing flow rate (the difference between blower flow and mouth flow rates was integrated from the moment that mouth flow rate exceeded blower flow rate until the fog was observed to reach the mouth. This gave the volume of filtered air that could be inhaled before outside contamination began to be inhaled. This determination was made for three breaths and the average calculated.

Results

In Figure 1 is shown the comparative calibration of the two pneumotachographs used, showing that they matched extremely well. Thus, flow rate differences measured from the two flow meters could be calculated with confidence. Each flow meter had a quadratic pressure-flow characteristic [3] that was linearized mathematically before flow differences or flow integration was performed (Figure 2).

In Figure 3 is shown a typical image showing the path of the fog across the face and inside the face shield. In general, there were no significant differences between flow pathways seen with the breathing machine or the human face. The three-dimensional curling and twisting path taken by the fog as it enters the facepiece, flows to the visor and reverses toward the mouth was seen for both human face and machine headform.[2]

In Table 1 are summarized results of the human subject testing. Average volume inhaled before contaminants (fog) reached their mouths (Total Prior Volume) is 1.11 L. For tidal volume less than this value, airborne contaminants leaking in from around the periphery of this respirator would not be inhaled by an average wearer. Also given are standard deviations and ranges of the data. The range of individual breaths is 0.82 to 1.47 L before fog reaches the mouth. Although this range is wide, the standard deviations for all subjects are mostly within 10% of individual means.

The Net Prior Volume is the Total Prior Volume inhaled by the subject subtracting the volume of air supplied by the blower from the beginning of the inhalation up to the point where fog reached the mouth. This assumes that all blower flow is inhaled and none short-circuits to the outside while the wearer is inhaling. The average Net Prior Volume is 0.66 L.

The Net Post volume is the volume of air inhaled that contains contaminants. It is the volume inhaled after fog reached the mouth and less the volume supplied by the blower at the same time, again assuming all blower volume is inhaled. The average value for Net Post Volume is 1.22 L, but this value would be expected to vary widely among individuals depending on their depths of breathing.

Discussion

Being able to see the path taken by flow inside a PAPR facepiece can help to understand flow dynamics of the protective device. Visualization is needed to substantiate results from computational fluid dynamics computer programs, and, perhaps, to improve protection of these devices.

The flow patterns proved to be complex, with twists and curls of a multi-planar nature. This twisting and curling has at least one positive and one negative effect. On the negative side, changing the magnitude and direction of a mass of fluid air required energy, so that the work required of the respiratory muscles during overbreathing of the PAPR blower is greater than it would have had to be had the flow pathway been simpler and straighter. Because the mass of air is very low, however, this extra work is usually insignificant. On the positive side, the twisting and curling of the air entering the facepiece periphery effectively lengthens the flow pathway and increases the amount of "dead" air that can be inhaled before contaminated air reaches the mouth. Thus, effective dead volume of this respirator is increased by the complexity of the pathway. One goal of respirator designers might then be to cause contaminated air to curl in a vortex pattern before it reached the mouth, thus lengthening the flow path manyfold. This may provide

more efficient protection than would increasing the blower or battery capacity. In the limit, it might be possible to provide as much wearer protection for a wearer of a loose-fitting respirator without a blower as loose-fitting devices presently with a blower.

So, continuing along this line of discussion a little further, why might a blower be needed at all? The answer lies in the nature of the air in the dead volume. The flow pathway for exhaled air is different from the flow pathway for inhaled air. Therefore, the dead volume fills with CO_2-rich and O_2-poor air during exhalation. This is the air that is first inhaled during the subsequent breath. If the effective inhaled flow pathway is lengthened too much, then it is only this air that is inhaled. It would not be contaminated, but it wouldn't be fresh air, either.

It is the function of the blower to purge exhaled air from the dead volume during the exhalation portion of the breathing cycle. Filling the dead volume with fresh, filtered air is all that the blower needs to do. It does not need to supply inhaled air as long as the inhaled flow pathway is long enough.

This almost inverts the traditional concept of dead volume as something undesirable. Dead volume in a PAPR such as this now becomes protective, and not burdensome. The more protective dead volume present, the more effective is a loose-fitting respirator. With enough protective dead volume, there is essentially no difference between a loose-fitting respirator and a tight-fitting respirator. Thus, it is seen that some loose-fitting hoods can be treated as if they were tight-fitting respirators.

Hoods, however, have taken an extensive approach toward providing protective dead volume. They are large, and require proper wear. Just as filtering materials and membranes can be folded to fit a very large surface area into a small volume, it may be

possible to design a facepiece that fits a long flow pathway into a small volume. This would be an intensive approach, and should trade technology for materials.

One challenge that would be faced if this strategy were to be implemented is how to prove the protection afforded. Sampling contaminants inside the facepiece would have to be very carefully done, or else measurements would be too high. Most of the volume inside a facepiece could conceivably contain unacceptably high contaminant concentrations. Yet, if contaminants never reached the mouth then the respirator would have achieved its purpose. New approaches are called for.

Another challenge would be isolating sensitive tissues from contaminants. We have thus far been concerned only with inhaled contamination, but if the contaminants can irritate or damage the eyes or the skin, then this approach is not likely to succeed. In this case, tight-fitting PAPRs, APRs, or SCBAs would be required. Hence, as we already know, the selection of an appropriate respirator depends on the conditions under which it is to be used, and shouldn't be determined solely on price.

The most valuable figure determined by this study is the Net Prior Volume, because that is an estimate of protective dead volume. Koh et al.[2] measured this as 1.55 L with inhalation supplied by a breathing machine. The same volume was measured as 1.11 L in the present study with human volunteers. The difference between these two figures is not totally unexpected because facial configuration may have a substantial effect on flow pathways inside the facepiece. The flow curling that was observed would have been somewhat haphazardly formed as long as this characteristic were not specifically designed into the facepiece. The other two volumes in Table 1 depend upon the assumption that blower flow is totally inhaled, and does not leak to the outside during

inhalation. The assumption needs to be checked, and our guess is that it is not totally correct. A study has been conducted using CO_2 gas as a contaminant to determine, with a different method, the Net Post Volume of contaminated air inhaled.[4]

The value of Net Post Volume measured in that study was 0.6 L for the same respirator tested with a breathing machine set to produce a tidal volume of 2.4 L. The value of the same volume in this study is 1.22 L with human subjects breathing with an average tidal volume of 2.1 L. As mentioned before, the Net Post Volume depends strongly on the depth of breathing, so different results are to be expected.

Acknowledgement: This work was funded in part by the National Institute for Occupational Safety and Health (NIOSH), and the National Personal Protection Technology Laboratory (NPPTL) Contract 200-2002-00531.

Table 1. Human Subjects Results. Volumes given are averages of three breaths in Liters. Also given are standard deviations and range of values.

Subject Number	Total Prior Volume	Net Prior Volume	Net Post Volume	Average Tidal Volume
501	0.97 ± 0.04 (0.93-1.02)	0.42 ± 0.02 (0.40-0.45)	1.16 ± 0.11 (1.06-1.27)	2.25 ± 0.10 (2.16-2.37
502	1.16 ± 0.08 (1.06-1.22)	0.74 ± 0.06 (0.67-0.79)	1.66 ± 0.10 (1.56-1.75)	2.66 ± 0.04 (2.63-2.71)
503	0.99 ± 0.11 (0.90-1.11)	0.60 ± 0.09 (0.51-0.68)	1.54 ± 0.08 (1.49-1.63)	2.59 ± 0.12 (2.46-2.69)
505	1.21 ± 0.05 (1.18-1.27)	0.76 ± 0.02 (0.74-0.78)	1.53 ± 0.64 (0.80-2.02)	2.41 ± 0.97 (1.31-3.16)
507	1.24 ± 0.04 (1.20-1.28)	0.79 ± 0.13 (0.66-0.92)	1.65 ± 0.12 (1.55-1.77)	2.67 ± 0.12 (2.48-2.70)
508	1.08 ± 0.24 (0.82-1.27)	0.71 ± 0.20 (0.49-0.86)	0.94 ± 0.19 (0.73-1.11)	1.70 ± 0.22 (1.50-1.94)
509	0.84 ± 0.01 (0.83-0.86)	0.32 ± 0.04 (0.28-0.35)	0.32 ± 0.04 (0.28-0.36)	1.00 ± 0.03 (0.98-1.04)
510	1.26 ± 0.14 (1.11-1.39)	0.90 ± 0.12 (0.77-1.01)	1.33 ± 0.21 (1.09-1.4	1.90 ± 0.23 (1.63-2.07)
511	1.25 ± 0.19 (1.09-1.47)	0.77 ± 0.18 (0.58-0.95)	1.42 ± 0.32 (1.06-1.65)	2.80 ± 0.21 (2.55-2.96)
512	1.11 ± 0.16 (0.95-1.27)	0.57 ± 0.09 (0.47-0.62)	0.67 ± 0.09 (0.57-0.73)	1.40 ± 0.16 (1.25-1.56)
Avg	1.11 ± 0.14 (0.84-1.26)	0.66 ± 0.18 (0.32-0.90)	1.22 ± 0.45 (0.32-1.66)	2.12 ± 0.57 (1.00-2.80)

Notes: Subject Number refers to the number assigned in our laboratory. Total Prior Volume is the total volume inhaled by the subject before the fog reached the mouth. Net Prior Volume is the difference between subject inhalation volume and volume delivered by the blower before the fog reached the mouth. Net Post Volume is the difference in volume inhaled by the subject and supplied by the blower after the fog reached the mouth.

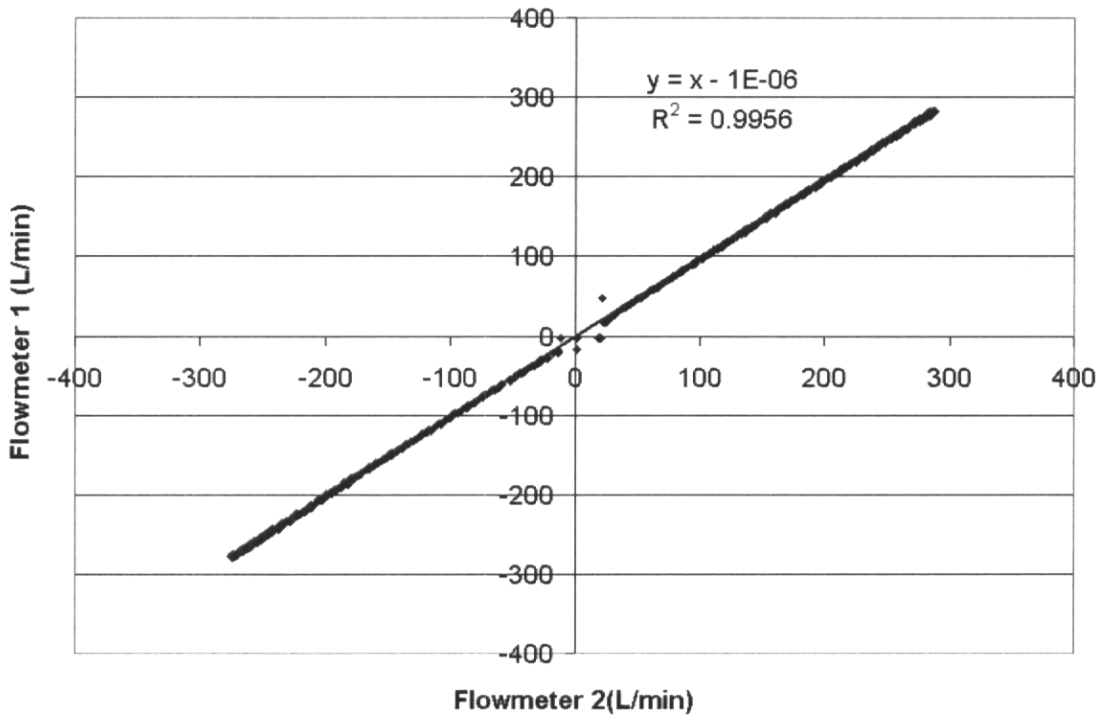

Figure 1. Comparison of calibrations between two flowmeters, showing that their outputs are nearly identical.

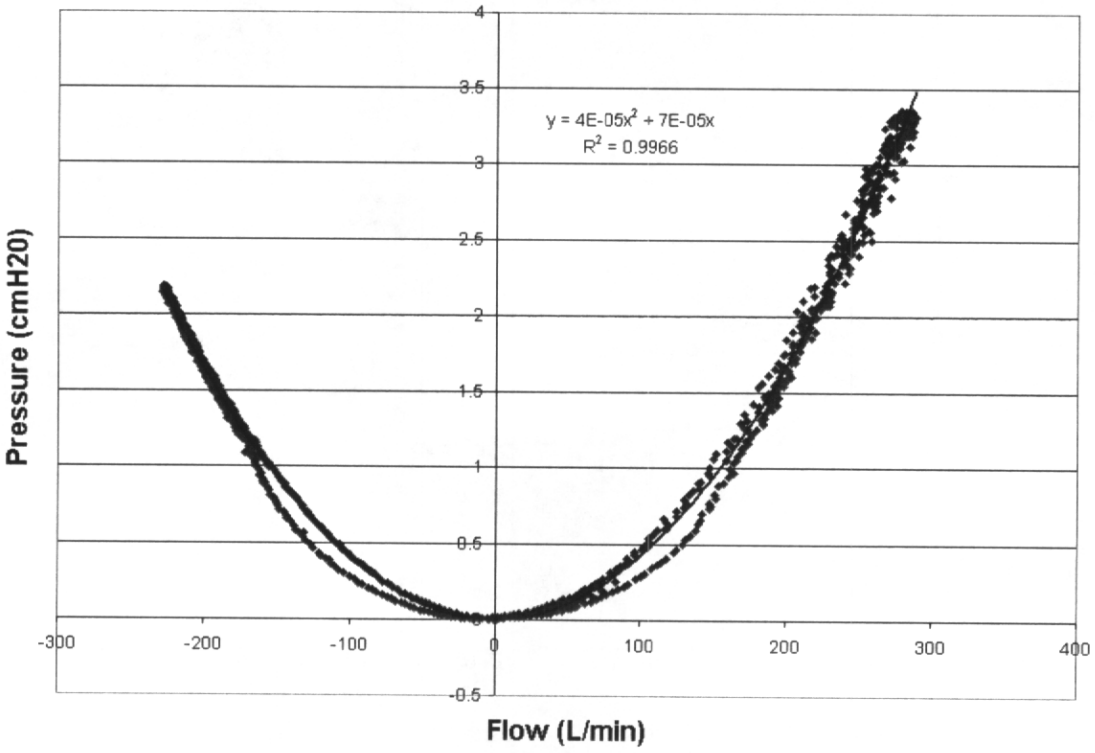

Figure 2. Quadratic calibration response of the Medgraphics pitot tube flowmeter. The flowmeter output was linearized mathematically.

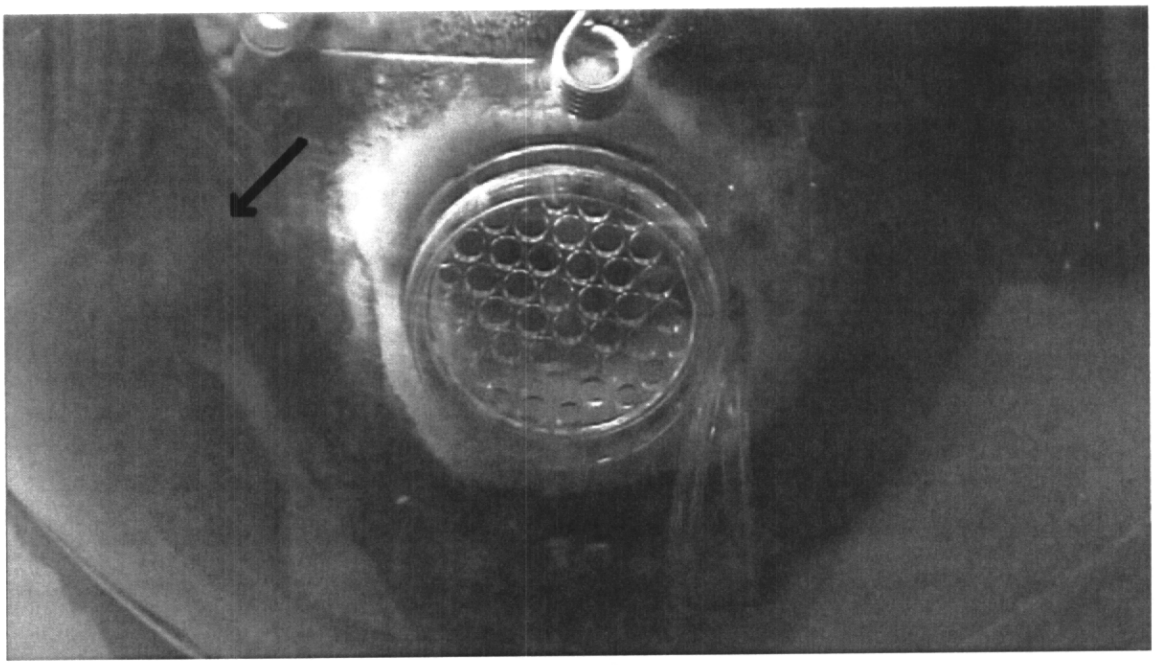

Figure 3a. Typical facial image showing the mouth and pneumotach. The face was covered with black face paint to enhance fog visibility. The Medgraphics pneumotach appears in the mouth, and is situated almost entirely within the oral cavity. Pressure tubes attached to the pneumotach can be seen on the right side of the pneumotach. Above the mouth is a spring belonging to a nose clip. Fog is slightly visible in this view (at arrow) as it reaches the mouth of the deeply inhaling subject.

Figure Captions

Figure 1. Comparison of calibrations between two flowmeters, showing that their outputs are nearly identical.

Figure 2. Quadratic calibration response of the Medgraphics pitot tube flowmeter. The flowmeter output was linearized mathematically.

Figure 3a. Typical facial image showing the mouth and pneumotach. The face was covered with black face paint to enhance fog visibility. The Medgraphics pneumotach appears in the mouth, and is situated almost entirely within the oral cavity. Pressure tubes attached to the pneumotach can be seen on the right side of the pneumotach. Above the mouth is a spring belonging to a nose clip. Fog is slightly visible in this view (at arrow) as it reaches the mouth of the deeply inhaling subject.

References

[1] Mackey, K. R. M., A. T. Johnson, W. H. Scott, and F. C. Koh, Overbreathing a Loose Fitting PAPR: *J. ISRP* 22:1-10 (2005).

[2] Koh, F. C., A. T. Johnson, and T. E. Rehak, Flow Visualization in a Loose-Fitting PAPR: *J. ISRP* (submitted 2006).

[3] Koh, F. C., A. T. Johnson, and T. E. Rehak, Inward Leakage in Tight-Fitting PAPRs, *J. Occup. Environ. Hyg* (submitted 2006).

[4] Johnson, A. T., F. C. Koh, and T. E. Rehak, Net Contaminant Volumes Inhaled While Wearing Respirators (2006).

APPENDIX 9

Protection Factors and Net Contaminant Volumes Inhaled While Wearing Respirators

Arthur T. Johnson
Professor

Frank C. Koh
Faculty Research Assistant

William H. Scott, Jr.
Faculty Research Assistant

Fischell Department of Bioengineering
University of Maryland
College Park, MD 20742

Timothy E. Rehak
General Engineer
National Personal Protection Technologies Laboratory
National Institute for Occupational Safety and Health
Pittsburgh, PA

corresponding author:
Arthur T. Johnson
Fischell Department of Bioengineering
University of Maryland
College Park, MD 20742
tel: 301-405-1184
email: artjohns@umd.edu

Abstract:

This experiment was conducted to determine how much contaminant could be expected to be inhaled when overbreathing a respirator. CO_2 was used as a tracer gas in the ambient air, and several loose-and tight-fitting respirators were tested on a breathing machine. CO_2 concentration in the exhaled breath was monitored as well as CO_2 concentration in the ambient air. This concentration ratio was able to give a measurement of protection factor, not for the respirator necessarily, but for the wearer. Flow rates in the filter/blower inlet and breathing machine outlet were also monitored, so blower effectiveness (defined as the blower contribution to inhaled air) could also be determined.

Protection factors were found to range from 1.1 for the Racal AirMate loose-fitting PAPR to infinity for the 3M Hood, 3M Breath-Easy PAPR and SE 400 breath-responsive PAPR. Inhaled contaminant volumes depend on tidal volume, but ranged from 2.02 L to 0 L for the same respirators, respectively. Blower effectiveness was about 1.0 for tight-fitting APRs, 0.18 for the Racal, and greater than 1.0 for two of the loose-fitting PAPRs. With blower effectiveness greater than 1.0, some blower flow during the exhalation phase contributes to the subsequent inhalation. Results from this experiment point to different ways to measure respirator efficacy.

keywords: contaminants, protection factor, dead volume, respirator, inhalation

Introduction:

Development of methods and determination of inhaled volumes are important for protection of wearers from airborne contaminants and assignment of minimal expected respirator protection factors (OSHA, 2006).

Previous work in our laboratory has lately concentrated on leakage in tight-fitting, loose-fitting, and breath-responsive powered air-purifying respirators (PAPRs) (Koh et al., 2006 a & b; Mackey et al., 2005; Johnson et al., 2006a). This work has involved flow visualization with fog generation, breathing machine tests, and human subject tests. Despite the assurance that visual detection of fog gives regarding flow pathways and the carriage of airborne contaminants to the mouth, this is still not a direct indication of contaminant protection offered by the respirator.

Other methods to measure protection have their shortcomings as well. Respirator protection factors are defined as contaminant concentration outside the facepiece divided by contaminant concentration inside the facepiece. These two concentrations are often measured by non-discriminating particle counters that require a finite amount of time to reach a valid measurement. Although this is a relatively simple measurement to make, it cannot be used accurately for rapidly changing particle counts.

Concentration ratio is only valid as a measure of protection factor as long as there are no particle sources or sinks in the system. It is known that the respiratory system is a source for moisture particles, and these can be counted along with particles of the challenge substance. Protection factors would, in this case, appear lower than they should. Deposition of particles within the respiratory system can also occur, leading to apparent protection factors higher than they ought to be.

In this study, we investigated measurement of respirator protection factors using a different method of a challenge gas and collection of exhaled breath. It was intended that results from this method could be compared to results using fog flow visualization with a breathing machine (Koh et al., 2006b) and human wearers (Johnson et al., 2006a).

Methods:

PAPR leakage was determined by operating the PAPR inside a chamber containing a tracer gas. Air supply to the PAPR blower came from the outside atmosphere containing a negligible concentration of the tracer gas. A breathing machine was used to simulate the effect of a human wearer, but exhaled air from the breathing machine was collected in a separate container. The presence of the tracer gas in the exhaled air was quantitative proof of PAPR inward leakage (Figure 1).

The chamber of dimensions 137 cm (54 in) by 76 cm (30 in) by 180 cm (71 in) was constructed of plywood and Lexan transparent plastic for visibility. Placed inside the chamber was a headform on which the PAPR was mounted. The mouth of the headform was connected to a breathing machine (Krug Life Sciences; Houston, TX) outside the chamber by means of a 3.8 cm (1.5 in) flexible ventilator hose (A-M Systems Spiral Tubing; Carlsborg, WA). Two one-way valves directed inhaled air from the PAPR into the breathing machine and exhaled air into a separate container. The valves had been salvaged from U. S. Army M17 air purifying respirators

The container to collect exhaled breath was constructed from several 2L soft drink plastic bottles sealed with black electrical tape. The ability of the tracer gas to diffuse through the walls of the container was not investigated, but the short time between

breaths and the volume inside the container made significant concentration errors unlikely.

CO_2 was used as the tracer gas. The test chamber was filled with 6-7% CO_2 from a cylinder, and the gas concentration was monitored continuously with a mass spectrometer (Model 1100; Perkin-Elmer; St. Louis, MO). Because CO_2 inside the test chamber was continuously being replaced by fresh air passing through the respirator, CO_2 was added continuously from the gas cylinder.

The exhalation container began with a negligible CO_2 concentration, which proceeded to climb as more exhaled air displaced initial air. The air/CO_2 mixture was sampled continuously by the mass spectrometer and at 50/sec by the data acquisition system. When CO_2 concentration had reached its final steady-state value, this concentration was used as the value in exhaled air.

PAPR blowers were operated with fully-charged batteries, and each test lasted approximately 2 min. Hoses were attached to the inlets of each blower so that ambient air could be drawn from outside the chamber. Hose inlets were located about 1m above the chamber, and excess gas was exhausted from the chamber floor in order not to cycle CO_2 from the chamber back into the respirator inlets (CO_2 is denser than air). MedGraphics (St. Paul, MN) #5038773 pitot tube flowmeters were used to measure blower flow and breathing machine flow. These were carefully calibrated beforehand to ensure that they gave identical measurements for identical flow rates (Koh et al., 2006b).

Data were collected with an analog-to-digital data acquisition board (National Instruments; Austin, TX) connected to the Universal Serial Bus (USB) of a PC computer.

Custom software developed in LabView 7 (National Instruments; Austin, TX) recorded flow and concentration data, calculated flow differences, and exhaled volumes.

The volume of inhaled CO_2 is the leakage volume times the concentration of CO_2 in the exhalation collection chamber atmosphere, which also equals the exhaled volume times the exhaled CO_2 concentration. Thus, leakage volume can be obtained as the exhaled volume times the ratio of CO_2 concentrations in the exhaled breath and chamber atmosphere.

Respirators tested were the Racal AirMate 3 (Racal; Frederick, MD) loose-fitting PAPR; Breathe Easy (3M; St. Paul, MN) tight-fitting PAPR, Butyl Head Cover with Cape, #522-02-23 (3M) loose-fitting hood, Centurion MAX (Martindale Protection; Thetford, Norfolk, UK) multi-purpose loose-fitting PAPR, SE 400 (SEA; Meadowlands, PA) breath-responsive PAPR, and FRM 40 (3M) air-purifying respirator. Penumotachs were adapted to blower inlets for the Racal, Centurion, and SEA devices. Pneumotachs were placed in the connecting hose between blower and facepiece for the two 3M powered devices. An inlet hose was connected to the filter of the FRM40.

The breathing machine was set to generate a minute volume of 112 L/min, tidal volume of 2.4 L, and a peak flow of 317 L/min. The breathing waveshape was sinusoidal. These settings have been used in this and previous experiments in order to induce respirator leakage if the respirator is going to leak at all. The breathing machine minute volume is nearly the same as most PAPR blower flow rates, but peak flows are much higher than blower flow rates.

Results

Results are summarized in Table I. It has been shown previously (Koh et al., 2006a) that PAPR blower flow rates vary during the breathing cycle, and this is reflected in the entries for blower flow rates. Exhaled tidal volumes were nearly constant at 2.32 to 2.42L. The ratio of CO_2 concentrations in the exhaled breath and enclosing chamber is also shown. The inverse of these figures are the measured protection factors for each of the respirators as worn and used. In the column labeled "Leakage Volume" are found volumes of inhaled contaminant-laden air, obtained by multiplying the concentration ratios by exhaled volumes. These figures also represent nominal leakage volumes for the respirators.

In Figure 2 are shown breathing machine flow rate, blower flow rate, and inhaled contaminant volumes for the Racal AirMate 3 loose-fitting PAPR. This figure is intended to show that blower flow rate for this respirator is almost constant, and that inhaled contaminant volume (integrated breathing machine flow rate times CO_2 concentration in the captured exhaled breath) is slightly more than 2 L.

Figure 3 is similar to Figure 2, but shows that blower flow rate for the 3M Breathe Easy tight-fitting PAPR varies throughout the inhalation phase of breathing. The volume of inhaled contaminants is indistinguishable from zero.

Figure 4 illustrates responses by the SE 400 breath-responsive tight-fitting PAPR. Blower flow rate tracks breathing machine flow rate in an attempt to maintain positive pressure inside the facepiece. Again, inhaled volume of contaminants is zero.

Discussion

It can be noted that, although the Racal AirMate 3 blower flow rate was higher than the Centurion MAX blower flow rate, contaminant exposure with the Racal is much higher and protection factor is much lower. In a previous paper (Koh et al., 2006a) it was shown that fog was drawn into the facepiece by blower turbulence, and this is reflected by CO_2 concentration measurements here.

The SE 400 breath-responsive respirator attempts to maintain positive pressure inside the facepiece, although that is not always the case (Koh et al., 2006b). The SE 400 blower flow can be seen to peak above the peak flow of 317 L/min produced by the breathing machine. When the blower was turned off, blower flow was much lower, and the respirator operated as an air-purifying respirator (APR). The FRM 40 APR has a similar flow rate through its filter, but a somewhat lower protection factor.

Three of the respirators tested had no evidence of contamination in the exhaled air. These were the 3M Hood, 3M PAPR, and SE 400 PAPR. In very demanding environments, these respirators would afford the best protection. Even if the power fails on the SE 400, protection is still reasonably good.

Protective dead volumes of some of these respirators had previously been measured. For the Centurion MAX, that value was about 1.4 L, and for the Racal AirMate, it was close to zero (Koh et al., 2006a). Dead volume of the FRM 40 is about 1.0 L, and the other two tight-fitting facepieces were presumed to have about the same amount (Koh et al., 2006b). The protective dead volume of the 3M Hood was measured on a mannequin by connecting the inlet port at the mannequin mouth to a vacuum hose and the inlet hose from the blower was closed off. The mannequin with Hood was placed

inside a fog-filled chamber. Mouth flow was recorded for the length of time for the fog to reach the mouth. As expected, fog entered the facepiece from below the ear and chin along the neck. The total volume of air inhaled before the fog reached the mouth was 2 L.

Despite advances in filter technology, contaminant levels inside respirators can still become unacceptably high if the respirators can leak ambient air through alternate pathways. In fact, weak links in wearer protection are the facial fit and the exhalation valve (Koh et al., 2006a). The figure of merit for respiratory protection has been the protection factor (PF) defined as the concentration of contaminant outside the respirator divided by the concentration inside the respirator. Results from this study are not in agreement with some of the Assigned Protection Factors published by OSHA (2006). OSHA assigns a protection factor of 50 to a full facepiece APR. Our results for the FRM 40 give a protection factor of 17, and for the unpowered SE 400 a value of 20. The OSHA value for full-facepiece tight-fitting PAPR is 1000; our results for the 3M PAPR and powered SE 400 are ∞. The OSHA value for the loose-fitting PAPR is 25; we obtained values of 1.1 for the Racal, 4 for the Centurion, and ∞ for the 3M Hood.

There are two difficulties with this ratio. First is that contaminant concentration inside the respirator can be nonuniform, and thus the measurement can be dependent upon location. Recent studies on flow visualization inside respirator facepieces (Koh et al., 2006b; Johnson et al., 2006a) have shown that flow pathways can twist and curl, with clear delineation between contaminant-filled air and clean air over very short distances. Placing a contaminant-detection probe in a stagnant zone could yield measurements that probably underestimate contaminant concentration. Placing the probe in the flow

pathway, where contaminant concentration might be particulary high, could overestimate average concentration in the facepiece.

The second difficulty with PF is that some contaminants can deposit or be absorbed in the respiratory system, thus making the respiratory airways into a contaminant filter. Measured average containment concentration inside the facepiece would, therefore, be underestimated.

In this study, we used an alternative means to measure protection factor as it related to respirator leakage. If the respirator was operated in an atmosphere containing a tracer gas, but the supply of air to the respirator through the filter circuit was free of tracer gas, then the only means for the gas to enter the facepiece and be inhaled was if the gas leaked inward from some path different from the filter circuit. If this test was conducted with a breathing machine, then the tracer gas would neither be deposited nor absorbed in the machine. The average concentration of the gas in the collected exhaled breath should then be equal to the average concentration inside the facepiece, thus averaging regions of high and low concentrations due to preferred contaminant flow pathways. The ratio of tracer gas concentration in the collected exhaled breath to the gas concentration in the surrounding atmosphere should then be the inverse of PF, at least from the wearer's standpoint.

This experiment was motivated by a need to measure leakage volumes. The volume of leakage into the respirator can be determined from the concentration ratio stated earlier and the measured exhaled volume, because air that leaks into the respirator has the gas concentration of the surrounding atmosphere.

Thus, this experiment had two possible outcomes, both of which can be of interest to respirator use experts. Comparing results from this and other recent fog flow visualization studies shows that protective respirator dead volume measurements are generally in agreement no matter what procedure is used. Using flow visualization with a breathing machine gave an inhaled volume before fog reached the mouth of about 1.4 L for the Centurion MAX PAPR (Koh et al., 2006b). Flow visualization with human subject breathing gave 1.1 L before fog reached the mouth for the same respirator (Johnson et al., 2006a).

The ratio of CO_2 concentrations in the chamber to that in the collected exhaled breath is the actual protection factor of the respirator, and these ranged from 1.1 to infinity for the particular set of respiratory conditions used. It was made clear from flow visualization studies (Koh et al., 2006a); Koh et al., 2006b) that contaminants can enter the respirator facepiece without being inhaled. There is, inside each respirator, a certain dead volume that acts to protect the wearer against inhaling contamination. This protective dead volume was measured in several respirators at about 1.4 L (Koh et al., 2006a; Koh et al., 2006b), meaning that, unless the inhaled tidal volume exceeded 1.4 L, no contaminant would reach the wearer. Exhaled breath or blower flow sweeps the protective dead volume clear of contamination during the exhalation phase of the breathing cycle, and the protective dead volume inside the respirator facepiece is renewed. Only in the case of the Racal AirMate 3 was it found that turbulence of blower flow inside the facepiece drew ambient contamination into the facepiece and reduced protective dead volume to a very small value.

It is known that peak respiratory flows can often exceed blower flows (Johnson, et al., 2005; Berndtsson, 2004; Coyne et al., 2006; Caretti and Coyne, 2006; Anderson et al., 2006). If PAPR blowers and batteries were made powerful enough to perform up to peak flow levels, bulk of the devices would probably increase greatly and the extra weight could reduce work performance (Johnson et al., 2006b). An alternate strategy, one that seems to have worked thus far, is to ensure a large enough protective dead volume that any contaminants entering the facepiece do not reach the mouth. Without accounting for exhalation air coming from the mouth, blower flow rate does not need to be any larger than that required to purge the dead volume of contaminants during the exhalation phase, so long as the distribution of blower air is wide enough to sweep the entire dead volume. Taking exhaled air into account reduces required blower flow rate even further, at least as far as contaminants are concerned. Smaller blower flow rates might result in CO_2 accumulation in the dead volume. The net result is that peak inhalation flow rates do not have to be met by the blower as long as stored clean air is available inside the facepiece.

This is a different way to look at dead volume. Dead volume in air-purifying respirators is considered to be a problem, accumulating CO_2 and limiting physical work performance (Johnson et al., 2000). Dead volume in powered air-purifying respirators (PAPRs) in contrast, can actually be a significant help to provide wearer protection. PAPR dead volume might be purposely designed to be large in order to achieve protection goals.

How large should protective dead volume be? It could be made large enough so that no contaminated air would reach the mouth even under extreme circumstances. Inhaled tidal volumes during physical exertion are normally in the 1.5 L range,

sometimes reach 2.0 L, and only rarely exceed 2.5 L. Protective dead volumes greater than 2.5-3.0 L should then be at least as effective as continuous positive pressure in the facepiece in providing wearer protection, as long as the blower can purge the dead volume during the exhalation phase of the breathing cycle. Dead volumes larger than 2.5 - 3.0 L require larger blower flow rates and may be unnecessary and undesirable.

There has been concern expressed when the pressure inside a respirator facepiece intended to be positive pressure becomes negative momentarily (Campbell et al., 1994). As long as positive pressure is maintained, it is asserted, any leakage would flow from inside the facepiece to the outside, and contaminated air would not enter the facepiece. This does not always have to be the case, as illustrated by the extreme example of the Racal Air-Mate 3, which ought to have a very slightly higher pressure inside the facepiece than outside as long as the blower pushes air through the region in front of the face. But, turbulence along the periphery of the visor draws contamination into the facepiece anyway. Negative pressure excursions are short and variably located.

Nevertheless, results in this and other recent experiments have shown that it is not necessary to maintain positive pressure inside the facepiece at all times just as long as contaminated (leakage) air never reaches the mouth. The blower must be able to remove contaminated air from the protective dead volume before the next negative pressure incident.

Many of the newer hood-type loose-fitting respirators use the protective dead volume principle, and so can be considered at least as protective as APRs and tight-fitting PAPRs. They have the advantage over APRs in that there is no high resistance to breathe

through, but have the disadvantage compared to tight-fitting PAPRs that, should the blower be inoperable, there is no contaminant protection afforded.

The validity of the methods used in this study depend upon filter efficacy. The tracer gas used in this study was CO_2, and we did not allow CO_2 to challenge the filter; each filter inlet was supplied by clean air. Hence, perfect filter efficiency was assumed, and we were mainly interested in respirator leakage.

If a different gas was used, one that the filter should remove, then the inlet to the filter could be in contact with the same atmosphere that surrounds the respirator under test. That way the filter circuit would also be tested.

Clayton et al. (2002) calculated respirator protection factors for human wearers while they simulated asbestos removal operations. They used a method similar to that used in the present study, except that their subjects worked in a chamber containing a small concentration of sodium hexafluoride instead of carbon dioxide. They also continuously measured SF_6 concentrations inside and outside the respirator, and thus could measure protection factors as they varied throughout the breathing cycle. In the present study, we were more interested in knowing how much of the contaminated air was actually inhaled, so inhaled contamination (CO_2) was collected when it was expelled from the breathing machine. Obviously, CO_2 could not be used as a test gas with human test subjects; SF_6 or CH_4 might be a better choice. However, collecting exhaled gas and determining contaminant levels there rather than monitoring contaminant levels inside the respirator facepiece gives the actual protection factor experienced by the wearer as compared to the respirator protection factor (insofar as there is no gas absorbed in the respiratory system).

The average concentration of tracer gas in the exhaled breath would not be expected to equal the average concentration inside the facepiece. Rather, the average exhaled-breath concentration reflects the concentration of contaminant actually inspired. This means that regions of high flow leading to the mouth are weighted substantially more than regions of nearly-stagnant flow. In this respect, measurement of exhaled-breath concentration is an honest measure of the exposure of the wearer.

Reports have been published relating facial measurements of wearers to respirator fit (Zhuang et al., 2005). One reason for this, of course, is that some facial configurations result in large leaks, and this lower protection factors. However, results from this study indicate another possible cause, and that is flow pathway of contaminated air. Different facial configurations could channel leakage flows differently in different people. Depending on the exact position of the particle counter used in those studies (Zhuang et al., 2005; Coffey et al., 2006; Myers et al.,1996) the counter could register higher average values or lower average values when contaminants were drawn into the respirator facepiece. Although several of these studies were conducted with half facepiece or filtering facepiece respirators (Zhuang et al., Coffey et al., 2006, Myers et al., 1996; Myers and Zhuang. 1998; Zhuang et al., 2003) there is no reason to suspect that preferential flow pathways discovered in our studies with loose-fitting PAPRs or tight-fitting APSs are not also present in other types of respirators. Facial configuration, especially nose protrusion, could easily affect leakage flow pathway to the mouth.

Calculation of net overbreathed volume as the integral of the difference between mouth flow and blower flow depends on the assumption that all the blower flow is captured within the facepiece. Likewise, the statement made earlier that the blower

needed to supply a flow rate no larger than the facepiece dead volume divided by the exhalation time is contingent upon no blower flow escaping the facepiece before it sweeps the facepiece. It is likely that some blower flow escapes directly to the outside, either through leaks or through the exhalation valve. This represents inefficient use of blower capacity. At present, there are no known published measurements of ineffectual blower flow, but these measurements are able to be made with the same method as used in this experiment.

If contaminated air can leak from outside the facepiece into the inhaled breath, then blower air can flow directly out of the facepiece without contributing to clean air in the protective dead volume. For this reason, blower contribution to the inhaled breath was calculated from:

$$V_{bl,inh} = V_{inh} [1\text{-}C_{co2,\,inh}/C_{co2,\,amb}] \quad (1)$$

This equation indicates that the blower/air contribution ($V_{bl,inh}$) to inhaled volume (V_{inh}) is the proportion of air not identified as leakage ($1\text{-}C_{co2,\,inh}/C_{co2,\,amb}$). Blower effectiveness is the ratio of the $V_{bl,inh}$ to blower flow rate integrated over the total inhalation time ($V_{bl,\,tot}$):

$$V_{bl,tot} = \int_{o}^{n} \dot{V}_{bl}\, dt \quad (2)$$

These values appear in Table 1 as Blower Contribution and Integrated Blower Flow.

It can be seen that blower effectiveness is very low for the Racal respirator. This indicates that most of the air propelled by the blower does not contribute to the volume of air inhaled, and is consistent with other data relating to protection factor (this study) and flow visualization (Koh et al., 2006b).

The 3M Breathe Easy tight-fitting PAPR has a blower effectivenss of about 1.0, which indicates that nearly all of the blower flow contributes to inhalation. The same is true for the SE 400 with blower turned off and FRM 40 APR; nearly all the air flowing through the blower or filter pathway contributes to inhaled air.

When the SE 400 blower was turned on, positive pressure is maintained in the facepiece (at least most of the time—see Koh et al., 2006a), and some of the blower air leaks out, probably through the exhalation valve. It has previously been observed that there is some inward leakage through this valve (Koh et al., 2006a). Blower effectiveness for this PAPR is about 90%.

Blower effectivenesses for both the Centurion MAX and 3M hood were greater than 1.0. In both of these cases, there apparently was enough protective dead volume that air supplied by the blowers during the exhalation phase of breathing contributed to inhaled volume. In these two cases, blowers conform to the recommendation we made that the blower need not supply all inhaled air volume but it does need to purge dead volume air during the exhalation interval. Thus, the blower can contribute to inhaled air volume even during exhalation.

Blower effectiveness analysis is only approximate at this time. The flow situation inside the respirator facepiece is complex, involving air leaking in as well as out simultaneously. Dead volume within the facepiece accumulates air from all sources over time. Breathing is periodic and not steady, and flow pathways inside the facepiece most likely change between inhalation and exhalation, and probably over time within breathing phase as well. If significant physical movement accompanies work performance, then the respirator can shift on the face, or in the case of the hood, the volume of air inside the

hood covering the torso can change greatly. Under extremely difficult breathing conditions, the facepiece itself can deform, which changes the boundary of the flow domain. At this point, successful determination of flow dynamics within a respirator has not been accomplished, to our knowledge.

Acknowledgement:

This work was funded in part by the National Institute for Occupational Safety and Health National Personal Protection Technology Laboratory (NIOSH-NPPTL) Contract 200-2202-00531.

Table 1. Summary of Results

Respirator	Blower Flow Rate (L/min)	Exh Vol (L)	CO_2 Ratio	Protection Factor	Leakage Volume (L)	Inhaled Volume (L)	Blower Contribution (L)	Integrated Blower Flow (L)	Blower Effectiveness
Racal PAPR	191-200	2.41	0.84	1.1	2.02	2.66	0.43	2.42	0.18
Centurion PAPR	88-101	2.37	0.25	4	0.60	2.66	1.99	1.17	1.70
3M Hood PAPR	157-161	2.39	0	∞	0	2.63	2.63	1.87	1.41
3M PAPR	121-278	2.42	0	∞	0	2.62	2.62	2.51	1.04
SE 400 PAPR	64-322	2.32	0	∞	0	2.58	2.58	2.90	0.89
SE 400 APR (blower off)	(0-284)	2.37	0.048	20	0.11	2.58	2.46	2.50	0.98
FRM 40 APR	(0-289	2.37	0.057	17	0.14	2.62	2.47	2.51	0.99

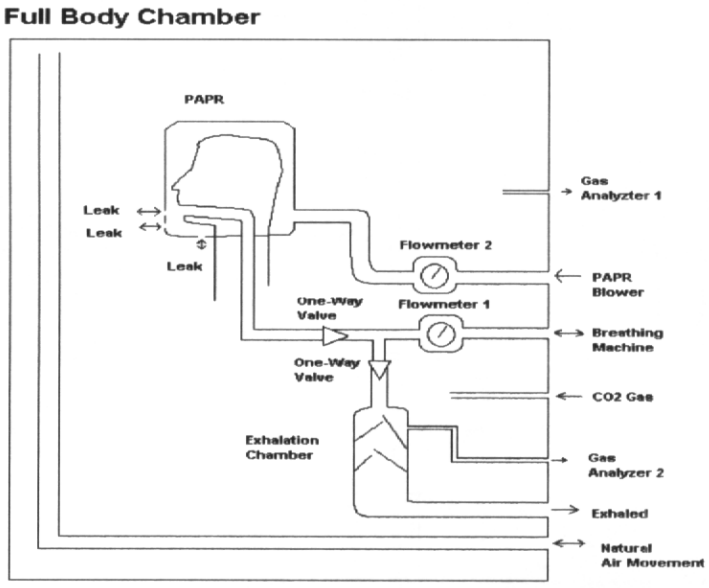

Figure 1. Diagram of the experimental apparatus used. The respirator under test was mounted on a headform inside a large chamber. A breathing machine was used with CO_2 gas to detect leaks. Exhaled air was collected and CO_2 concentration was measured and compared to CO_2 concentration in the chamber.

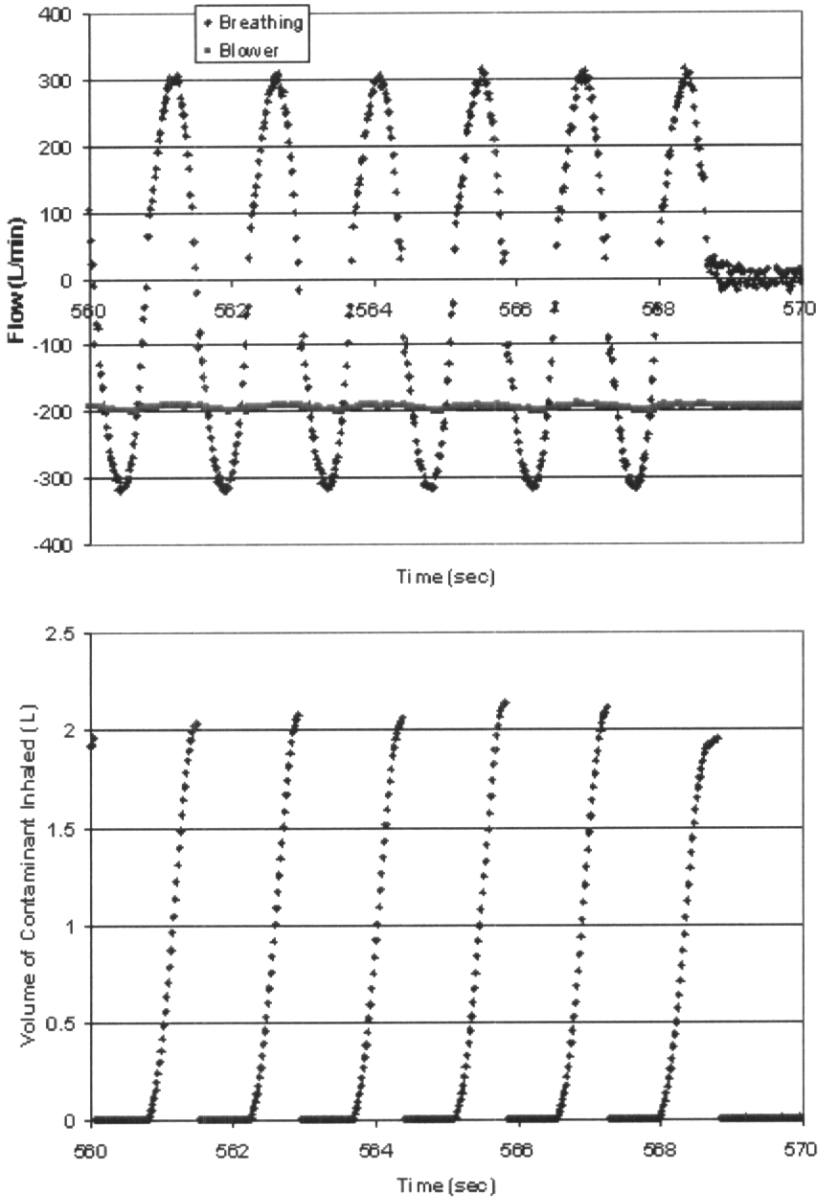

Figure 2. Flows and volumes for the Racal AirMate 3 loose-fitting PAPR. Breathing machine flow is sinusoidal with exhalation in the positive direction. Blower flow rate changes hardly at all. Corresponding contaminant volumes were calculated as the CO_2 concentration in the exhaled air times the integral of the breathing machine exhalation flow rate.

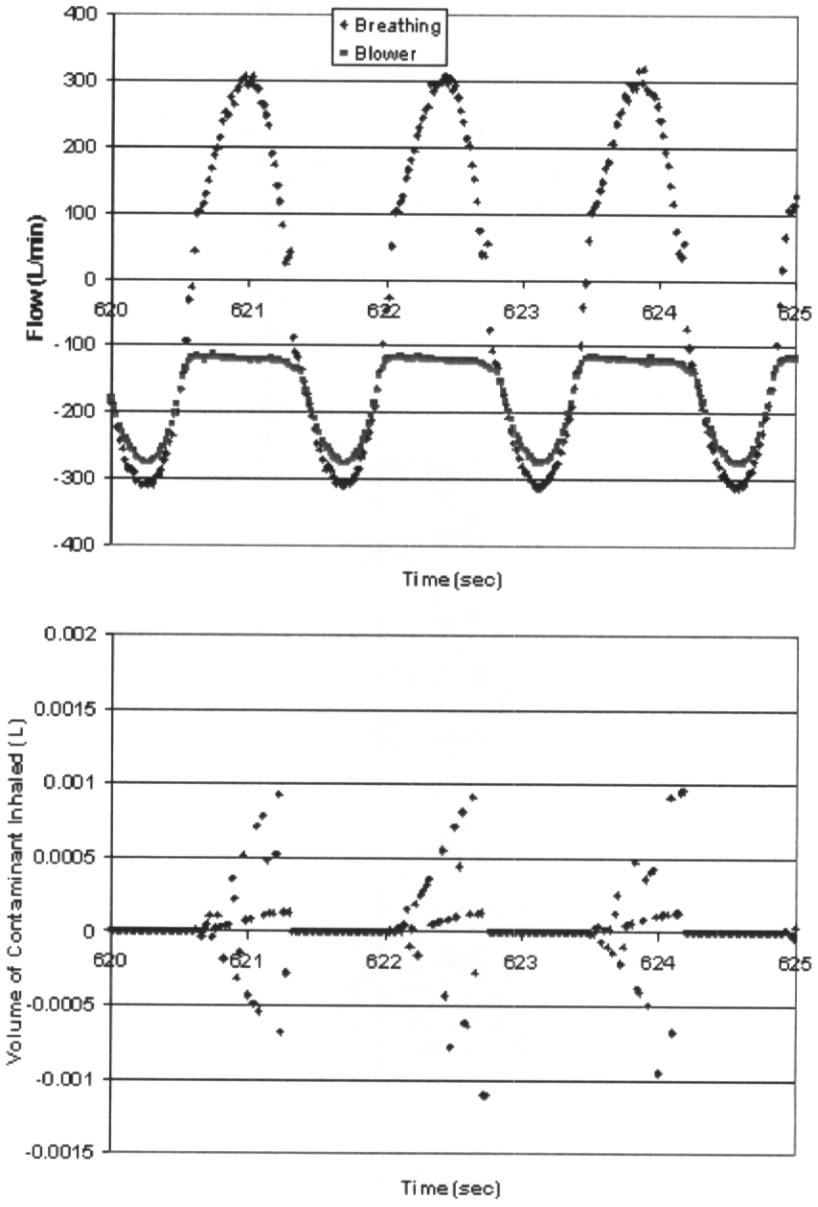

Figure 3. Flows and volumes for the 3M BreatheEasy tight-fitting PAPR. Blower flow rate can be seen to track breathing machine flow during inhalation. The corresponding contaminant volumes (below) are so small that they are inconsequential.

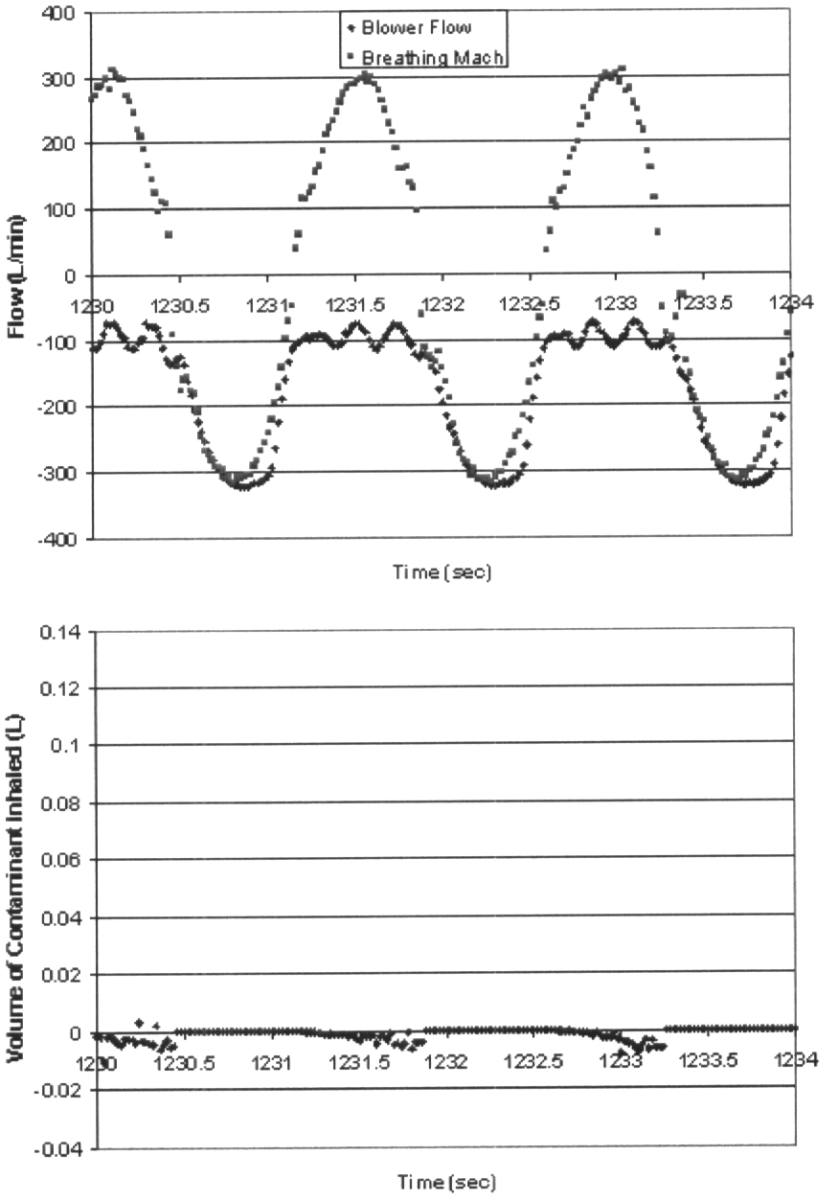

Figure 4. Flows and volumes for the SE 400 breath-responsive PAPR. Blower flow rate is adjusted to maintain positive pressure inside the facepiece. Corresponding contaminant volumes (below) are neglible.

Figure Captions

Figure 1. Diagram of the experimental apparatus used. The respirator under test was mounted on a headform inside a large chamber. A breathing machine was used with CO_2 gas to detect leaks. Exhaled air was collected and CO_2 concentration was measured and compared to CO_2 concentration in the chamber.

Figure 2. Flows and volumes for the Racal AirMate 3 loose-fitting PAPR. Breathing machine flow is sinusoidal with exhalation in the positive direction. Blower flow rate changes hardly at all. Corresponding contaminant volumes were calculated as the CO_2 concentration in the exhaled air times the integral of the breathing machine exhalation flow rate.

Figure 3. Flows and volumes for the 3M BreatheEasy tight-fitting PAPR. Blower flow rate can be seen to track breathing machine flow during inhalation. The corresponding contaminant volumes (below) are so small that they are inconsequential.

Figure 4. Flows and volumes for the SE 400 breath-responsive PAPR. Blower flow rate is adjusted to maintain positive pressure inside the facepiece. Corresponding contaminant volumes (below) are neglible.

References

Anderson, N. J., P. E. Cassidy, L. L. Janssen, and D. R. Dengel, 2006, Peak Inspiratory Flows of Adults Exercising at Light, Moderate, and Heavy Work Loads, *J. ISRP* 23:53-63.

Berndtsson, G., 2004, Peak Inhalation Air Flow and Minute Volumes Measured in a Bicycle Ergometer Test, *J. ISRP* 21:21-30.

Campbell, D. J., G. P. Noonan, T. R. Merinar, and J. A. Stobbe, 1994, Estimated Workplace Protection Factors for Positive-Pressure Self-Contained Breathing Apparatus, *Amer. Indus. Hyg. Assoc. J.*, 55:322-329.

Caretti, D. M., and K. M. Coyne, 2006, A Quantitative Review of Ventilation Rates During Respirator Resistance Breathing, *J. ISRP* 23:1-20.

Clayton, M. P., A. E. Bailey, N. P. Vaughan, and R. Rajan, 2002, Performance of Power Assisted Respirators During Simulated Asbestos Removal, *Ann.. Occup. Hyg.* 46:49-59.

Coffey, C. C., R. B. Lawrence, Z. Zhuang, M. G. Dulling, and D. L. Campbell, 2006, Errors Associated with Three Methods of Assessing Respirator Fit, *J. Occup. Environ. Hyg.* 3:44-52.

Coyne, K., D. Caretti, W. Scott, A. Johnson, and F. Koh, 2006, Inspiratory Flow Rates During Hard Work When Breathing Through Different Respirator Inhalation and Exhalation Resistances, *J. Occup Environ. Hyg.* 3:490-500.

Johnson, A. T., Koh, F. C., S. Jamshidi, and T. E. Rehak, 2006a, Human Subject Testing of Leakage in a Loose-Fitting PAPR, *J. Occup. Environ. Hyg.* (submitted).

Johnson, A. T., W. H. Scott, F. C. Koh, E. B. Francis, E. R. Lopresti, and S. J. Phelps, 2006b, Effects of Helmet Weight on Voluntary Performance Time at 80-85% of Maximal Aerobic Capacity, *J. ISRP* (in review).

Johnson, A. T., W. H. Scott, C. G. Lausted, K. M. Coyne, M. S. Sahota, and M. M. Johnson, 2000, Effect of External Dead Volume on Performance Time While Wearing a Respirator, *Amer. Indus. Hyg. Assoc. J.*, 61:678-684.

Johnson, A. T., Koh, F. C. ,W. H. Scott, Jr., K. M. Mackey, K. Y. S. Chen, and T. Rehak, 2005, Inhalation Flow Rates During Strenuous Exercise, *J. ISRP*, 22: 79-96.

Koh, F. C., A. T. Johnson, and T. E. Rehak, 2006a, Inward Leakage in Tight-Fitting PAPRs, *J. Occup. Environ. Hyg.* (in review).

Koh, F. C., A. T. Johnson, and T. E. Rehak, 2006b, Flow Visualization in a Loose-Fitting PAPR, *J. ISRP* (in review).

Mackey, K. R. M., A. T. Johnson, W. H. Scott, and F. C. Koh, 2005, Overbreathing a Loose-Fitting PAPR, *J. ISRP* 22:1-10.

Myers, W. R., and Z. Zhuang, 1998, Field Performance Measurements of Half-Facepiece Respirators: Developing Probability Estimates to Evaluate the Adequacy of an APF of 10, *Amer. Indus. Hyg. Assoc. J.*, 59:796-801.

Myers, W. R., Z. Zhuang, and T. Nelson, 1996, Field Performance Measurements of Half-Facepiece Respirators, *Amer. Indus. Hyg. Assoc. J.*, 57:166-174.

OSHA (2006): Assigned Protection Factors: Final Rule – 71:50121-50192, Code of Federal Regulations 29 CFR 1910, 1915, and 1926.

Zhuang, Z. C. C. Coffey, P. A. Jensen, D. L. Campbell, R. B. Lawrence, and W. R. Myers, 2003, Correlation Between Quantitative Fit Factors and Workplace Protection Factors Measured in Actual Workplace Environments at a Steel Factory, *Amer. Indus. Hyg. Assoc. J.*, 64:730-738.

Zhuang, Z. C., C. C. Coffey, and R. Berry Ann, 2005, The Effect of Subject Characteristics and Respirator Features on Respirator Fit, *J. Occup. Environ. Hyg.* 2:641-649.

APPENDIX 10

RESPIRATORY

ANSI Z88.1 **Revision: 69** RESPIRATORY PROTECTION AGAINST RADON DAUGHTERS (17 Pages, $25)

ANSI Z88.10 **Revision: 01** RESPIRATORY FIT TESTING METHODS ($63)

ANSI Z88.2 **Revision: 92** RESPIRATORY PROTECTION ($57)

ANSI Z88.4 **Revision: 72** RESPIRATORY PROTECTION (not in stock/ no price)

ANSI Z88.5 **Revision: 81** RESPIRATORY PROTECTION FOR THE FIRE SERVICE (22 PAGES, $25)

ANSI Z88.6 **Revision: 84** FOR RESPIRATORY PROTECTION – RESPIRATOR USE (17 PAGES, $25)

ANSI Z88.7 **Revision: 01** COLOR CODING OF AIR-PURIFYING RESPIRATOR CANISTERS, CARTRIGES AND FILERS ($38)

BS 2091 **Revision: 69** RESPIRATORS FOR PROOTECTION AGAINST HARMFUL DUSTS, GASES AND SCHEDULED AGRICULTURAL CHEMICALS

BS 2617 **Revision: ?** RESPIRATORS FOR AGRICULTURAL WORKERS USING TOXIC CHEMICALS

BS 4555 **Revision: 70** SPECIFICATION FOR HIGH EFFICIENCY DUST RESPIRATORS

BS 4558 **Revision: 70** SPECIFICATION FOR POSITIVE PRESSURE, POWERED DUST RESPIRATORS

CNS Z 2024 **Revision: 87** DUST RESPIRATORS

JIS T 8151 **Revision: 91** DUST RESPIRATORS

JIS T 8152 **Revision: 94** GAS RESPIRATORS

JIS T 8153 **Revision: 02** SUPPLIED-AIR RESPIRATORS

JIS T 8157 **Revision: 91** POWERED AIR PURIFYING RESPIRATORS (PAPR)

JIS T 8159 **Revision: 95** LEAKAGE RATE TESTING METHOD FOR FACEPIECES OF RESPIRATORS

JIS T 8160 **Revision: 92** DUST RESPIRATORS FOR FINE PARTICLES

MIL-STD-6-9 **Revision: A** RESPIRATORS, AIR FILTERING

VISION

ANSI Z2 **Revision: 38** SAFETY CODE FOR THE PROTECTION OF HEADS, EYES AND RESPIRATORY ORGANS (101 pages, $43)

ANSI Z2.1 **Revision: 59** SAFETY CODE FOR HEAD, EYE AND RESPIRATORY PROTECTION (47 pages $20)

ANSI Z87.1 **Revision: 89** PRACTICE FOR OCCUPATIONAL AND EDUCATIONAL EYE AND FACE PROTECTION (44 pages, $94)

ASTM F 803 **Revision: 01** STANDARD SPECIFICATION FOR EYE PROTECTORS FOR SELECTED SPORTS (14 pages, $39)

BS 1542 **Revision: 82** SPECIFICATION FOR EQUIPMENT FOR EYE, FACE, AND NECK PROTECTION AGAINSTY NON-IONIZING

RADIATION ARISING DURING WELDING AND SIMILAR OPERATIONS (not in stock/ no price)

BS 2092 **Revision: 87** SPECIFICATION FOR EYE-PROTECTORS FOR INDUSTRIAL AND NON-INDISTRIAL USES (24 pages/ no listed price)

BS 7028 **Revision: 99** EYE PROTECTION FOR INDUSTRIAL AND OTHER USES-GUIDANCE ON SELECTION, USE AND MAINTENANCE (28 pages, $153)

BS EN 166 **Revision: 02** PERSONAL EYE-PROTECTION SPECIFICATIONS (38 pages, $153)

BS EN 167 **Revision: 02** PERSONAL EYE PROTECTION – OPTICAL TEST METHODS (30 pages, $153)

BS EN 168 **Revision: 02** PERSONAL EYE PROTECTION – NON-OPTICAL TEST METHODS (35 pages, $185)

CNS Z 2034 **Revision: 81** EYE PROTECTOR WITH PLASTIC LENSES (6 pages, $25)

CSA Z94.3 **Revision: 99** INDUSTRIAL EYE AND FACE PROTECTORS (57 pages, $68)

CSA Z94.3.1 **Revision: 02** PROTECTIVE EYEWEAR: A USER'S GUIDE (26 pages, $25)

DIN 4646 P2 **Revision: 75** GLASSES FOR EYE – PROTECTION EQUIPMENT; OPTICAL TE (in stock/ no price)

DIN 4646 P8 **Revision: 86** LENSES FOR EYE PROTECTORS; ANTIFOGGING TEST (in stock, no price)

DIN 58214 **Revision: 97** EYE-PROTECTORS; SHIELDS, SCREENS AND HELMETS; TERMS AND FORMS AND SAFETY REQUIREMENTS (German, 4 pages, $46)

ISO 4849 **Revision: 81** PERSONAL EYE PROTECTORS (8 pages, $39) – there are several revisions: ISO 4850, 4851, 4852, 4854, and 4855 which all deal with personal eye protectors/protection

ISO 4856 **Revision: 82** PERSONAL EYE-PROTECTORS-SYNOPTIC TABLES OF REQRMTS ($30)

JIS T 8147 **Revision: 94** EYE PROTECTOR ($62)

MIL-E-50069 **Revision: 00E** EYERING, FIELD PROTECTIVE MASK, C4 (6 pages, $28)

QPL-15042 **Revision: 4** ANTIFOGGING COMPOUND, EYE PROTECTIVE EQUIPMENT (not in stock/ no price)

SAA AS 1336 **Revision: 82** RECOMMENDED PRACTICES FOR EYE PROTECTION IN THE INDUSTRIAL ENVIRONMENT (16 pages, no price)

SAA AS/NZS 1336 **Revision: 97** RECOMMENDED PRACTICES FOR OCCUPATIONAL EYE PROTECTION (36 pages, $34)

SAA AS/NZS 13367 **Revision: 92** HEAD PROTECTIVE EQUIPMENT – EYE PROTECTORS FOR INDUSTRIAL APPLICATION (40 pages, $34)

HEARING

A-A 54890 **Revision: 93** PLUG, EAR, HEARING PROTECTION, UNIVERSAL SIZE, WITH HEADBAND (9 pages, $29)

A-A-58084 **Revision: 96** PROTECTOR, HEARING (5 pages, $26)

ANSI 12.19 **Revision: 96** MEASUREMENT OF OCCUPATIONAL NOISE EXPOSURE

ANSI S12.42 **Revision: 95** MICROPHONE-IN-REAL-EAR AND ACOUSTIC TEST FIXTURE METHODS FOR THE MEASUREMENT OF INSERTION LOSS OF CIRCUMNATURAL HEARING PROTECTION DEVICES ($117)

ANSI S3.19 **Revision: 74** METHOD FOR THE MEASUREMENT OF REAL-EAR PROTECTION OF HEARING PROTECTORS AND PHYSICAL ATTENUATION OF EARMUFFS ($117)

BS 5108 P1 **Revision: 91** SOUND ATTENUATION OF HEARING PROTECTORS – PART 1: SUBJECTIVE METHOD OF MEASUREMENT (no price)

BS EN 352-3 **Revision: 97** HEARING PROTECTORS – SAFETY REQUIREMENTS AND TESTING – PART 3. EAR-MUFFS ATTACHED TO AN INDUSTRIAL SAFETY HELMET (30 pages, $153)

CSA Z94.1 **Revision: 02** HEARING PROTECTION DEVICES – PERFORMANCE, SELECTION, CARE, AND USE (62 pages, $68)

DIN 32760 **Revision: 85** HEARING PROTECTORS; CONCEPTS, SAFETY REQUIREMENTS (no price)

DIN EN 352 P1 **Revision: 93** HEARING PROTECTORS – SAFETY REQUIREMENTS AND TESTING – EAR MUFFS (25 pages, $163)

DIN EN 352 P3 **Revision: 97** HEARING PROTECTORS – SAFETY REQUIREMENTS AND TESTING – PART 3. EAR MUFFS ATTACHED TO AN INDUSTRIAL SAFETY HELMET (17 pages, $176)

DIN EN ISO 4869-4 **Revision 00** HEARING PROTECTORS PART 4: MEASUREMENT OF EFFECTIVE SOUND PRESSURE LEVELS FOR LEVE-DEPENDENT SOUND-RESTORATION EAR-MUFFS (9 pages, $127)

ISO 4869-1 **Revision: 90** ACCOUSTICS – HEARING PROTECTORS – PART 1: SUBJECTIVE METHOD FOR THE MEASUREMENT OF SOUND ATTENUATION (7 pages, $39)

ISO TR 4869-4 **Revision: 98** ACCOUSTICS – HEARING PROTECTORS – PART 4: MEASUREMENT OF EFFECTIVE SOUND PRESSURE LEVELS FOR LEVEL-DEPENDENT SOUND-RESTORATION EAR-MUFFS (12 pages, $39)

MIL-H-87819/2 **Revision: 85** HEADSET-ELECTRICAL, HEARING PROTECTIVE TYPE HIGH AMBIENT NOISE LEVELS, 105-125 DB M87819/2-01 (4 pages, $28)

MIL-H-87819/3 **Revision: 85** HEADSET-NONELECTRICAL, HEARING PROTECTIVE TYPE HIGH AMBIENT NOISE LEVELS, 105-125 DB M87819/3-01 (6 pages, $28)

SAA AS 1270 **Revision: 88** ACCOUSTICS – HEARING PROTECTORS (no price)

SAA AS/NZS 1270 **Revision: 99** ACCOUSTICS – HEARING PROTECTORS (23 pages, $29)
STANAG 2899 **Revision: 87** PROTECTION OF HEARING (9 pages, $29)

CRANIAL

A-A 2269 **Revision: A** HELMET, SAFETY (9 pages, $29)
ANSI 289.1 **Revision: 97** INDUSTRIAL HEAD PROTECTION
BS 2826 **Revision: ?** INDUSTRIAL SAFETY HELMETS (HEAVY DUTY) (not in stock, no price)
BS 5240 P1 **Revision: 87** INDUSTRIAL SAFETY HELMETS – PART 1. SPECIFICATION FOR CONSTRUCTION AND PERFORMANCE (12 pages, no price)
BS 6489 **Revision: 84** SPECIFICATION FOR HEADFORMS FOR USE IN THE TESTING OF PROTECTIVE HELMETS (no price)
BS EN 397 **Revision: 95** SPECIFICATION FOR INDUSTRIAL SAFETY HELMETS (24 pages, $116)
BS EN 960 **Revision: 95** HEADFORMS FOR USE IN THE TESTING OF PROTECTIVE HELMETS (28 pages, $116)
BS EN 1835 **Revision: 00** RESPIRATORY PROTECTIVE DEVICES-LIGHT DUTY CONSTRUCTION COMPRESSED AIR LINE BREATHING APPARATUS INCORPORATING A HELMET OR A HOOD-REQUIRMENTS, TESTING, MARKING (66 pages, $231)
DIN 4840 **Revision: 89** PROTECTIVE HELMETS USED IN INDUSTRY, AGRICULTURE AND FORESTRY; SAFETY REQUIREMENTS, TESTING (9 pages, no price)
DIN 58648 P2 **Revision: 97 Chg: Date: 02/00/97** RESPIRATORY EQUIPMENT; COMPRESSED AIR LINE BREATHING APPARATUS INCORPORATING A HOOD, A HELMET, OR A SUIT; SAFETY REQUIREMENTS TESTING, MARKING ($84)
DIN EN 397 **Revision: 00** INDUSTRIAL SAFETY HELMETS (15 pages, $138)
DIN EN 960 **Revision: 98** HEADFORMS FOR USE IN THE TESTING OF PROTECTIVE HELMETS (17 pages, $176)
DIN EN 1835 **Revision: 00** RESPIRATORY PROTECTIVE DEVICES LIGHT DUTY CONSTRUCTION COMPRESSED AIR LINE BREATHING APPARATUS INCORPORATING A HELMET OR A HOOD REQUIREMENT, TESTING, MARKING (61 pages, $194)
GGG-H-142 **Revision: G** HELMET, CONSTRUCTION WORKER'S (18 pages, $32)-superseding document: A-A-2269
ISO 3873 **Revision: 77** INDUSTRIAL SAFETY HELMETS (8 pages, $39)
QPL-GGG-H-142 **Revision: 50** HELMET, CONSTRUCTION WORKER'S (no price)
SAA AS 1801 **Revision: 81** INDUSTRIAL SAFETY HELMETS (20 pages, no price)
SAA AS 2512.1 **Revision: 84** METHODS OF TESTING PROTECTIVE HELMETS – DEFINITIONS AND HEADFORMS (7 pages, $25)

SAA AS/NZS 1801 **Revision: 97** HEAD PROTECTIVE EQUIPMENT – OCCUPATIONAL PROTECTIVE HELMETS (30 pages, $29)

SAA AS/NZS 2512.1 **Revision: 98** METHODS OF TESTING PROTECTIVE HELMETS – DEFINITIONS AND HEADFORMS (31 pages, $29)